

Annual Report of Naka Fusion Research Establishment From April 1, 1999 to March 31, 2000

Naka Fusion Research Establishment

Japan Atomic Energy Research Institute
Naka-machi, Naka-gun, Ibaraki-ken

(Received October 25, 2000)

This report provides an overview of research and development activities at the Naka Fusion Research Establishment, JAERI, during the period from April 1, 1999 to March 31, 2000. The activities in the Naka Fusion Research Establishment are highlighted by high performance plasma research in JT-60 and JFT-2M, and progress in ITER EDA, including ITER technology R&D.

Objectives of the JT-60 project are to contribute to the physics R&D for International Thermonuclear Experimental Reactor (ITER) and to establish the physics basis for a steady state tokamak fusion reactor like SSTR. For the achievement of these objectives, some mechanical improvement of the centrifugal pellet injector have been done for stable production and successive ejection of pellet. In addition, a guide tube for an injection from top of high-field side was installed. As a result, pellets were successfully injected from the top of high-field side as well as the low-field side in February 2000. The injection power of electron cyclotron heating (ECH) system of the frequency of 110 GHz installed last year was increased up to ~0.75 MW for 2 seconds in this year using the control of RF beam angle. Two gyrotrons were newly installed with total power increased from 1 MW to 3 MW.

The JT-60 experiments have continued to be productive in many areas covering performance improvement of reversed shear plasmas, non-inductive current drive, physics study relevant to improved modes, stabilization of MHD modes, feedback control, disruption study, understandings on energetic particles and divertor studies with increased pumping capability. Highlights of FY 2000 experiments may be summarized as follows:

- (1) A reversed shear discharge with an equivalent fusion multiplication factor Q_{DT}^{eq} of ~0.5 was achieved successfully at plasma current of 2.4 MA for 0.8 seconds.
- (2) Quasi-steady operation of a low current reversed shear plasma with a large fraction (~80%) of bootstrap current was realized under full non-inductive current drive condition. H-factor of 3.3-3.8 at electron density as high as 73% of the Greenwald limit was sustained for 6

times the energy confinement time.

- (3) Normalized beta exceeding the ideal no-wall stability limit was obtained in reversed shear plasmas with a ratio of an outer-wall radius to a plasma minor radius less than 1.3.
- (4) L-H transition power was reduced by ~30% in the W-shaped divertor with pumping from both inside and outside slots compared with that in the open divertor. Helium exhaust rate in ELMy H-mode plasmas was improved up to 50% higher than the inside slot pumping.
- (5) Current drive efficiency of 1.3×10^{19} A/m²/W was attained by N-NBI at 350 keV in the high p ELMy H-mode with the central electron temperature of 8.6 keV. The efficiency is about 2.6 times higher than that of 100 keV.

On JFT-2M, advanced and basic research of tokamak plasma is being proceeded including the application of the low activation ferritic steel. A dramatic reduction of trapped ion loss due to the toroidal field ripple was identified for the first time in the tokamak experiment through measurements of the first wall temperature. Ferritic steel boards covering 20 % of the first walls have been installed inside the JFT-2M vacuum vessel for the coming experiments. Fast sampled measurement of potential and fluctuations by the heavy ion beam probe revealed characteristic time scales of the potential change at the plasma periphery for the first time at the L/H transition. The results would provide an important evidence for the L/H transition theory based on the change of electric field structure.

The principal objective of theoretical and analytical studies is to understand physics of tokamak plasmas. Much progress was made on analyzing dynamics of the internal transport barrier in JT-60U reverse shear plasmas. Progress was also made on the study of micro and macro instabilities. The NEXT (Numerical EXperiment of Tokamak) project has been progressed in order to investigate complex physical processes in core plasmas, such as transport and MHD, and in divertor plasma by using recently advanced computer resources. Remarkable progress was made on the development of divertor simulation codes.

R&D of fusion reactor technology has focused on the ITER EDA and DEMO-related areas including application to the other field. Major highlights in FY 1999 are as follows:

- (1) CS Insert Coil which is one layer solenoid with Nb₃Sn conductor was successfully fabricated and installed with inner and outer CS Model Coil modules into the CS Model Coil test facility.
- (2) Thermal fatigue test of the first wall panel made by reduced activation ferritic steel F82H has been performed and the first wall panel withstood 8500 cyclic heating by 5.5 MW/m² surface heat flux (surface temperature estimates 1000°C).
- (3) A new experiment to design the vacuum insulated beam source for the negative ion-based neutral beam injector (N-NBI) started. High-energy (725 keV) H⁻ ions, which was produced by the ion source for N-NBI, were implanted into the single-crystal Si wafer without mass separation to delaminate a thin Si layer. After annealing the implanted Si wafer at 600°C

for 10 minutes, the Si layer has been successfully delaminated at a thickness of 10 μm .

- (4) Critical heat flux test on screw tube under one sided heating conditions, thermal fatigue tests with 20 MW/m² on short dump target, and disruption erosion tests on various tungsten were performed.
- (5) Design study of International Fusion Material Irradiation Facility(IFMIF) responding to the deuterium beam current upgrade in three stages(50/125/250 mA), which corresponds with the fusion reactor program, has been progressed.

After the successful completion of the six year Engineering Design Activities (EDA) for ITER in July 1998, the three Parties of Japan, the European Union (EU) and the Russian Federation (RF) agreed to extend the period of the EDA for three years until July 2001 in order to modify the design of ITER so that the construction cost can be reduced as much as about a half of the cost of 1998 design, by taking account of the progress in plasma physics and technology R&D. For the design of the modified ITER (termed 'ITER-FEAT'), new technical guidelines were established, and various design options were examined in line with the guidelines. The concept of ITER-FEAT was eventually selected at the Program Directors' Meeting held in July 1999, with emphasis on high plasma density and the capability of steady-state operation. On the basis of this decision, the design of ITER-FEAT was developed, and the Outline Design Report together with its Technical Basis document were submitted by the ITER Director to the ITER Meeting of the Parties' representatives held in January 2000. The Technical Subcommittee of the Fusion Council of Japan reviewed these documents, and concluded in March 2000 that the predicted plasma performance and engineering performance are appropriate for fulfilling the technical objectives. Further development of detailed design of ITER-FEAT will be continued aiming at completing the Final Design Report, a full set of other technical documents, and ITER technology R&D by July 2001.

Based on the previous design studies of SSTR in 1990, advanced SSTR in 1996 and a concept of DREAM reactor with a high availability and an easy maintenance system, a new tokamak fusion power reactor (A-SSTR2) which meets both economical and environmental requirements was developed in 1999. Radiological toxic hazard potential is compared among all the radioactive materials contained in a fusion reactor, a pressurized light water reactor and a coal-fired power plant.

Keywords; Fusion Research, JAERI, JT-60, JFT-2M, NEXT, Fusion Engineering,
CS Model Coil, N-NBI, ITER, Fusion Reactor Design

Contents

I. JT-60 PROGRAM

1. Operation and Machine Improvements
 - 1.1 Tokamak Machine
 - 1.2 Control System
 - 1.3 Power Supply System
 - 1.4 Neutral Beam Injection System
 - 1.5 Radio-frequency Heating System
 - 1.6 Diagnostics System
 - 1.7 Data Analysis System
2. Experimental Results and Analysis
 - 2.1 Sustainment of High Performance and Non-inductive Current Drive
 - 2.2 Physics of Plasma Confinement
 - 2.3 High Energy Ions and MHD Instabilities
 - 2.4 Plasma Control and Disruption
 - 2.5 Particle Control and Divertor/SOL Physics
 - 2.6 High-radiation and High-density Experiments

II. JFT-2M PROGRAM

1. Advanced Material Tokamak Experiment (AMTEX) Program
 - 1.1 Ripple Reduction Experiments
 - 1.2 Preparation for Pre-testing of Compatibility with Plasma
2. High Performance Experiments
 - 2.1 H-mode Study with Heavy Ion Beam Probe Measurement
 - 2.2 RF Experiments
 - 2.3 Compact Toroid Injection
 - 2.4 Comparative Research on Closed and Open Divertor Geometries
3. Operation and Maintenance
 - 3.1 Tokamak Machine
 - 3.2 Neutral Beam Injection System and Radio-frequency Heating System
 - 3.3 Power Supply System

III. THEORY AND ANALYSIS

1. Confinement and Transport
2. Stability
3. Divertor

4. Numerical Experiment of Tokamak (NEXT)
 - 4.1 Development of Computational Algorithm
 - 4.2 Transport and MHD Simulation
 - 4.3 Divertor Simulation

VI. FUSION REACTOR DESIGN AND SAFETY RELATED RESEARCH

1. Fusion Reactor Design
2. Fusion Safety
 - 2.1 Study of In-vessel Abnormal Events
 - 2.2 Comparison of the Biological Hazard Potential in Fusion Reactor, Light-water Reactor and Coal-fired Power Plant

Appendices

- A.1 Publication List (April 1999-March 2000)
- A.2 Personnel

I. JT-60 PROGRAM

Objectives of the JT-60 project are to contribute to the physics R&D for International Thermonuclear Experimental Reactor (ITER) and to establish the physics basis for a steady state tokamak fusion reactor like SSTR. In the fiscal year 1999, JT-60 experiments were devoted to long time sustainment of high performance plasma, demonstration of steady state operation scenario of tokamak, confinement improvement, divertor physics, heating and current drive with negative ion-based neutral beam injectors (N-NBI), energetic particle physics and disruption study.

Highlight in long time sustainment of high performance plasma is successful sustainment of the equivalent fusion multiplication factor Q_{DT}^{eq} of ~ 0.5 for 0.8 sec in a reversed shear plasma with internal transport barrier. A principle of steady state operation of tokamak was demonstrated with reversed shear plasma in a high triangularity configuration, where fully non-inductive current drive condition was sustained for 2.6 sec with a high bootstrap current fraction of 80%. High confinement with H-factor of 3.8 (H_H -factor to IPB98(y, 2) scaling ~ 2.3) was achieved in a reversed shear plasma at electron density as high as 73% of the Greenwald density. Normalized beta exceeding the ideal no-wall stability limit was obtained in reversed shear plasmas with a ratio of an outer-wall radius to a plasma minor radius less than 1.3. Divertor studies were conducted in the modified W-shaped divertor, where the outside divertor slot was opened for improving the divertor pumping. It was confirmed that the power threshold of the L-H transition was reduced by $\sim 30\%$ in the W-shaped divertor with pumping from both inside and outside slots, compared to the threshold power in the open divertor. Helium exhaust rate in ELMy H-mode plasmas was improved up to 50% than the inside slot pumping. Current drive efficiency of 1.3×10^{19} A/m²/W was attained by N-NBI at 350 keV in the high β_p ELMy H-mode with the central electron temperature of 8.6 keV. The efficiency is about 2.6 times as high as that by NBI around 100 keV. Electron cyclotron (EC) waves of 110 GHz was injected continuously for 5 sec, which is the longest pulse in tokamaks in the world as the electron cyclotron frequency. Central electron temperature of 11 keV was obtained by the EC heating. Amplitude of the neo-classical tearing mode (NTM) considered to be one of important issues in ITER was reduced by the EC wave injection. Furthermore, understandings on energetic particle behavior and disruptions have been steadily progressed.

Two gyrotrons were newly installed and the total gyrotron power was increased from 1 MW to 3 MW. The system is expected to use for suppressing NTMs and for demonstrating high N-NBI current drive efficiency required in ITER at high electron temperature. Multiple pellet injection from both high field side and low field side was started with a centrifugal pellet injector.

1. Operation and Machine Improvements

1.1 Tokamak Machine

Operation and maintenance of JT-60 has been carried out on schedule in this fiscal year. During the maintenance period in May, regular inspection and maintenance of the high pressures gas facility was performed. In the next maintenance period from November to December, status of the cooling pipes inside the toroidal magnetic field coils was examined. Inspections were conducted through observation using a fiberscope with CCD camera and checking of air tightness using highly pressurized air. It has not found that extension of the existing cracks and newly produced cracks on the inside wall of the cooling pipes.

In vessel inspection, a small part of the first wall tiles was replaced isotropic graphite with carbon fiber composite (CFC), where the tile was damaged due to the high heat flux of the plasma discharges with highly triangular-shaped configurations. Rogowsky coils installed in/out vessel, which were found to be poor insulation, were replaced by new ones. The vessel port (port section P-3) was reconstructed to set up a diagnostic instrument on this port for measurement of plasma current profiles.

Eighty metal drums containing solid radioactive waste were transported from Naka site to Tokai Site, the facility of Low Level Waste Management Division (Department of Decommissioning and Waste Management) of JAERI. These were combustible wastes which has been put out in the period of every maintenance work. They have been stored in the radioactive waste storage building at Naka site. They were removed to be incinerated for their volume reduction because there is no incinerator for radioactive wastes at Naka. Regarding the activated materials exceeding the permitted radiation level, storage area for their temporarily keeping was located in the cable duct area in the second basement of JT-60 experimental building. These materials, metal tools, diagnostic instruments and other steel manufactures, irradiated by D-D neutrons inside the torus hall should be kept within the radiation controlled area because it is required to reuse them, but forbidden to take out from the controlled area of the JT-60 facility.

Following major modifications have been performed: (1) All of the piezoelectric valves (PEV) for supplying working gas were replaced by new type of PEVs using a stack type piezoelectric element which have been developed during the previous fiscal year. Replacement has been done to avoid a trouble due to old bimorph type PEVs because they have been deteriorated by 15 years use and it became difficult to get old ones owing to discontinuance of production. (2) In the control system for the tokamak machine, a part of hardware standard of CAMAC was changed to that of VME so as to have higher performance. For the other CAMACs, preventive measures were taken against the computer problem of 2000 year's millennium.

As for the centrifugal pellet injector, whole device was removed from the horizontal port of P-10 section into the next testing room to the torus hall in December 1998. Some mechanical

improvements have been done there in this fiscal year. Pellet production mechanism, cutter and acceleration parts were modified for stable production and successive ejection of pellets, and consequently the injector became to be able to eject trains of up to 40 cubic (2.1 mm^3) deuterium pellets at frequencies of 1~10 Hz and velocities of 0.2~1.0 km/s. The injector was installed again on JT-60 in December 1999. Figure I.1.1-1 shows the drawing of pellet injection system for JT-60. A guide tube for an injection from magnetic high-field side (HFS) was developed on a parallel with the mechanical improvements. The guide tube (5 mm in inner diameter and ~15 m in length) has three curves on the way to the nozzle at P-9 upper port. The first curvature is limited to $R = 600 \text{ mm}$ (the maximum curvature) because of obstructive devices around the guide tube. Pellet injection experiments began from February 2000. Pellets were successfully injected from both sides. Figure I.1.1-2 shows the ablating cloud of pellet injected from the upper port (HFS).

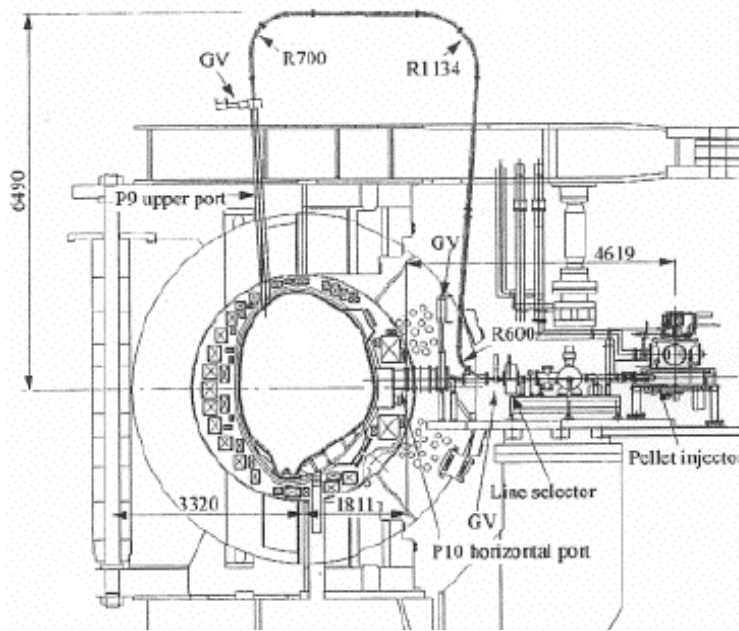


Fig. I.1.1-1 Schematic drawing of pellet injection system for JT-60

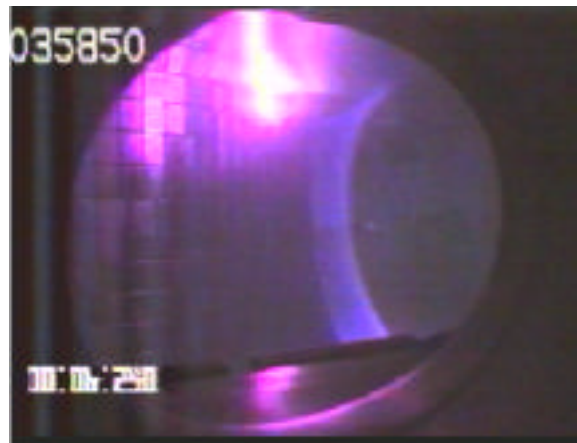


Fig. I.1.1-2 Light emission of pellets injected from upper port (High field side) inside vacuum vessel.

As regard the in-situ boronization system, the glow discharge with hydride decaboran ($\text{B}_{10}\text{H}_{14}$), which led a long boronization time, was examined.

Boronization is usually conducted with a mixed carrier gas of deuterium and He instead of He only. Deuterium is added to reduce hydrogen inside the boron film during the vapor deposition. It became clear that the methane gas, produced by deuterium sputtering on the surface of carbon first walls, exerted an influence on the discharge conditions, i.e., electrode voltages, gas pressures and so on. Based on the above result, a deuterated decaboran ($\text{B}_{10}\text{D}_{14}$), instead of the conventional hydride decaboran, was newly applied for the decaborane-based boronization. The deuterated decaboran which excludes hydrogen content makes it possible to

reduce the conditioning shots after the boronization, which is required for achieving a low isotopic dilution factor $H / (H + D)$. Consequently, this new method doesn't need deuterium as the carrier gas. The boronization time, therefore, is expected to be shortened due to stable glow discharges without precise control of methane gas. The first trial of the boronization with deuterated decaboran was conducted at the end of the fiscal year. Comparing to the previous method, boron coating time was reduced to $\sim 1/2$ and discharge conditioning shots were reduced to $\sim 1/5$. Due to application of the deuterated decaboran, the boronization time was actually shortened and efficiency of the first wall conditioning after the vessel vent was drastically improved.

In plasma-surface interaction study, R&D of the divertor material sample installation device was carried out for the surface analysis of the divertor tile. This device consists of a divertor material sample and a remote handling device to remove the sample after plasma experiments without a shut-down of JT-60. Various material surface analyses using the device are possible under a wide variety of plasma conditions. In this fiscal year, conceptual design and test-fabrication of a part of the handling device were performed. For reliable sample gripping by remote handling, the manipulator and the driver were tested under high vacuum and high temperature ($\sim 300^\circ\text{C}$) conditions.

1.2 Control System

1.2.1 Advanced Plasma Control System

A real-time plasma control system for particle and heating was installed to the JT-60 control system (ZENKEI) in May 1998. Since then, so called "advanced control algorithms" for following quantities have been developed and installed to the ZENKEI for improvement of plasma performance [1.2-1]; (i) neutron production rate, (ii) electron temperature at the plasma center, (iii) electron temperature gradient, (iv) plasma stored energy, (v) divertor radiation power and (vi) divertor neutral gas pressure ratio. The quantities (i), (ii), (iii) and (iv) are feedback-controlled by NBI and (v) and (vi) by gas puff. In this fiscal year, control algorithms for (ii), (iii), (iv) and (vi) were installed in correspondence to respective experimental purposes. In the application of a new control algorithm or in the modification of control algorithms, any change was not required in the interface and software of the heating systems (NBI, RF) or gas injection system. This made it possible to quickly modify control algorithms in correspondence to the experimental results.

1.2.2 Real-time Plasma Shape Reproduction System

A new real-time plasma shape reproduction system used for plasma equilibrium control is now under development. The calculation method used in this system is based on the Cauchy-condition surface method [1.2-2] that has been developed for a recent few years. In this fiscal

year, the design and construction of the system were carried out. The new shape reproduction system is shown in Fig. I.1.2-1. The calculation time of the shape reproduction concerning major equilibrium parameters (horizontal position, x-point height, triangularity etc.) is required to be within 500 μ s. However, the calculation time of plasma vertical position must be within 250 μ s to ensure the stability of vertical motion. To satisfy this requirement, the new system was constructed with six Compact-PCI boards with Alpha-21164 (500 MHz, 512 Mbyte memory made by DEC. Ltd.) as main processors and reflective memory modules for real-time communications. Two processors execute real time calculations of plasma vertical position and magnetic flux, communication to the other four processors and clock control in the period of 250 μ s. The other four processors execute real time calculation of the plasma shape reproduction in the period of 500 μ s. To minimize the calculation time of the plasma shape reproduction with keeping adequate accuracy, a look-up table method was adopted in the calculation. In this method, the calculation condition is classified to suitable cases corresponding to the position of plasma center. For each case, numerical values like Green function are calculated in advance and stored in the look-up table. The numerical values used are changed in each case, which reduces the calculation time. In the actual system, 81 cases were prepared in the look-up table. This system will be tested and is expected to come into operation in the middle of year 2000.

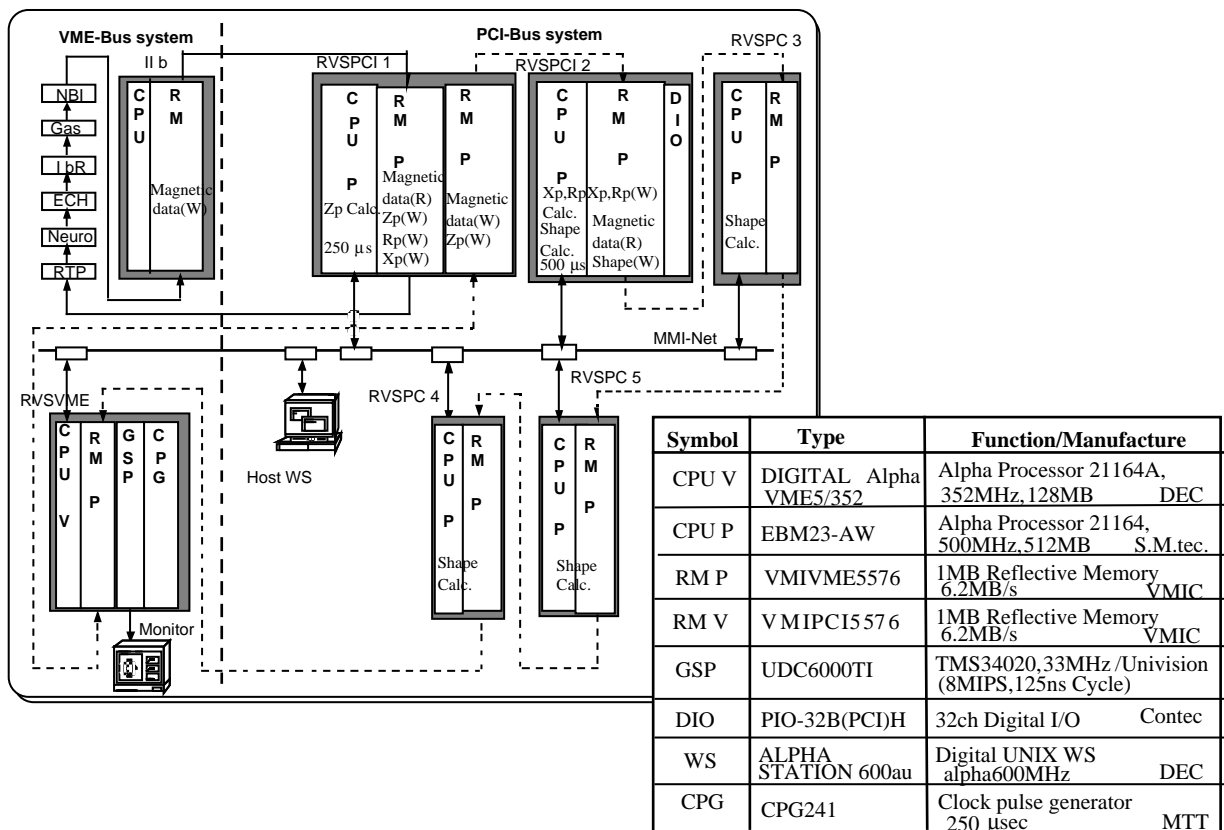


Fig. I.1.2-1 Configuration of a real-time plasma shape reproduction system

1.2.3 Long-time Digital Integrator

Some of the integrators for magnetic measurements used since the start of JT-60 had been unstable due to aged failures. Therefore, eight units of 75 old integrators were replaced by newly developed long-time digital integrators [1.2-3] in January 1999 to test their characteristics in the actual circumference of JT-60 operations. After the test and tuning of the new integrators for four months, the rest of the old integrators were replaced by the new ones in a short shutdown period of May 1999. According to the test and tuning results, the following improvement and correction were conducted: Input protection resistors for the analog circuit board were changed to larger ones because very high voltage was input by disruptions. Also, an initial program fault found in the ROM for controlling the direction of plasma current was corrected. Currently, all of the integrators are operating well with low drift and good linearity performance. In addition, a disruption free integrator, which has such a sufficient dynamic range as to operate throughout a shot without saturation even when large disruptions occur, is now under development.

References

- [1.2-1] Kurihara K., Kawamata Y., Akiba K., et al., Nucl. Sci., **47** 205 (2000).
- [1.2-2] Kurihara, K., "A New Shape Reproduction Method Based on the Cauchy-condition Surface for Real-time Tokamak Reactor Control", to be published in Fusion Eng. Des.
- [1.2-3] Kurihara, K., Kawamata, Y., "Development of a Precise Long Time Digital Integrator for Magnetic Measurements in a Tokamak," Proc. of 17th Symposium on Fusion. Engineering, San Diego, 1997.

1.3 Power Supply System

1.3.1 Replacement of Filter Capacitors for Three Motor-generator Sets

One of the capacitors in the harmonic filters of the toroidal magnetic field coil power supply burnt out in June 1998. The cause of the fault was carefully investigated and was concluded as a synergetic effect of aged deterioration of the insulator in the capacitor and the load of repeated transient high voltage owing to the connection and disconnection of switches. Therefore, it was determined that the old capacitors connected to 18 kV or 11 kV AC line should be replaced to new ones step by step, and the replacement started in 1998. The replacement completed in May 1999 by replacing the remaining ten capacitors of the filter capacitors for three motor-generator sets.

1.3.2 Replacement of Battery of Uninterruptible Power Supply

The lifetime of the battery used in the uninterruptible power supply (UPS) is usually from 5 to 7 years. However, the battery of JT-60 UPS had been used for 9 years. Therefore, half of the batteries in the AC UPS (HS-2500E, 165 units) and all of the batteries in the DC UPS (HS-500E, 102 units) were replaced with new ones.

1.3.3 Development of Forced Air-cooling VCB

A forced air-cooling VCB (Fig. I.1.3-1) has been developed as a backup switch at the pulse operation of the ITER superconducting center solenoid coil (CS coil). The developed VCB is constructed with three parallel connection of vacuum valves and has a continuous current rating of 36 kA DC. The power test was successfully performed, but the current interruption test was postponed because of the limitation of the test facilities [1.3-1]. This VCB was installed to the JT-60 poloidal field power supply as a backup switch for the pulse operation test of ITER CS model coil.

1.3.4 Preparations for Pulse Operation Test for ITER-CS Model Coil

The pulse operation test of the ITER CS model coil is one of the highlights of ITER R&Ds, and is planned in May 2000 using the JT-60 poloidal field power supply. Therefore, safety measures such as installations of a higher ground resistor of 10 ohm and a backup switch (forced air-cooling VCB) for the protection make-switch were performed for this test [1.3-2].

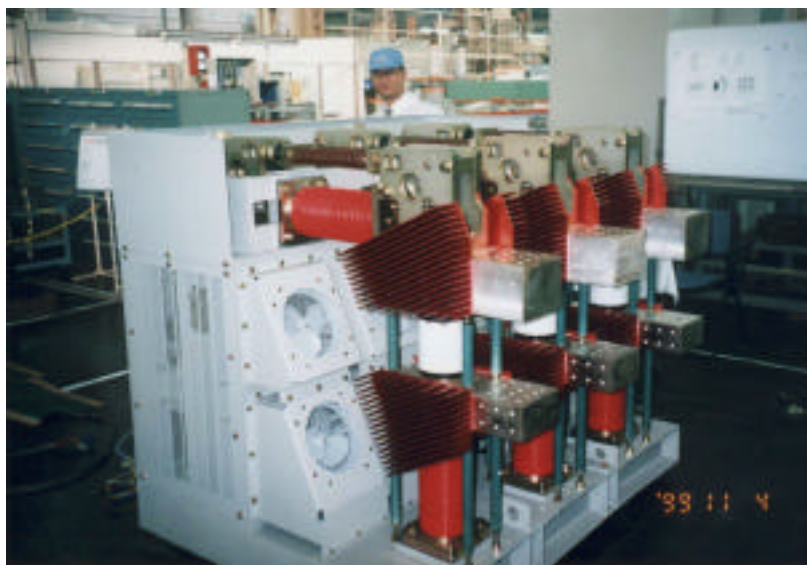


Fig. I.1.3-1. A photograph from back side of the forced air-cooling VCB.
The total performances are 12 kV and 36 kA DC.

References

- [1.3-1] Matsukawa M., Miura Y. M., Terakado T., et al., "Development of a Vacuum Switch Carrying a Continuous Current of 36 kA DC," to be published in Proc. of 19th International Symposium on Discharges and Electrical Insulation in Vacuum, China, 2000.
- [1.3-2] Matsukawa M., Miura Y. M., Terakado T., et al., IEEE Trans. on Appl. Supercond., **10**, 1410 (2000).

1.4 Neutral Beam Injection System

The positive ion based NBI system, which comprises fourteen beam-line units, injected a deuterium neutral beam power of around 25 MW at 90 keV for 9 sec in maximum with 11 beam-

lines. The rest of beam-lines (3 units) was used as the evacuation system for JT-60 W-shape divertor region using beam-line cryopumps. The cryopump is able to evacuate not only deuterium gas but also helium gas by argon gas trapping method. The divertor evacuation has contributed to the study of divertor physics and demonstration of helium ash exhaust.

Concerning the negative ion based NBI system, there are some issues of the ion sources and power supplies which have to be solved for increasing furthermore the beam power. The most important issue is source plasma non-uniformity in the arc chamber, which causes a bad beam divergence by a perveance mismatching of the accelerated beam. The bad beam divergence gives rise to a higher heat load onto the accelerator grids as much as more than 40%. As countermeasures against the source plasma non-uniformity, a few attempts to improve have been made. One is to change an arc current spatial distribution by regulating the arc current resistor which is connected in series to each of the eight filament groups. The second is to change the filament temperature for optimizing arc discharge mode since the alteration of arc discharge mode between emission limit and space charge limit seems to affect the source plasma uniformity. The third is removing a bad uniformity plasma region to minimize the grid heat load by masking at the both edges of the plasma grid. As a preliminary result, the acceleration efficiency, defined by ratio of negative ion current to acceleration drain current, went up by 10% from 0.65 to 0.72, and the injection power into JT-60 plasma has begun increasing as shown in Fig.I.1.4-1.

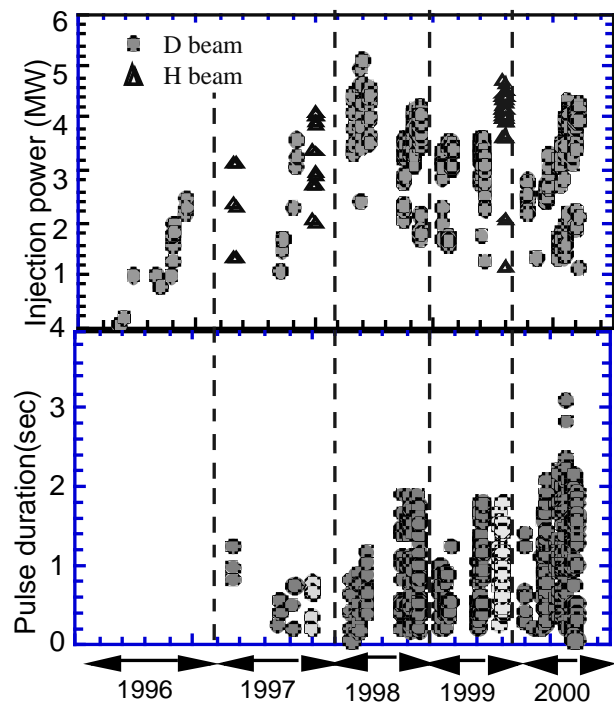


Fig. I.1.4-1 Time evolution of the injection power and beam duration time on the negative ion based NBI

1.5 Radio-frequency Heating System

1.5.1 ICRF System

The frequency of ion cyclotron range of frequencies (ICRF) heating system was changed from 102 MHz to 112 MHz in order to obtain better antenna-plasma coupling resulting in higher coupled power, and to enable effective combined experiments with 110 GHz electron cyclotron heating (ECH). The initial experiments at the new frequency showed improvement in the coupling resistance by 40 - 70%, because the frequency is closer to 120 MHz which is the center of the frequency range of the antenna. A first test of the feedback control of the separatrix-antenna gap, δ_0 , was performed. It precisely controlled the δ_0 of the ICRF configuration as shown

in Fig.I.1.5-1. Antenna coupling resistance, R_c , reasonably responded to the step like scan of δ_0 . Reflected power, P_{ref} , was kept small with frequency feedback control (Δf). To keep δ_0 is quite effective to couple stable ICRF power to the plasma. It is expected that the control improve the ICRF heating of the plasma that tends to change the separatrix position, i.e., reversed magnetic shear plasma.

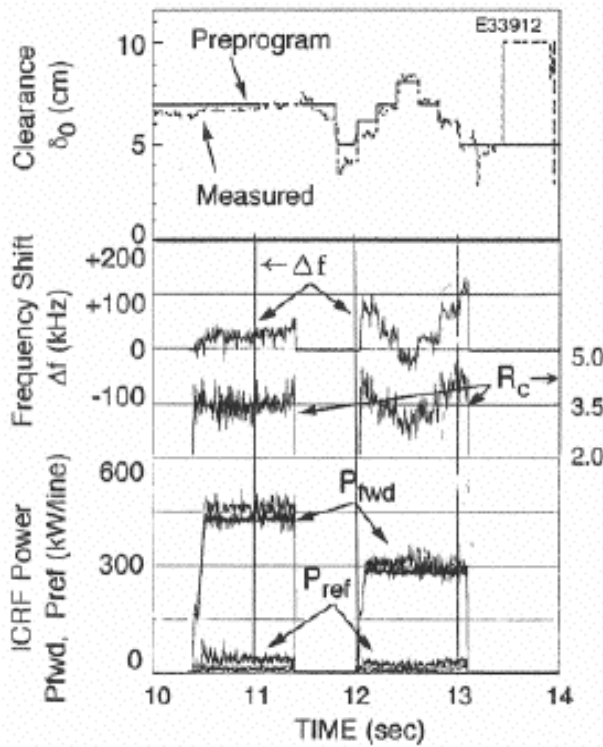


Fig.I.1.5-1 Feedback control of the separatrix-antenna gap controlled the δ_0 of the ICRF configuration.

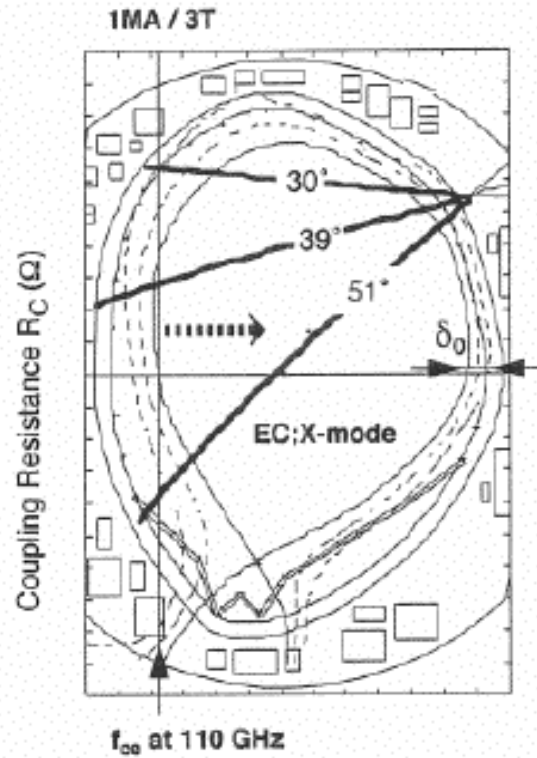


Fig. I.1.5-2 EC beam angles in combined LH and EC heating. The resonant position shifts to the lower field side due to Doppler-shift and relativistic effects.

1.5.2 LHRF System

The Lower Hybrid Range of Frequencies (LHRF) system was operated for the experiments concerning on 1) forming higher electron temperature, 2) maintaining negative shear plasmas, 3) controlling a plasma current profile. Typical injection powers with negative shear plasmas were 1.5 MW – 5 sec / 2 MW - 2 sec and 1 MW - 2 sec from A- and C-antennas, respectively. Better coupling was obtained with these antennas settled even behind from the first wall up to ~13 mm for negative shear plasmas compared with normal shear plasmas. The current profile control was performed changing $N_{||}$ spectrum launched from the LH antennas up to now. On the other hand in this campaign, the profile control was tried by changing the LH driven current by electron cyclotron (EC) beams injected with different angles as shown in Fig. I.1.5-2. For example, if the

resonance condition satisfies at the central part, the enhanced energetic electrons lead a peaking current profile. Here Doppler-shift and relativistic effects must be considered on the resonance condition. The EC beam angle was changed as 30, 39 and 51 degrees in the poloidal direction. The EC power was ~ 700 kW of X-mode at 110 GHz, and the LH power was ~ 1000 kW at 2 GHz. Plasma current was 1 MA and toroidal magnetic field was 3 T at center. Internal inductance l_i remarkably decreased at the 39-degree case. This suggests that current profile become flat by EC injection during LH injection. Hard x-ray profiles observed are consistent with the behavior in l_i . Therefore, it was shown that the current profile could be controlled by changing the EC beam angle under the fixed spectrum of LH power.

The 110 GHz 1 MW Electron Cyclotron Range of Frequencies (ECRF) system was designed and constructed on JT-60U to locally heat and control plasmas. The gyrotron has a diamond window to transmit RF power with Gaussian mode that is easily transformed to HE_{11} mode for the transmission line of corrugated waveguides. The other diamond window is installed at the inlet of the antenna for a vacuum seal between the transmission line and the JT-60U. The total length of the transmission line from the gyrotron to the antenna is about 60 m including

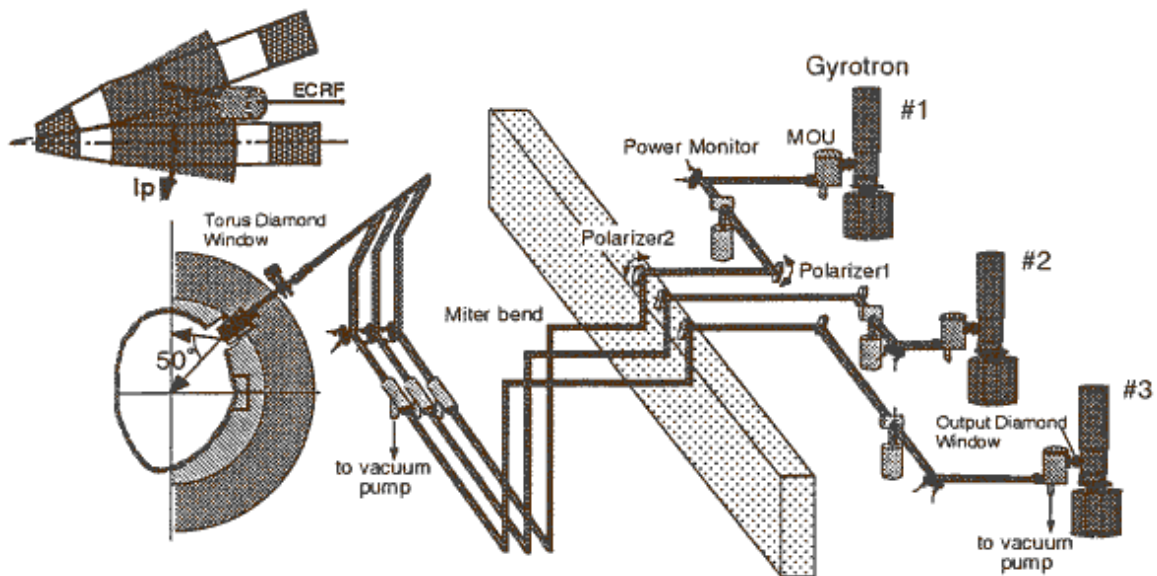


Fig.I.1.5-3 Overview of a 3 MW ECRF system for JT-60

nine miter bends. The antenna has a focusing mirror and a flat steerable one to focus and to control the RF beam angle mainly in the poloidal direction. In the initial operation, the power of $P_{EC} \sim 0.75$ MW for 2 sec was successfully injected into plasma when the gyrotron generated power up to 1 MW. The total transmission efficiency from the gyrotron to the plasma was about 75%. A controllability of local electron heating with the deposition width of ≤ 15 cm was well demonstrated by using the steerable mirror. Strong central electron heating was obtained from 2.2 keV to 6.6 keV for $P_{EC} \sim 0.75$ MW, 0.3 sec at the optimized polarization [1.5-1, 2]. On the basis of the successful operation of the first ECRF line, two lines have been newly installed on

the JT-60U ECRF system at the end of March 2000 as shown in Fig. I.1.5-3.

References

- [1.5-1] Ikeda Y. et al., Proc. Of IAEA Tech. Com. Meeting on ECRH Phys. and Tech. for Fusion Devices and 11th Joint Workshop on ECE and ECRH (EC-11) (1999).
- [1.5-2] Shinozaki S. et al., Proc. of 18th Symposium on Fusion Engineering (1999).

1.6 Diagnostics System

1.6.1 Bolometer Tomography [1.6-1]

The in-vessel bolometer cameras were recently made operational by improving the electrical and thermal insulation of the sensors during the last two years. The modifications include adding a 3 mm thick ceramic plate at the windows, replacing the first collimator with small apertures and a grounded point for the vacuum feed-through flange. The small apertures of the in-vessel cameras enable detailed radiation profile measurements. Those hardware improvements of in-vessel divertor bolometer cameras to withstand severe electrical and thermal loads and the development of tomography software have made more detailed visual studies of divertor radiation possible. Line integrated bolometer signals of 48 total sight lines are successfully mapped onto the JT-60U divertor geometry indicating characteristic profiles for tokamak operational regimes. Tomographic analysis was confirmed to be consistent with an independent measurement of the radiating layer width at the target plate.

1.6.2 Development of O-mode Reflectometer for Density Fluctuation Measurement

The X-mode core correlation reflectometer successfully measured the decay length of density fluctuations. The frequency range of the system is optimized for toroidal magnetic field, B_T , from 3.3 to 4.0 T and a typical density profile. Therefore, the system can not measure in lower B_T discharges due to disappearance of a cut-off layer. On the other hand, in the case of O-mode propagation, the cut-off layer depends only on the electron density. In order to measure various case of plasma configurations, 3ch O-mode reflectometer has been designed for density fluctuation measurement to complement X-mode system. The targets of O-mode reflectometer are the change of fluctuation level and correlation during formation of the transport barrier, L-H and H-L transition, ELM and MARFE activity and so on. These targets are varying from edge to core plasma region. To cover these region, we chose 3 frequencies, 34 GHz fixed, 34 to 40 GHz selectable and 50 GHz fixed, which correspond to the cut-off density of 1.43 , $1.43 - 1.98$ and $3.10 \times 10^{19} \text{ m}^{-3}$, respectively. The 50 GHz reflectometer is scheduled to be constructed in July 2000.

1.6.3 Visible Spectrometer with Spatial Resolution for Divertor Plasma

A new visible spectrometer has been installed in order to investigate atomic and molecular processes in divertor plasmas such as divertor detachment possibly caused by plasma

recombination. The system has 16 viewing-codes to cover the divertor region with spatial resolution of about 3 cm. The maximum time resolution is about 5 mseconds by using a frame transfer CCD detector. The wavelength resolution is possible to change from 0.054 nm to 1.25 nm flexibly with 3 different gratings at the wavelength of 546 nm and the slit width of 30 μm .

1.6.4 Development of Collective Thomson Scattering Based on Pulsed CO₂ Laser [1.6-2]

Collective Thomson Scattering (CTS) measurement in JT-60U has been developed to measure the ion temperature using pulsed CO₂ laser, and to demonstrate alpha particle measurement for ITER. In FY 1999, the laser guide tube and optical system were installed in the torus hall and all of the CTS system installation has been finished. The incidence of the CO₂ laser was started. The ion temperature measurement in comparison with the result of the charge exchange recombination spectroscopy measurement and the detection of fast ions in NNB heated plasma will be carried out in FY2000.

1.6.5 The 24-channel Heterodyne Radiometer System

In JT-60U, the heterodyne radiometer system is mainly used for the measurement of the structure of electron temperature perturbations. In FY 1999, the number of channels was doubled to 24 by adding a new heterodyne radiometer. By using this system, ECE ranging from 176 to 200 GHz can be measured. It means that the measurable space is about 40 cm with the spatial resolution of about 2 cm. The system made it possible to measure the formation process of internal transport barrier in the electron temperature and to find the precise position and amplitude of MHD instability.

1.6.6 Increasing of the YAG Laser Repetition Rate

In the improvement of performance for YAG laser Thomson scattering system, the laser repetition rate was increased from 20 Hz to 30 Hz. Increasing the repetition rate with high-gain amplification, the thermal gradients in the Nd-YAG rods cause stress induced birefringence, which leads to depolarization and energy loss in the output pulse. However, the laser repetition rate could be achieved up to 30 Hz with the conventional energy (2 J) by optimizing the compensation optics. Thus, time evolution of electron temperature and density profiles that were changed every moment (i.e. formation status of internal transport barrier (ITB) in the negative magnetic shear plasma) became measurable with higher time resolution.

1.6.7 Calibration Improvement on Infrared Laser Polarimeter [1.6-3]

The infrared laser polarimeter has been operated for electron density measurement based on the tangential Faraday rotation diagnostic in tokamak plasma. It is remarkable that polarimetry is pretty reliable in comparison with interferometry. The polarimeter system has two

CO₂ laser polarimeters with different laser wavelength of 10.6 and 9.27 μm. Such a dual CO₂ combination enables not only independent density measurement with each wavelength but also the two-color polarimetry with the elimination of Faraday rotation component at vacuum windows. For system calibration, a polarizer plate which is temporary inserted into the probing laser path is used to provide preset polarization angles. While the 9.27 μm polarimeter was usually well calibrated, it was difficult to calibrate the 10.6 μm polarimeter because serious non-linearity of its detected signal was observed and an angle step of the polarizer on manually rotating stage was poor. In order to improve the calibration accuracy, a rotating stage system that is controlled by a workstation computer has been applied in FY 1999. By use of this new calibration tool, electron density diagnostics has been successful by the two independent polarimeters and also by the combination of two polarimeters.

References

- [1.6-1] Konoshima S., Leonard A. W., et al., to be submitted to Plasma Physics and Controlled Fusion.
- [1.6-2] Kondoh T., et al., submitted to Review of Scientific Instruments.
- [1.6-3] Kawano Y., Chiba S. and Inoue A., submitted to Journal of Plasma Fusion Research.

1.7 Data Analysis System

1.7.1 Data Analysis Tools, Database and Computer System

The data analysis tools for JT-60 experiment database have been updated. Some new diagnostic data related to the real time plasma control feedback loop are included in the data illustration system (DAISY) such as the gradient of electron temperature, the electron density in divertor region. Also the shot number selection facilities of DAISY have been improved for easier use. The software for displaying and manipulating a time slice of various plasma quantities, SLICE, now incorporates a ray tracing calculation of ECRF (electron cyclotron range of frequencies). The available fitting functions of SLICE are also extended. The impurity density profile is estimated in SLICE by using the impurity radiation intensity measured by the charge exchange recombination spectroscopy. The 1.5 dimensional tokamak prediction and interpretation code system, TOPICS, has been revised in accordance with the progress of JT-60U experiments. The D-He³ fusion reaction rate is calculated by TOPICS. The subroutines of 2D Fokker-Planck equation, the neoclassical transport and so forth in TOPICS have been updated. The experimental logbook system, FELLOW, now produces an index of discharges with major plasma parameters along with waveform files in a PDF format. The fast plasma-boundary identification code (FBI) can now make use of the alternate diagnostic data from different channels when the primary data are not available.

The JT-60 experimental database has enriched the content. Appropriately for the update of data analysis of diagnostic data, such as MSE (motional Stark effect) diagnostics, these analyzed data have been added to the experimental database. Plasma equilibrium data calculated with

MSE diagnostics have also been added to the database.

Some subsystems of the JT-60 data processing system have been improved according to the demands of plasma diagnostic subsystems and the JT-60 control system by utilizing the progress of the computer and network technology. TMDS (transient mass data storage system) composed of a mini-computer with bulk memory boards has been replaced by workstations with VMEbus memory modules. These workstations are connected with the main computer ISP (inter-shot processor) of Fujitsu GS8300 and the UNIX file server, which has a capacity of ~100 GB RAID disks and ~900 GB MO (magneto-optical disk) auto-exchangers, via the gigabit ethernet switch to cope with the increase of data transfer. Aged ACM-A (auxiliary crate controller with microprocessor type A) in one of diagnostic subsystems has been replaced by a workstation with a VMEbus byte serial highway driver, based on the technologies used in new CICU (CAMAC interface control unit).

The communication method of the JT-60 experimental sequence using a special link between ISP and the JT-60 control system has been changed to network connection by introducing a relaying workstation. The ways of data exchanges via CAMAC serial highways between a communication computer and the JT-60 control system has been also changed to network connection. In RTP (real time processor), reflective memories has been introduced to send processed diagnostic data to the feedback computer of the JT-60 control system in real time, which have drastically shorten a data transfer time compared with former time-consuming communication using CAMAC memory modules

1.7.2 FAME System

By utilizing a high speed 7 CPUs parallel computer IBM RS/6000 SP (the maximum theoretical speed of 3.42 GFLOPS and the large capacity of the data storage of 50 GB), the Fast Analyzer for MHD Equilibrium system (FAME) has been successfully providing MHD equilibria of 2095 JT-60U tokamak discharges in last year. The MHD reconstruction of each discharge within a shot interval consists of about 130 equilibria in time series being enough for the non-stationary analysis of the experimental data of JT-60U. After tuning up the SELENE and FBI codes on FAME parallel computing system, the computational performance becomes more than 3 times faster than the original system (FAME-1). Additionally, a direct data transfer from the ZENKEI control system have made the waiting time after shot, typically ~ 11 min in past, much shorter as ~ 6 min. An equilibrium animating system arranged in the central control room also enabled to provide animations of MHD equilibrium analyzed by the FAME, incorporated with SLICE.

1.7.3 Data Link System and Remote Participation in JT-60 Experiments

The remote participation in JT-60 experiments from PPPL and GA has been carried out by

utilizing the Data Link System and the video conference systems. The Data Link System provides standard JT-60 data analysis tools: DAISY, FBI, EQREAD (MHD equilibrium display code), and SLICE. Participants from both JAERI and PPPL/GA jointly analyzed and discussed the JT-60 data together.

Eight projects have started as remote collaboration under the Cooperation among the Three Large Tokamak Facilities and the Japan-US Cooperation on Fusion Research and Development. These eight projects cover a wide range of research topics and the total number of participants amounts to more than one hundred.

2. Experimental Results and Analysis

2.1 Sustainment of High Performance and Non-inductive Current Drive

2.1.1 Sustainment of High Fusion Performance in High Current Reversed Shear Plasmas

Efforts to sustain high fusion performance in high current reversed shear (RS) plasmas were attempted. Trials for sustaining an H-mode edge and those for passing through q_{\min} (minimum value of q) = 2 were done but they need more adjustments. Through optimization of the evolution of plasma beta by using the stored energy feedback control, we were successful to sustain DT-equivalent fusion power gain $Q_{\text{DT}}^{\text{eq}} \sim 0.5$ quasi-stationarily for 0.8 sec or nearly equal to the energy confinement time in a 2.4 MA RS discharge with an L-mode edge [2.1-1]. Other typical parameters are β_{N} (normalized beta) = 1.1 - 1.2, $H_{89} = 2.5 - 2.7$, $HH_{98y2} \sim 1.4$, $T_i(0) = 12 - 14$ keV, $n_{\text{D}}(0)\tau_{\text{E}}T_i(0) \sim 4 \times 10^{20} \text{ m}^{-3} \cdot \text{keV} \cdot \text{s}$, $B_{\text{T}} = 4.35$ T, $q_{95} = 3.4$, $\kappa(\text{elongation}) = 1.84$ and $\delta(\text{triangularity}) \sim 0.05$. Here H_{89} denotes the confinement enhancement factor to the L-mode scaling while HH_{98y2} denotes the confinement enhancement factor to the ELMy H-mode scaling. The sustained performance in $P_{\text{DT}}^{\text{eq}} / P_{\text{NB}}^{\text{abs}}$ ($P_{\text{DT}}^{\text{eq}}$ denotes DT-equivalent fusion power and $P_{\text{NB}}^{\text{abs}}$ denotes the absorbed neutral beam power) was improved significantly compared to the previous higher $Q_{\text{DT}}^{\text{eq}} (\sim 1)$ discharges; the duration for $P_{\text{DT}}^{\text{eq}} / P_{\text{NB}}^{\text{abs}} > 0.45$ was extended 0.5 sec to 0.85 sec.

2.1.2 Quasi Steady Reversed Shear Plasmas with High Bootstrap Current Fraction and High Confinement

A quasi-steady RS plasma accompanying internal transport barriers (ITBs) with a large fraction ($\sim 80\%$) of bootstrap current was realized under full non-inductive current drive condition [2.1-2]. This result demonstrates the basic scenario for steady state operation of advanced tokamak. Waveforms of this discharge are shown in Fig. I.2.1-1. High confinement and high beta were sustained for 6 times the energy confinement time τ_{E} ; $\tau_{\text{E}} = 0.4 - 0.5$ sec, $\beta_{\text{N}} = 1.9 - 2.2$, $\beta_{\text{p}} = 2.6 - 3.2$, $H_{89} = 3.3 - 3.8$ and $HH_{98y2} = 2.1 - 2.3$ sustained for 2.7 sec in a plasma with $B_{\text{T}} = 3.4$ T, $I_{\text{p}} = 0.8$ MA, $q_{95} \sim 9$, $\kappa \sim 1.5$ and $\delta \sim 0.4$. The density, temperature and q profiles were also sustained stationarily with large radii ($\sim 65\%$ of plasma minor radius) of ITB and q_{\min} . Full

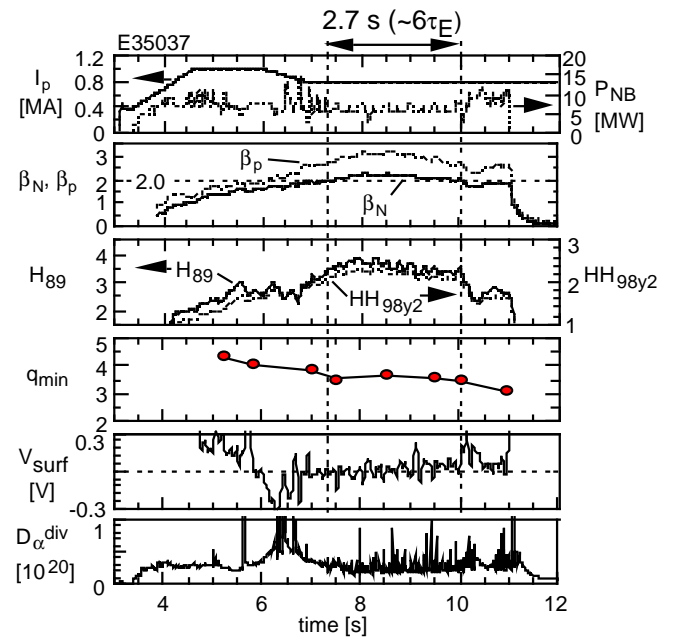


Fig. I.2.1-1. Waveforms of a RS plasma in which high confinement and high bootstrap current fraction were sustained for 2.7 s. From the top, plasma current (I_{p}) and NBI power (P_{NB}), β_{p} (dotted line) and β_{N} (solid line), H_{89} (solid line) and HH_{98y2} (dotted line), q_{\min} , surface loop voltage V_{surf} deuterium recycling emission at the divertor.

non-inductive current drive was achieved with large fraction of bootstrap current together with beam driven current (~25% of plasma current) by tangential beams. The sustainment of large radius of q_{\min} was attained only in high β_p discharges, which indicates the role of bootstrap current for preventing the shrinkage of radius of q_{\min} and for the sustainment of current profile.

2.1.3 Sustainment of High Beta RS Plasmas by LHCD

In 1998, an RS plasma with $\beta_N \sim 0.9$ accompanying ITBs was successfully maintained in a quasi-steady state. Almost all plasma currents were sustained non-inductively by the lower hybrid (LH) driven current (~77%) and the bootstrap current (~23%) [2.1-3]. Efforts to sustain higher beta RS plasma by LHCD were done in FY 1999. Higher β_N was pursued by simply raising neutral beam power. Feedback control of the distance between the plasma surface and the first wall of the vessel in the low-field side was employed in this campaign, which was found very effective to keep the efficient coupling of LH wave to the plasma. As a result, $\beta_N > 1.5$ was sustained for 1 sec with $I_p = 0.85$ MA, $B_T = 2.0$ T and $q_{95} \sim 4.4$.

2.1.4 Extension of High Integrated Performance Regime with High Current Drive Efficiency of NNB [2.1-1]

With application of the negative ion based neutral beam (NNB) injection, the regime of high β_p H-mode plasmas with a high fraction of non-inductive current drive, high β_N and high confinement was expanded toward a higher plasma current regime.

A nearly full-CD with $\beta_N = 2.4$ and $H_{89} = 2.56$ was obtained in a high β_p H-mode plasma with $I_p = 1.5$ MA, $B_T = 3.7$ T, $q_{95} = 4.2$, $\kappa = 1.6$ and $\delta = 0.35$. NNB (360 keV, 3.4 MW) and co-tangential positive ion based neutral beam (85 keV, 4.1 MW) were injected for current drive. According to the ACCOME code, the total beam driven current was 670 kA including 410 kA by NNB and the bootstrap current was 710 kA. In total, the calculated non-inductive driven current was 92% of the plasma current. Figure I.2.1-2 shows that the current drive efficiency η_{CD} of NNB is increasing with central electron temperature and the value for the above discharge is 1.3×10^{19} A/W/m². This is the highest efficiency in the neutral beam current drive in the world.

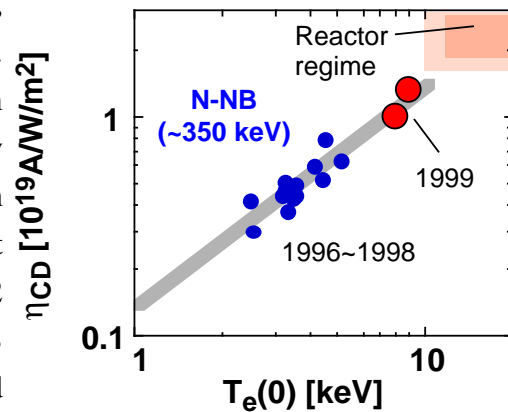


Fig. I-2.1-2. The current drive efficiency η_{CD} of NNB increasing with the central electron temperature $T_e(0)$. The highest value reached 1.3×10^{19} A/W/m².

2.1.5 Current Drive by LH and EC

An EC wave injection system was installed in FY1999 for local heating and current drive

[2.1-4]. The system has one gyrotron, which is designed to generate 1 MW for 5 sec. The torus injection power was ~0.75 MW. Two more gyrotrons are planned to be installed in FY 2000. In FY 1999, preliminary experiments on EC current drive were done and changes in MSE (motional Stark effect diagnostics) pitch angles were observed during EC wave injection into a low density plasma. The current profile control by combination of LH and EC injection was also attempted. It was found that the injected EC wave coupled to the LH-driven electrons via resonance condition with Doppler effect and relativistic effect, and that the LH-driven current profile could be changed by EC injection angle. To optimize the direction of EC wave for driving a current with maximum current density at the aimed position, the numerical evaluation by the full relativistic adjoint method is fully operational [2.1-5].

References

- [2.1-1] Kamada Y. and the JT-60 team, Plasma Phys. Control. Fusion, **41** B77 (1999).
- [2.1-2] Fujita T. and the JT-60 team, to be published in J. Plasma and Fusion Res.
- [2.1-3] Ide S., Naito O., Oikawa T., et al., Nucl. Fusion, **40** 445 (2000).
- [2.1-4] Ikeda Y et al., to be published in Fusion Eng. Design.
- [2.1-5] Hamamatsu K., Fukuyama A., Joint Meeting of IAEA Technical Committee Meeting on ECRH Physics and Technology for Fusion Devices and The 11th Joint Workshop on Electron Emission and Electron Cyclotron Resonance Heating, (1999).

2.2 Physics of Plasma Confinement

2.2.1 Reduction of L-H Transition Threshold Power under the W-shaped Pumped Divertor Geometry [2.2-1]

Remarkable reduction of the L-H threshold power was documented in JT-60U under the W-shaped pumped divertor geometry, in comparison with the results of previous open divertor. The range of density was extended to $0.6n_{\text{GWL}} (= I_p / \pi a^2)$, and apparently stronger than linear density dependence was found at high density. Accordingly, the threshold power scaling has been re-established in the international database group and modified to the form.

$$P_{\text{th}} = 3.24 B_T^{0.75} n_{20}^{0.6} R^{0.98} a^{0.81} M^{-1}. \quad (1)$$

The prediction interval was reduced to 32 MW for ITER-FEAT, whereas the previous scaling (2), for which the open divertor results were consistent with, provides 57 MW.

$$P_{\text{th}} = 0.45 B_T^{0.75} n_{20}^{0.75} R^2 \times (0.6 n_{20} R^2)^{\pm 0.25}. \quad (2)$$

However, the new scaling (1) considers the JT-60U results as a scatter and is not concerned with the strong density dependence stated above. If it were to be included, the scaling takes the form

$$P_{\text{th}} = 9.46 \times 10^{-3} B_T n_{19}^{1.25} R^3, \quad (3)$$

and it predicts 93 MW for ITER-FEAT. Here, the regression analysis was performed only with the JT-60U database to derive the scaling (3), where the reduction of edge temperature as well as

the nonlinear increase of edge density at high density was also observed. Although the scalings (2) and (3) show substantially different density exponents, the threshold power exhibit similar dependence on n_e^{95} , regardless of the divertor geometry. Therefore, it is suggested to elaborate a scaling with n_e^{95} .

The effect of divertor geometry on the L-H transition threshold power, which has long been an issue of controversy, was investigated to the detail with emphasis on edge plasma quantities, including the poloidal distribution of neutrals. The reason why the neutrals are emphasized is that atomic processes cannot be ignored to understand the L-H transition at the plasma edge, especially at a high density, where a large amount of fuel gas is supplied from the outside.

The performed neutral particle density analysis with DEGAS indicates that at lower n_e^{95} , neutral penetration length becomes larger, and its negative contribution to the threshold power can be predominant. Namely, the edge ion collisionality (v^{*95}) defined at right before the L-H transition is slightly reduced, partly owing to the reduction of Z_{eff} in the W-shaped divertor. However, due to the decrease of edge density and consequent increased heating efficiency, the power threshold is notably reduced. At medium to high density region, however, n_0^{95} near the X-point in the W-shaped divertor is substantially larger than that of the open divertor. On the other hand, v^{*95} is near unity, whilst it is much lower in the open divertor, although the high density data is scarce for the open divertor. It indicates that the negative contribution of the edge neutral particles, related to the charge exchange friction loss, disappears with an increase of density, which might be ascribed to the scattering model of trapped ions outside the separatrix near the X-point. Here, it should be noted that n_0^{95} at the midplane for the W-shaped divertor is approximately 60% of that of the open divertor. Further indications is that the value of v^{*95} starts to decrease at high density close to the Greenwald limit, which may be indicative of the fact that the negative influence of the edge neutrals near the midplane or inside the separatrix is taking over the scattering effect near the X-point. Thus, the negative CX and positive scattering effects of neutral particles compete with each other in different density range and contribute to the apparently complex dependence of the density dependence of the threshold power.

2.2.2 Degradation of Thermal Energy Confinement of ELMy H-mode Plasmas [2.2-2]

The dominant causes of the degradation of thermal energy confinement with an increase in plasma density were analyzed in JT-60U ELMy H-mode plasmas. As density is raised the energy stored in the pedestal remains almost constant because of the destabilization of type-I ELMs, while the core component also tends to be constant. The enhancement factor of the core confinement remarkably decreases with density. The reduction in the pedestal temperature due to strong gas puffing seems to bring about an increase in the effective thermal conductivity for the core plasma. On the other hand, as shown in Fig. I.2.2-1, a continuous increase of the core

enhancement factor based on the offset nonlinear, H (ONL-Core), scaling was observed with increase in pedestal ion temperature, T_i^{ped} . Therefore an increase in the energy stored in the pedestal plasma due to high triangularity is expected to produce thermally improved energy confinement performance even at a high density in JT-60U.

2.2.3 Comparison of Edge Pedestal Parameters between JT-60U and DIII-D H-mode Plasmas [2.2-3]

Edge pedestal parameters (pedestal temperature and density, pedestal width) between JT-60U and DIII-D are studied. For the discharges used in the study, the JT-60U H-mode operation space is in the high edge ion temperature and low edge electron density region, whereas DIII-D discharges have higher edge electron density and lower electron temperature. A new pedestal width scaling for T_e and T_i based on this study of the two machines is proposed. The new scaling includes normalized poloidal gyroradius and Greenwald density: $\Delta \propto a \rho^{*0.4} n_{G*}^{0.3} \kappa^{-1.5}$. The result of the comparison of these scalings is that the new scaling and $\Delta / R \propto (\beta_p^{\text{PED}})^{0.4}$ are well fitted and the fitting errors are almost the same as experimental error.

2.2.4 On Threshold Power for ITB Formation in JT-60U RS Plasmas [2.2-4]

On JT-60U, the dependence of power required to form an ITB in a RS plasma (P_{th}) on B_t was investigated. In the experiments the NB power was scanned during the I_p ramp-up phase at different B_t with other parameters, including I_p , and the plasma configuration as fixed as possible. The experiment was carried out both in deuterium and hydrogen plasmas with the same configuration and operational scenario but with different density. The experimental results show that the minimum absorbed power required ITBs to form is almost independent to B_t , in both the deuterium and hydrogen discharges. Further investigation on ITB formation will be continued, concerning other parameters.

2.2.5 Confinement Improvement in Region of $T_e > T_i$ in JT-60U [2.2-4]

Towards the study of improved confinement with internal transport barriers (ITBs) in reactor relevant plasmas, that is conditions under electron heating dominant and low central fueling, operational regime of JT-60U improved confinement plasmas has been tried to extend. By utilizing LHRF and ECRF system, the region of RS plasma operation, mainly hydrogen discharges, has been extended up to T_e / T_i in the plasma core region $\leq \sim 2$. Confinement improvement factor of about 1.8 was found to be maintained in the regime. The ITBs were

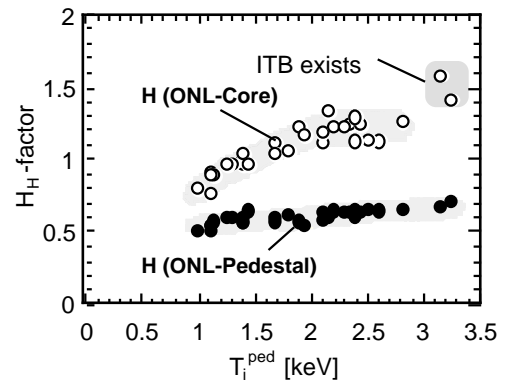


Fig.I.2.2-1 Dependence of H (ONL-Core) and H (ONL-pedestal) on T_i^{ped} in type-I ELMy H-mode plasmas.

confirmed to be maintained even in such a regime, which is encouraging toward fusion plasma research.

2.2.6 Location of Internal Transport Barrier

The safety factor value and profile affect the internal transport barrier formation and propagation in the core improved confinement plasmas. The ITB firstly appeared in a core region and then moved outward and final location of the ITB stagnated near the location of minimum magnetic shear in the reversed shear plasmas. However the reduced gradients of T_i seem to allow that location of ITB foot became greater than the location of minimum magnetic shear. These results suggest that the outward propagation of the ITB is limited by increasing instability drive such as high n ballooning mode when the local gradient at the ITB foot goes to positive shear region across the q_{\min} surface.

2.2.7 Correlation Measurement during ITB Degradation by Minor Collapse in JT-60U Reversed Shear Plasma [2.2-5]

By using an X-mode reflectometer, radial correlation measurement in the ITB region have been performed for the first time during ITB degradation phase in JT-60U reversed shear plasma. The correlation is that of the complex amplitude of the reflectometer signal for frequencies with highest correlation with higher than 10 kHz. The measured correlation is fit by an exponential function, $\exp(-\delta r / \Delta L)$. The radial decay length, ΔL , which can scale with the correlation length, increased from 12 mm to 62 mm for E32845, which suggests that the density correlation length significantly increases after the minor collapse. Therefore, in the case of an abrupt degradation with a minor collapse, the relaxation of ITB correlates with the enhancement of the radial correlation length of the electron density fluctuations.

References

- [2.2-1] Fukuda T., et al., Plasma Phys. Control. Fusion. **42** A289 (2000).
- [2.2-2] Urano H. et al., to be published in Plasma Phys. Control. Fusion (2000).
- [2.2-3] Hatae T. et al., Plasma Phys. Control. Fusion, **42** A283 (2000).
- [2.2-4] Ide S. et al., Phys. Plasmas **7**, 1927 (2000).
- [2.2-5] Shinohara K., et al., Rev. Sci. Instrum., **70**, 4246 (1999).

2.3 High Energy Ions and MHD Instabilities

2.3.1 Alfvén Eigenmodes

Study of Alfvén Eigenmodes (AEs) was carried out in collaboration with Princeton Plasma Physics Laboratory. One of the main topics is understanding of instabilities with a frequency sweep in the frequency regime of AEs driven by negative-ion-based neutral beam (NNB) injection in weak magnetic shear discharges [2.3-1]. Two kinds of modes with a frequency sweep were observed after NNB injection. One is that the toroidal mode number n is one and the

frequency changes slowly around 20 kHz corresponding to the frequency inside the Alfvén continuum. The other appears as a burst-like frequency sweep in the range of ~20 kHz within 10 msec around 60 kHz corresponding to that of the toroidicity-induced AEs (TAEs). Toroidal mode number of the later one is $n = 1 - 2$. We refer to the former and later modes as slow-frequency-sweep (SFS) modes and fast-frequency-sweep (FFS) modes, respectively.

Experimental study revealed that the threshold volume-averaged hot ion beta $\langle\beta_h\rangle$ to destabilize SFS and FFS modes are between $\langle\beta_h\rangle \sim 0.07$ and 0.1 % and these modes could be destabilized by larger β_h or larger gradient of β_h than those of a continuous TAE. These modes are also found to be destabilized in the condition of $v_{b//}/v_A = 1.2 - 1.4$ ($v_{b//}$: beam velocity in the toroidal direction, v_A : the Alfvén velocity) and $\langle\beta_h\rangle \sim 0.15\%$ which is in the expected region of α particle condition (v_α/v_A ; v_α : the birth velocity of α particles) in ITER [2.3-2].

Theoretical analysis of these modes was carried out using the linear kinetic nonperturbative code “HINST”, which is able to resolve resonant branches of TAE called resonant TAE (RTAE). Calculations by HINST were in qualitative agreement with observed MHD characteristics of these modes such as the frequency region with the frequency sweep, toroidal mode number and $\beta_h(0)$ to be excited [2.3-3].

Ellipticity induced Alfvén Eigenmodes (EAEs) were also studied in ICRF heated plasmas together with TAEs. Utilizing occurring conditions of these AEs residing at well-determined safety factor, q , surfaces in the plasma core, the behavior of the q -profile in the plasma center was studied [2.3-4]. It was found that just before a sawtooth crash the central value of the q -profile, q_0 , reached values between 0.8 and 0.9, and at the crash q_0 did not usually relax back to unity. Immediately after the crash, q values from below to above unity were also found. Moreover, for sawteeth where q_0 relaxes back to above unity, a typical change in q_0 was found to be between 0.15 and 0.2.

2.3.2 Tearing Modes and Their Stabilization in Long Pulse High β_p H-mode Discharges

Characteristics of tearing modes in quasi-steady state high poloidal beta, β_p , H-mode discharge have been investigated. In FY 1999, density dependence of onset conditions of tearing modes was investigated with a fixed configuration. It was found that the onset normalized beta $\beta_N = \beta (I_p/aB)^{-1}$ (%mT/MA) is almost linearly increases with the electron density and the onset β_N normalized by the ion Larmor radius has positive dependence on collisionality ($\sim v_e^{0.36}$). In some discharges with low collisionality, no tearing mode was observed even when β_N is high enough, which suggests that tearing modes can be stable in the low collisionality region. Tearing mode stabilization experiment was performed using Electron Cyclotron Range of Frequency (ECRF) heating (ECH) and current drive (ECCD) with 0.75MW of injection power. Stabilization of tearing modes was confirmed while complete suppression was not achieved. After increase in the in injection power up to 2.3 MW in 2000, complete suppression of $m/n = 3/2$ tearing modes

was demonstrated [2.3-5].

2.3.3 Effects of ECH/ECCD on Sawteeth

After the installation of the ECRF injection system in FY 1999, effects of ECH/ECCD on sawtooth oscillations were begun to investigate [2.3-6]. It was found that sawtooth-free period was drastically extended by ECRF injection near the $q = 1$. It is also found that both ECH and ECCD contribute to the sawtooth stabilization in the case of ECRF injection near the $q = 1$ surface, while sawtooth stabilization by counter-ECCD near the magnetic axis was not observed. From these results, we may say that it is possible to control a sawtooth period by ECH/ECCD.

2.3.4 Edge Stability in H-mode Discharges

In JT-60U H-mode discharges, giant (Type I) edge localized modes (ELMs) disappear and minute grassy ELMs appeared in the operation regime such that the triangularity δ , edge safety factor q_{95} and poloidal beta β_p are high enough. Complete suppression of giant ELMs was observed at $\delta \sim 0.45$, $q_{95} \sim 6$, and $\beta_p \sim 1.6$. Giant ELMs could be suppressed at a lower q_{95} (~ 4.0) in the higher δ ($= 0.54$) discharges. In the grassy ELMy H-mode discharges, edge temperature and pressure could be higher than those in the giant ELMy ones and a favorable confinement could be sustained without increase in impurity concentration. Stability analysis based on equilibria reconstructed using the EFIT code with detailed treatment of the edge pressure and current profiles was carried out in collaboration with General Atomics. The results suggest that the edge region of the grassy ELMy plasmas is accessing to the second stability regime of infinite n ballooning modes while that of the giant ELMy plasmas is in the first regime and the stability is limited by the infinite n ballooning mode [2.3-7].

2.3.5 Stability of Reversed Shear Discharges

Stability of reversed shear discharges was studied to understand stability of tokamak operation in steady-state high bootstrap current fraction [2.3-8]. The disruptive upper limit of the normalized beta is $\beta_N \sim 2$ at $q_{\min} \sim 2$ (q_{\min} : the minimum safety factor) in discharges with the L-mode edge and is close to the stability limit against an ideal $n=1$ kink mode in the free boundary condition. Resistive MHD instabilities give rise to major collapses at the lower β_N regime than the ideal stability limit. Linear stability analysis with a two-dimensional marginal stability analysis code MARG2D [2.3-9], showed that a double tearing mode can be unstable at the $q = 3$ surface in the experimental situation, and the numerical result is not in contradiction to the experimental one. Major collapses often occur when the safety factor at the plasma surface is close to integer values, suggesting that external kink modes relate to the causal mechanism for major collapses. The numerical analysis revealed that a stable external kink mode play a destabilizing role of tearing modes in the reversed shear configuration.

2.3.6 Wall Stabilization and Resistive Wall Mode

Experimental study on stabilizing effects of the JT-60U wall and resistive wall modes (RWMs) was started on JT-60 to provide physics basis about them from a large tokamak. For this purpose, we employed plasma shapes with the large plasma volume, V_p , of 70 ~ 85 m³ such that the plasma surface is close enough to the wall to be $d/a = 1.1 \sim 1.3$ (d : wall radius, a : plasma minor radius). We employed high- β_p H-mode discharges with (weak) positive central magnetic shear and reversed shear discharges with the negative central magnetic shear to study the wall stabilization in different q -profiles. A theoretical model predicts RWMs suppression by toroidal rotation is more effective in positive magnetic shear configurations.

In the case of the high β_p H-mode discharge, $\beta_N = 3.42$ was obtained at $q_{95} = 3.4$ with $V_p = 80$ m³ and $d/a \sim 1.2$. The high beta phase was terminated after appearance of a $m/n=3/1$ mode that seemed to be locking to the wall and β_N was saturated. No clear RWM was observed while stability analysis with an assumed q profile showed that the achieved β_N is above the no-wall ideal stability limit.

In the case of reversed shear discharges, the stability limit without wall, $\beta_N^{\text{no-wall}}$, is relatively lower due to the broad current profile or the lower plasma internal inductance. Reversed shear discharges with $\beta_N > 2.4$ were obtained with the plasma shape of $V_p > 70$ m³ or $d/a < 1.3$ frequently and the highest achieved β_N was 2.8. Calculated $\beta_N^{\text{no-wall}}$ with measured pressure and q profiles was $\beta_N = 2.2$. Thus, stabilizing effects of the JT-60U wall on pressure driven low n kink modes was confirmed and reversed shear discharges with $\beta_N > \beta_N^{\text{no-wall}}$ were obtained. An $n = 1$ MHD activity with the growth rate of ~ 100 s⁻¹ $\sim 1 / \tau_{\text{wall}}$ (estimated τ_{wall} of the JT-60U wall is ~ 10 msec) and with the toroidal rotation frequency of ~ 20 Hz $\sim 1 / (2\pi\tau_{\text{wall}})$ appeared followed by disruption in the wall-stabilized high beta discharges. The MHD activity is attributed to RWM [2.3-10].

References

- [2.3-1] Kusama Y., et al., Nucl. Fusion, **39** 1837 (1999).
- [2.3-2] Shinohara K., Kusama Y., et al., to be submitted to Nucl. Fusion.
- [2.3-3] Grelenkov N.N., et al., to be submitted to Nucl. Fusion.
- [2.3-4] Kramer G.J., Cheng C.Z., Fu G.Y., et al., submitted Nucl. Fusion.
- [2.3-5] Isayama A., Kamada Y., et al., to be submitted to Nucl. Fusion.
- [2.3-5] Ikeda Y., Ide S., Suzuki T., et al., to be submitted to Nucl. Fusion.
- [2.3-7] Kamada Y., et al., Plasma Phys. Control. Fusion, **42** A247 (2000).
- [2.3-8] Takeji S., Tokuda S., Fujita T. et al., J. Plasma and Fusion Res., **76** 575 (2000).
- [2.3-9] Tokuda S., Watanabe T., Phys. Plasmas, **6** 3012 (1999).
- [2.3-10] Takeji S., Fujita T., Tokuda S., et al., to be submitted to Nucl. Fusion.

2.4 Plasma Control and Disruption

The recent development of the real time feedback control is more focused on the control of local quantities for the improvement of global stability or confinement. In order to maximize the efficiency of the experiment and prepare for the advanced plasma control in fusion reactors,

several tools of the real time feedback control were additionally developed and designed. On the basis of developed feedback control tools, the multiple feedback algorithm was explored in JT-60U, aimed at the establishment and sustainment of the integrated plasma performance in the fusion reactor, where more than two real time feedback schemes are simultaneously applied to the plasma [2.4-1]. Plasma density, stored energy, and divertor radiation loss were feedback-controlled simultaneously by main gas puff, injected neutral beam power, and divertor gas puff, respectively. Mutual relationship between the control variables was estimated by the step modulation of specific variable during another variables fixed. A feedback control to simulate the reactor plasma was performed in low-q ELMy H-mode plasma. During the constant plasma density at around half the Greenwald density, the fraction of divertor radiation loss to the total heating power at 40 - 50%, and the stored energy at 1.2 - 1.5 MJ were kept for 6 sec. For the reactor relevant parameters, normalized β -value, β_N , and H-factor, H_{89} , were investigated in addition to controlled parameters. β_N and H_{89} showed antagonistic feature depending on the neutral beam heating power, while relatively high β_N value of 2.5 was obtained. In order to simulate the burning plasma, it is necessary to modify the control algorithm so that the base heating power, which is not directly controlled, changes according to β_N .

Halo current is one of the critical issues in ITER because of an intense electromagnetic force on the in-vessel component. Reduction of halo current was performed by the impurity gas puffing to decrease the electron temperature in the halo region effectively because the magnitude of halo currents depends on resistivity of current path of halo current [2.4-2]. The electron temperature in the halo region at the time of the maximum halo current was around 10 eV. To confirm the causes of reduction of halo current more clearly, the effect of impurity species, such as neon, argon, and helium was investigated. The magnitude of the maximum halo current of $TPF \times I_h / I_{p0}$ with neon gas puff decreased to 30% of that for no gas puff. The reduction rate of halo current depended on total impurity gas injected in vacuum vessel. In the case of helium puff, more than 10 times large amount of gas puff (8-10 Pam³) was required to reduce the $TPF \times I_h / I_{p0}$. Thus, the neon and argon puff is more effective to reduce the halo current because of the reduction of the edge plasma temperature even in short time of order 10 ms. The $TPF \times I_h / I_{p0}$ was around 0.2 in low safety factor of plasma surface, q_s , which was larger than that of high q_s case of typically < 0.12 . These results suggest that both reduction of electron temperature and high q_s are possible cause of the low halo current for neon gas puffing. Edge electron temperature was decreased with the increase in total amount of gas puff. Whereas the central electron temperature after the energy quench did not differ so much. The result suggests that the edge cooling is essential for the halo current reduction and cooling of plasma center is not necessary. This means that impurity gas puffing is a reliable method for the halo current reduction even in large size plasma.

Runaway electrons generated at the major disruption are considered to significantly reduce

the lifetime of the first wall in tokamak fusion reactors. Hence, establishment of methods for avoidance, suppression and termination of runaway electrons is a key issue in present tokamaks. Fast termination of runaway current was first demonstrated in JT-60U by reducing the safety factor at the plasma surface q_s (or the effective safety factor at the plasma edge, q_{eff} , for divertor plasma). The safety factor was reduced by either a controlled inward plasma shift, a VDE (uncontrolled vertical plasma shift) or a ramp-up of plasma current by 1 MA/s [2.4-3]. A sudden decrease of runaway current was always observed at q_s around 2 or 3 (or q_{eff} around 3). This suggests that runaway current may be spontaneously terminated for VDEs in tokamak fusion reactors like ITER due to a natural decrease in q_s . Degraded confinement of runaway electrons in macroscale magnetic turbulence, as observed during major disruptions in JT-60U, can be explained by the breakdown of toroidal momentum conservation due to the toroidal asymmetry of magnetic perturbations. Possible free-boundary MHD activities that cause abrupt termination are low- n external kink modes or surface tearing modes, which should be investigated by experiments and theoretical analyses. The spontaneous and intrinsic termination of runaway current will greatly reduce the energy flux on the first wall and the halo current, which should be also experimentally confirmed.

The development of low voltage startup scenarios for large tokamaks is necessary to reduce breakdown loop voltage. In JT-60U, study of low voltage startup by electron cyclotron preionization and preheating was carried out in which ECH assisted startup with $E \sim 0.24$ V/m (loop voltage of 4 V) was demonstrated. The experiments were carried out in the vicinity of the fundamental cyclotron resonance using an ordinary mode launch from low field side [2.4-4]. ECH injection was started 30 ms before the excitation of ohmic heating coils and vertical coils with constant voltage during 100 ms. Then feedback control system was started to increase the plasma current at the ramp-up rate of $dI_p / dt = 0.2$ MA/s. The density of pre-ionized plasma was roughly estimated about $1 \times 10^{18} \text{ m}^{-3}$ with the prefilling pressure of 8×10^{-4} Pa. The breakdown time is 10 ms. It is much faster than OH breakdown. In the constant voltage phase, steep increase rate of the plasma current at $dI_p / dt = 1.36$ MA/s is observed. The results are compared with a quasi-0D code analysis, developed for ITER burnthrough scenario.

References

- [2.4-1] Fukuda T., *et al.*, Fusion Eng. Des., **46** 337 (1999).
- [2.4-2] Neyatani Y., Yoshino R., Nakamura Y., Sakurai S., Nucl. Fusion, **39** 559 (1999).
- [2.4-3] Yoshino R., Tokuda S., Nucl. Fusion, **40** 1293 (2000).
- [2.4-4] Kajiwara K., Yoshino R., submitted to Nucl. Fusion.

2.5 Particle Control and Divertor / SOL Physics

The pumping scheme in the W-shaped divertor was modified from pumping through the inner side private flux region (Inner-leg pumping) to pumping through the inner and outer side

private flux regions (both-leg pumping) in November-December 1998. The both-leg pumping has been considered to improve controllability of divertor plasma and neutral particles in the high density regime, where in-out asymmetry of the recycling neutral flux becomes weak. The effective pumping speed for the both-leg pumping was estimated to be $15.9 \text{ m}^3/\text{s}$ at about 0.1 Pa by using a gas filling method, which is 25% higher than that for the inner-leg pumping. Furthermore, all graphite tiles of the dome were changed to carbon fiber composite tiles. So far, the distance from the strike point to the dome (Gap_in for inner divertor and Gap_out for outer divertor) was limited to be larger than 3 cm to avoid high heat load to the dome. The divertor operation with Gap_in and Gap_out of 0.5 - 1.0 cm has been possible after the modification.

2.5.1 Particle Exhaust in Both-leg Pumping [2.5-1]

The pumping rate to the recycling neutral flux was quantitatively estimated in the both-leg pumping and compared with that in the inner-leg pumping. The ratio of the pumping flux to the total D_α emission integrated in the whole plasma was in the range of 0.03 - 0.27 for the both-leg pumping with Gap_in = 3.5 cm and Gap_out = 3 cm. The pumping rate to the recycling neutral flux can be estimated to be 0.2 - 1.8%, where (ionization events) / (D_α emission) = 15 was used. The pumping rate in the both-leg pumping was smaller than that in the inner-leg pumping at the same gap, especially in the attached divertor plasma. The ratio of the integrated D_α emission in the inner divertor to that in the outer divertor was estimated to be 3.3 - 3.8 in the attached divertor plasma and 1.5 - 2 in the detached divertor plasma with x-point MARFE. This result indicated that the back-flow from the inner pumping slot to the outer pumping slot through under-dome due to in-out asymmetry of the recycling neutral flux could cause a reduction of pumping rate in the both-leg pumping. The simulation using the UEDGE and DEGAS2 codes also suggested the back-flow at the outer pumping slot. Consequently, the smaller pumping rate was observed for the both-leg pumping compared with that for inner-leg pumping in this simulation.

The pumping rate decreased with increasing gap for the both- and inner-leg pumping. The pumping rate in the detached divertor plasma with x-point MARFE increases to 4.5% at Gap_in = 1.5 cm and Gap_out = 0.5 cm for the both-leg pumping, which is larger than that in the inner-leg pumping with Gap_in = 3.5 cm.

2.5.2 Pumping Effect on Divertor Plasma and Detachment [2.5-2]

The SOL plasma flow for the cases of gas-puffing at plasma top in the both-leg pumping was investigated using the reciprocating Mach probes installed at the outer midplane and the x-point. Effect of bypath between the inner and outer divertors under a dome on the particle recycling was also studied. The profiles of ion saturation current ratio between down stream side (divertor side) and up stream side (midplane side) for the both-leg and inner-leg pumping were

comparable both at the midplane and near x-point. Flow reversal occurred at the midplane, while the plasma flowed from the x-point to the divertor plate. A mechanism to produce the flow reversal at the midplane has been proposed based on the in-out asymmetry in the ion poloidal drift in a torus. The flow reversal at the midplane decreased with increasing density and the plasma flow just below the x-point increased under conditions in which the attached plasma was maintained. For the both-leg pumping, the divertor plasma flow tended to increase at high density. At the same time, small reduction of the flow reversal was observed at midplane. These facts suggested that the increase in the plasma flow at the outer divertor by the both-leg pumping is not large enough to change the plasma flow pattern.

An improvement of the divertor operation was observed for the both-leg pumping case: partial-detached plasma at both divertor targets without appearance of the x-point MARFE was maintained in the main plasma density range of $2.3 - 2.56 \times 10^{19} \text{ m}^{-3}$. In the partial-detached divertor, an increase in the plasma flow at the x-point was amplified by a reduction in the downstream plasma pressure using the both-leg pumping. The neutral flux from the inner divertor to outer divertor through under-dome is so small that the in-out asymmetry of the neutral recycling did not change.

2.5.3 Efficient Helium Exhaust in Divertor-closure Configuration [2.5-3]

Helium exhaust has been studied in the ELMy H-mode plasmas by injecting a neutral beam of helium atoms as central fuelling of helium. A global particle confinement time of $\tau_{\text{He}}^* = 0.36 \text{ s}$ and $\tau_{\text{He}}^*/\tau_E = 2.8$ were achieved in attached plasmas with $\text{Gap}_{\text{in}} = \text{Gap}_{\text{out}} = 0.5 - 1 \text{ cm}$ (divertor-closure configuration). The helium exhaust efficiency in the both-leg pumping was enhanced by 45% as compared to that in the inner-leg pumping with $\text{Gap}_{\text{in}} = 3.5 \text{ cm}$. In the high X_p configuration for the both-leg pumping with $\text{Gap}_{\text{in}} = \text{Gap}_{\text{out}} = 4 \text{ cm}$, the helium exhaust efficiency and the pumping rate deteriorated. The global particle confinement time τ_{He}^* in the high X_p configuration became longer about two times as compared to that in the divertor-closure configuration. Longer τ_{He}^* in the high X_p configuration could be related to the back flow at the outer pumping slot as well as deuterium pumping.

2.5.4 Helium Removal from Core Plasma inside ITB in Reversed Shear Plasmas

Helium ash exhaust in the reversed shear plasma is a matter of concern, because the helium particle confinement is remarkably improved inside the ITB. A previous study of helium exhaust in reversed shear plasmas using helium gas-puffing indicated that helium removal inside the ITB was 2 - 3 times as difficult as outside the ITB [2.5-4].

Helium exhaust was also investigated in reversed shear plasmas with L-mode edge using a neutral beam of helium atoms. The residence time of helium density (equivalent to the local τ_{He}^*) was evaluated to be 3.7 sec inside the ITB and 2.8 sec outside the ITB, respectively. The

local helium residence time was almost the same at the central and peripheral regions in ELMy H-mode plasmas. However, the local helium residence time inside and outside the ITB in the reversed shear plasmas was clearly different. If the local residence time of inside the ITB was assumed as $\tau^{\text{ITB}^*}_{\text{He}}$, the ratio of $\tau^{\text{ITB}^*}_{\text{He}}/\tau_E = 11$ (major contribution of τ_E was from inside the ITB) was achieved.

The reversed shear discharge with the L-mode edge by low-power NB heating is unfavorable for helium removal because of the low-density edge. Recently, the reversed shear discharge with H-mode edge by high-power NB heating of $P_{\text{NB}} = 10$ MW was successfully sustained. In this discharge, the recycling neutral flux in the divertor region was a factor of two high compared with the L-mode edge. Improvement of the helium exhaust efficiency in the core plasma will be attempted under the condition with high recycling and ELMs.

2.5.5 Chemical Sputtering in Divertor Plasma

Chemical sputtering yield of sum of C_2D_2 and C_2D_4 was estimated in addition to that of CD_4 in the L-mode plasmas based on measurements of CD and C_2 spectral bands intensities. The CD spectral bands are emitted from CD radicals originating not only from CD_4 but also from C_2D_2 , C_2D_4 and other heavier hydrocarbon molecules. According to the laboratory experiment, the chemical sputtering yields of C_2D_2 and C_2D_4 are comparable and the yields of C_2D_6 and other heavier hydrocarbons are about one order of magnitude smaller than those of CD_4 , C_2D_2 and C_2D_4 . Therefore only CD_4 and $(\text{C}_2\text{D}_2 + \text{C}_2\text{D}_4)$ were taken into account to evaluate the yields. It is difficult to measure the accurate ion flux to the divertor plates by Langmuir probes in detached plasma conditions. Therefore, the estimation of the yields is restricted to attached conditions. The chemical sputtering yield was measured at the outer divertor plate. The electron temperature was assumed to be 20 eV. Sputtering yields of both CD_4 and $(\text{C}_2\text{D}_2 + \text{C}_2\text{D}_4)$ were around 1% to 2%. This result reveals that C_2D_2 and C_2D_4 are also sputtered by chemical reaction to an extent comparable to CD_4 .

References

- [2.5-1] Takenaga H., et al., submitted to Nucl. Fusion.
- [2.5-2] Asakura N., et al., to be published in J. Nucl. Mater.
- [2.5-3] Sakasai A., et al., to be published in J. Nucl. Mater.
- [2.5-4] Sakasai A., et al., the 17th IAEA Fusion Energy Conf., Yokohama 1998, EX6/5.

2.6 High-radiation and High-density Experiments in JT-60U

In order to demonstrate impurity seeding operational scenario in ITER under high-power heating conditions in a large tokamak, Ne seeding has been applied to ELMy H-mode plasmas and reversed shear plasmas in JT-60U [2.6-1]. In FY 1999, the JT-60U W-shaped divertor was modified to pump both the inner and outer divertor. The pumping efficiency was enhanced and

the pumping time constant for noble gas impurities was reduced from ~2 to ~0.5 sec. This improved pumping efficiency enabled to control the edge plasma radiation loss with a feedback technique by Ar puffing into the main plasma chamber and extended the possibility to control the ELMy H-mode plasmas and reversed shear plasmas with the high radiation loss and high plasma density.

2.6.1 ELMy H-mode Plasmas with Impurity Seeding

In ELMy H-mode plasmas with high beam power (< 21 MW), the electron density was raised without increase in recycling and a quasi-steady state with high radiation and high confinement was sustained for ~2.5 sec (The duration was limited by the poloidal coil system). With Ar seeding, the radiation loss power was enhanced up to ~ 80% of the heating power with high confinement ($H_{99} \sim 1.5$). With Ar seeding, while the Z_{eff} was increased from 2.4 to 4.5 and the plasma purity (n_D / n_e) was decreased from 72 % to 62%, the energy confinement time was improved by a factor of 1.35, the ion temperature was doubled. As a result the fusion product ($n_D \tau_E T_i$) was enhanced by a factor of 2.4 [2.6-2].

A new operational scenario to reduce deuterium gas puffing for high density plasmas was proposed in FY 1999. Plasma configurations of near-limiter were used to increase the plasma density at low deuterium gas puff rate during low NB power (PNB = 4.3 MW) phase. Then Ar gas puff rate was adjusted to follow programmed edge radiation power using feedback control during the ELMy H-mode phase with PNB = 17 MW. Feedback control of deuterium gas puff was also used to increase the plasma density slowly, where the gas puff rates (maximum rate of less than $10 \text{ Pa m}^3/\text{s}$) was smaller than that in the near-limiter phase. Relatively high H-factors of 1.4 - 1.45 was maintained during 0.5 - 1.5 sec with large radiation fraction of ~0.8, where Greenwald density fraction was 0.7.

Kr injection was applied to hydrogen discharges of ELMy H-mode plasma, confinement degradation is observed with Kr seeding, unlike Ar seeding, when the radiation loss power is increased. While confinement improvement by Kr seeding was observed in super shots in TFTR [2.6-3], where the electron temperature was 5 - 9 keV at the plasma center, radiation loss profile seemed to be unfavorable in the plasmas with $T_e \sim 2$ keV in JT-60U.

2.6.2 Reversed Shear Plasmas with Impurity Seeding

High confinement ($H_{99} > 2$) with an ITB and high radiation loss power fraction ($P_{\text{rad}} / P_{\text{net}} > 0.7$) were simultaneously obtained with Ne and Ar seeding. A radiation mantle was produced in the scrape-off layer in the case with Ne seeding. In the case with Ar seeding, although the radiation loss fraction was higher than that in the case with Ne seeding, the radiation loss power density was also high in the core region and at the vicinity of the null point. Therefore, Ar seeding was not better with respect to the energy confinement, though Ar is a

better radiator than Ne. The values of Z_{eff} with and without impurity seeding were ~ 3 and ~ 5 , respectively. Since impurity contamination is a critical issue for reversed shear discharges, the impurity transport [2.6-4] will be investigated further.

2.6.3 Impurity Transport Analysis in Collaboration with PPPL

In FY1999, the collaborative effort between physicists at JT-60U and the Princeton Plasma Physics Laboratory (PPPL) was significantly increased including analysis of radiative improved (RI) modes in JT-60U and comparison with RI experience in TFTR.

A preliminary comparison of the Ar ion charge-state distributions predicted by IMPACT (JAERI code) and MIST (PPPL code) for an ELMy H-mode discharge with Ar puffing was performed. The peak locations and ion densities for the fully stripped, hydrogen-like, and helium-like ions showed reasonable agreement between the two codes predictions. Some differences in the predicted densities for lower charge states are being investigated. Efforts are underway to insure that both codes have the same and latest and best ionization and recombination rates included in their atomic databases. Also, differences between the measured radiated power profiles and the predictions of the two codes are being investigated. Improvements in the atomic physics databases and/or understanding of the impurity transport may result from these studies.

References

- [2.6-1] Itami K., et al., in Fusion Energy 1997 (Proc. 16th Int. Conf. Montreal, 1996), Vol. 1, 385 (1996).
- [2.6-2] Sakurai S., et al., to be published in J. Nucl. Mater.
- [2.6-3] Hill K., et al., Nucl. Fusion, **39** 1949 (1999).
- [2.6-4] Takenaga H., et al., J. Plasma and Fusion Res., **75** 952 (1999).

II. JFT-2M PROGRAM

On JFT-2M, advanced and basic research for the development of high performance tokamak plasma is being promoted, making use of the flexibility of a medium-sized device and the research cooperation with universities and other research organs. From this fiscal year, the application of the low activation ferritic steel, which is a leading candidate for structural material of a demonstration reactor, to plasma (called Advanced Material Tokamak Experiment (AMTEX)) has been started. As for the high performance experiments, the H-mode research with the heavy ion beam probe, the radio-frequency heating and current drive study, the advanced fuelling study by compact toroid injection as well as the research on divertor characteristics were carried out under continued collaboration with universities and other institutions.

1. Advanced Material Tokamak Experiment (AMTEX) Program

The low activation ferritic steel had never been applied in fusion devices, because it has a possibility to disturb magnetic field for plasma confinement because of its ferromagnetism. In addition, ferritic steel is likely to rust and the gas desorption in the vacuum is larger compared with stainless steel. Therefore, compatibility of the low activation ferritic steel with plasma should be tested. In JFT-2M, the advanced material tokamak experiment program (AMTEX) concerned with the low activation ferritic steel (F82H) is being proceeded in stages, with a final target to realize high performance plasma in the vacuum vessel, inside of which will be fully covered with ferritic steel. In this fiscal year, ripple reduction experiments were performed as the first stage and installation of the ferritic steel inside the vacuum vessel was completed for the pre-testing on compatibility with plasma (second stage).

1.1 Ripple Reduction Experiments [1.1-1, 1.1-2, 1.1-3, 1.1-4]

It is important to reduce the toroidal field ripple for realizing a tokamak reactor, because the magnetic field ripple increases the fast ion losses (ripple loss). Therefore ripple reduction test with installation of the ferritic board (FB) outside the vacuum vessel (just under the toroidal field coils) was carried out on JFT-2M. An infrared camera (IRTV) was mainly used for the measurement of the ripple losses. Parameter dependence of the ripple losses was investigated by varying the thickness of FBs and the magnetic field strength. As a result, it was shown that ripple

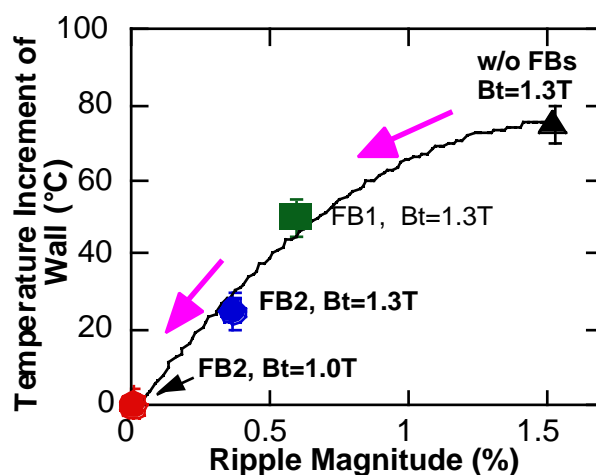


Fig. II.1.1-1 Temperature increment of the first wall due to the ripple trapped losses against the ripple magnitude.

trapped losses almost disappeared in the ideal condition, as shown in Fig. II.1.1-1. Furthermore, no deteriorating effects were observed on the plasma production, control and confinement. Moreover, an H-mode was obtained in the single null divertor configuration after the FB installation as well, and the toroidal rotational speed of the plasma increased from 20 - 30 km/s to 50 - 60 km/s at the plasma periphery in ELM-free H-mode.

This demonstration of the magnetic field ripple reduction by the FB installation was achieved for the first time in the world. The result is important for making the magnetic field coils of a fusion reactor be compact and high performance.

References

- [1.1-1] Sato M., Miura Y., Kimura H., et al., "Advanced Material Tokamak Experiment (AMTEX) Program with Ferritic Steel on JFT-2M", J. Plasma and Fusion Research, **75** 741 (1999).
- [1.1-2] Sato M., Kawashima H., Miura Y., et al., "Design and first experimental results of toroidal field ripple reduction using ferritic insertion in JFT-2M", to be published in Fusion Engineering and Design.
- [1.1-3] Tsuzuki K., Sato M., Kawashima H., et al., "Ripple reduction and surface coating tests with ferritic steel on JFT-2M", to be published in J. Nucl. Mater.
- [1.1-4] Kawashima H., Sato M., Tsuzuki K., et al., "Ripple reduction test by ferritic steel board insertion in the JFT-2M tokamak", J. Plasma and Fusion Research, **76** 585 (2000) (in Japanese)

1.2 Preparation for Pre-testing of Compatibility with Plasma

For the preliminary testing of the magnetic effects and the plasma-wall interaction with respect to the ferritic steel, FBs, which cover partly inside of the vacuum vessel, were installed as shown in Fig. II.1.2-1.

FBs (32 sectors in total) were arranged uniformly in the toroidal direction, so that the influence to the ripple is minimized and the magnetic effect can be evaluated separately from the ripple. FBs outside the vacuum vessel are still retained for the ripple reduction. Magnetic probes and flux loops, a part of which was installed both front and back sides of FBs, and thermocouples, which were set in upper FBs at each toroidal section, were newly equipped. The former is used for the evaluation of the magnetic effect and the latter for the measurement of the toroidal distribution of ripple losses. Furthermore, a boronization system was newly prepared for improvement of the plasma wall on FBs.

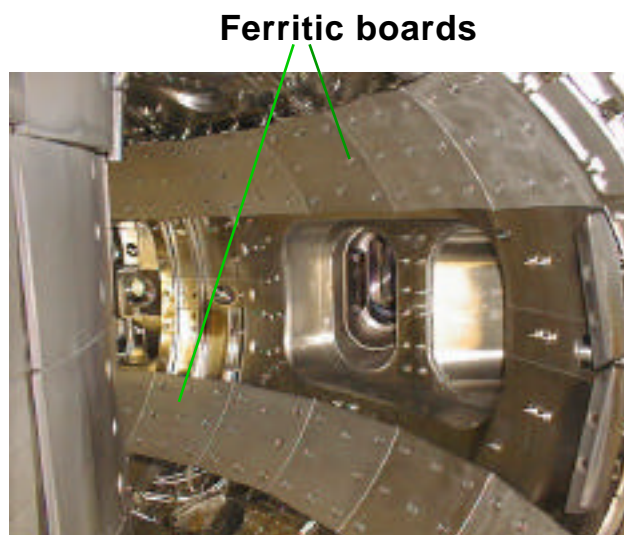


Fig.II.1.2-1 Inside of the JFT-2M vacuum vessel after installation of ferritic steel boards (covering 20% of the inside wall)

2. High Performance Experiments

2.1 H-mode Study with Heavy Ion Beam Probe Measurement

It is pointed out theoretically that radial electric field at the plasma periphery plays an important role in the L/H transition. In JFT-2M, fast measurement of potential and fluctuations by the heavy ion beam probe was further proceeded in collaboration with the National Institute for Fusion Science and detailed time scales of the potential change at the plasma periphery have been clarified for the first time [2.1-1, 2.1-2, 2.1-3].

Figure II.2.1-1 indicates time variations of the plasma potential and the soft-X ray intensity at the plasma periphery in the cases where the heating power is much higher than or at the same level with the threshold power. It was found that there are two patterns of the potential variation at the L/H transition, such as rapid reduction (10 ~ 100 μ sec) just after the arrival of the heat pulse associated with a sawtooth crash, and relatively slow reduction (200 ~ 500 μ sec) which occurs several 100 μ sec to several msec after the arrival of the heat pulse. Potential change at the L/H transition appears in the manners such as only the former, the both and only the latter, depending on the heating power.

The results of this research give experimental evidence of the theory of the L/H transition based on the change of electric field structure. The measured time scales are important to clarify the physical process contributing the formation of the electric field.

References

- [2.1-1] Ido T., Kamiya K., Hamada Y., et al., "Behaviour of Sample Volumes of the Heavy Ion Beam Probe on JFT-2M", *Plasma Phys. Control. Fusion*, **41** 1013 (1999).
- [2.1-2] Ido T., Kamiya K., Miura Y., et al., "Temporal Behaviour of the Potential and Fluctuations at the L/H Transition on JFT-2M", *Plasma Phys. Control. Fusion*, **42** A309 (2000).
- [2.1-3] Hamada Y., Ido T., Kamiya and JFT-2M Group, "Fast Potential Changes at H-Mode Transition in the JFT-2M Tokamak", *Proc. of Fusion Energy 1998 (IAEA, Vienna)*, **4** 1681 (1999).

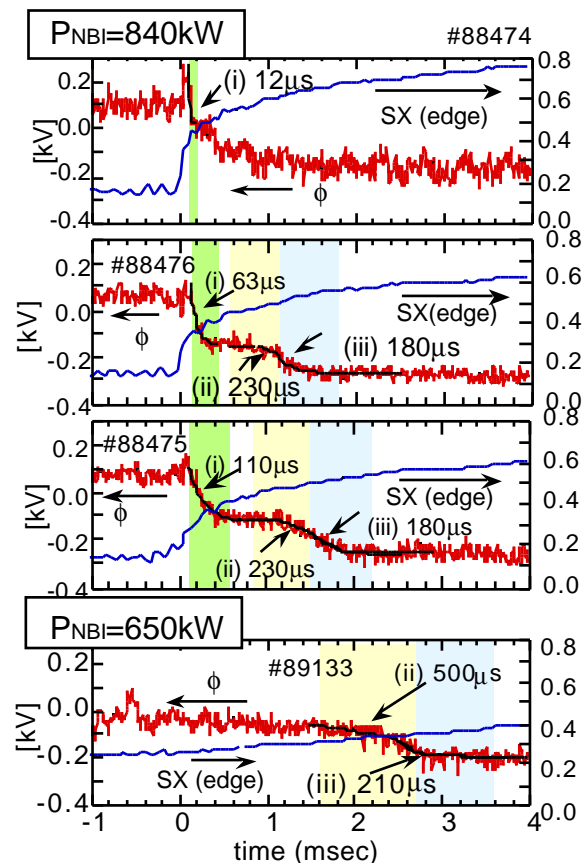


Figure II.2.1-1. Time variation of the space potential near the separatrix and the soft X-ray intensity at edge. In the columns from the top to the third, NBI power is sufficiently larger than the threshold power. In the fourth column, it is at the same level. The time 0 is chosen as the timing when the heat pulse of the sawtooth crash reached the plasma boundary.

2.2 RF Experiments

2.2.1 Fast Wave Experiments with Traveling Wave Antenna

Plasma current profile control is very important for high performance tokamak operation. In JFT-2M, experiments on fast wave, which is suitable for current drive at high density, have been proceeded by using a traveling wave type antenna (comblin antenna [2.2-1]) which has high directivity and sharp radiation spectrum. By injecting fast wave of 200 MHz and 230 kW into a target plasma heated by electron cyclotron wave of 230 kW, it was observed that high energy electrons of at least 10 keV were produced and that the electron temperature evaluated as a slope in the energy range of 5 - 10 keV raised from 2.1 keV to 3.0 keV (Fig. II.2.2-1). Coupling of fast waves and electrons with Comblin antenna was thus confirmed for the first time. Furthermore, by injecting two frequencies of 199.95 MHz and 200.05 MHz simultaneously from the comblin antenna, we succeeded in observation of the ponderomotive potential produced by the beat wave (100 kHz) in the core plasma region with the heavy ion beam probe measurement. This experimental technique is expected to be useful for the direct measurement of the electromagnetic field profile of the fast wave.

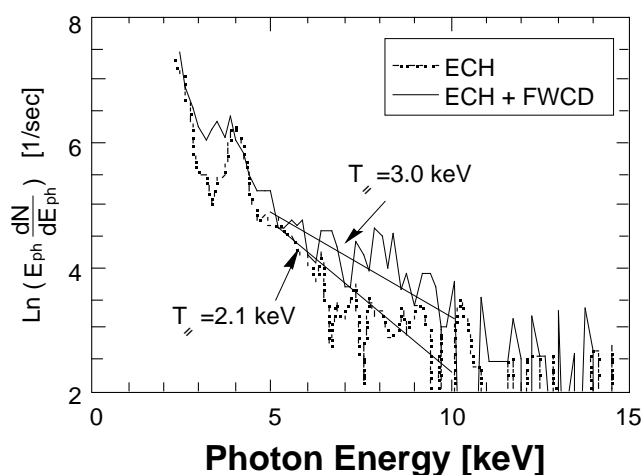


Fig.II.2.2-1 Soft X-ray energy spectra during fast wave injection (combination of fast wave and electron cyclotron wave, ECH+FWCD) and before injection (electron cyclotron wave, ECH, only).

2.2.2 Disruption Control with Electron Cyclotron Wave

It had been clarified in JFT-2M that the tearing instability, which causes plasma disruption, can be suppressed by the local heating with the electron cyclotron wave [2.2-2]. On the other hand, it is theoretically predicted that the tearing instability can be suppressed by the plasma rotation. Therefore, in this year, comparison was made between the electronic cyclotron (ECH) local heating and the rotation by the neutral particle injection (NBI) of the co-direction and the counter-direction. As a result, it was made clear that the stabilizing effect of ECH local heating is much stronger under the present condition, although the suppression by NBI was observed to some extent when the rotation was fast. The second mirror antenna system, beam injection angle of which can be variable, was installed to increase the electron cyclotron current drive power.

References

- [2.2-1] Pinsker R.I., Moeller C.P., Petty C.C., et al., Fusion Technology 1996 (Elsevier Science B.V., Amsterdam) 629 (1997).
- [2.2-2] Hoshino K., et al., Phys. Rev. Lett. 69, 2208 (1992); Hoshino K., et al., AIP Conference Proceedings, 289, Radio Frequency Power in Plasmas (1993, Boston), 149 (1994).

2.3 Compact Toroid Injection

Development of the fueling method by the compact toroid (CT) injection, which is expected as a fueling method to a core plasma of a fusion reactor, is being proceeded in JFT-2M [2.3-1]. The velocity of CT of 300 km/s, which is the best until now, was achieved at $B_T = 0.8$ T. The corresponding increment of the line-average electron density was $0.4 \times 10^{19} \text{ m}^{-3}$ with 40% of the fueling efficiency. It was estimated that the electron temperature of the CT plasma was about 10 eV from the spectroscopic measurement. Furthermore, optimization of the CT injection system (such as optimization of the electrode configuration, the development of the fast gas injection valve) as well as preparation of measuring instruments (such as fast PIN diode array, multiple channel electrostatic probe, etc.) were completed.

References

[2.3-1] Ogawa T., Fukumoto N., Nagata M., and JFT-2M Group, "Compact Toroid Injection Experiment in JFT-2M", Nuclear Fusion. **39** 1911 (1999).

2.4 Comparative Research on Closed and Open Divertor Geometries

Generally, a confinement characteristic of H-mode degrades or H-mode itself disappears, when strong gas puffing is made to get a high density during H-mode. In JFT-2M, sustainment of high confinement at high density and compatibility with low temperature and high density divertor plasma had been demonstrated, by installing baffle plates between the divertor region and the main plasma region (closed divertor) [2.4-1]. In this year, experiments under the open divertor condition were done, and comparison with the closed divertor was made. Radiation loss and D_α intensity were larger with strong gas puffing during NBI heating to get low temperature and high density divertor, compared with the closed divertor. Moreover, a sustainment time of the H-mode became short and remarkable low temperature and high-density divertor could not be obtained. It can be evaluated that screening effect of baffle plates against neutral particles and impurities are effective.

References

[2.4-1] Kawashima H., Sengoku S., Ogawa T. and JFT-2M Group, "Study of a Closed Divertor with Strong Gas Puffing on JFT-2M", Nuclear Fusion. **39** 1679 (1999).

3. Operation and Maintenance

3.1 Tokamak Machine

The vacuum vessel of JFT-2M started vacuum exhaust and baking from April. The displacement measurement of the vacuum vessel was done at the same time. It confirmed that there was no movement of the vacuum vessel by the ferritic steel boards (FBs) inserted in the space with 16 TF coils and the vacuum vessel for the ripple reduction last year. During a vacuum vessel baking, Taylor discharge cleaning (TDC) was carried out. Experiment operation about ripple reduction started in May after checking a plasma control. The experiment operation of JFT-2M was done on schedule for eight months until January 2000. In FY99, the plasma experiment of JFT-2M was

2232 shots and TDC was 131 hours.

Capacitors of the harmonic filters for the poloidal field coils power supply and the NBI power supply were renewed during the annual maintenance because of deterioration. Plasma excitation capacitors were also renewed for the same reason. The control system of vacuum exhaust equipment, gas puff equipment and the leakage test device was superseded by the new one. This newly installed control system has improved efficiency of the operation and acquisition of data. From the viewpoint of maintenance of tokamak machine, the following improvements were done: The first was the installation of an electric potential measurement device, which makes it easy to detect the deterioration of the vacuum vessel insulation. The second was measures against the minute vacuum leakage of the vacuum vessel: namely, magnetic probes supposed to be one of the causes of the leakage were replaced, and a movable limiter was removed.

Preparation for compatibility with plasma and FBs was the second stage of Advanced Material Tokamak Experiment (AMTEX), and it was done in cooperation with Experimental Plasma Physics Laboratory in the remodeling term in March from February 2000. FBs were installed on the outboard side of the vacuum vessel in the toroidal direction. The installation area of FBs is equivalent to about 20% of the interior of a vacuum vessel. The energization test of the toroidal magnetic field coils was done to confirm the deformation of FBs and its deviation. The result was within the allowable error range. A boron coating apparatus was installed in order to control impurities which could be increased due to the installed FBs and improve an interaction between the plasma and wall.

3.2 Neutral Beam Injection System and Radio-frequency Heating System

A NBI device was operated through the year for the injection experiment. The check was carried out for the NBI device: the vacuum exhaust, the beam line, the sources of ion, and the power supply. The replacement and repairs of their parts were done at the same time. As a result, the soundness of the NBI device was maintained. An annual check for an ECH device was carried out in September. Cooling of the device was done, and the ECH device was operated for the injection experiment for about three months until December. The ECH power supply was repaired and its grounding electrode was improved in the remodeling term. The maintenance check for the FW and PIB device was carried out at the same time.

3.3 Power Supply System

The operation duration of the toroidal magnetic field coil power supply (DC Generator, DCG) is very long because it is used for TDC and the pulse experiment. Operation condition is severe to DCG because an acceleration and slowdown are repeated. A filter was installed in the air inlet, and control of the dust in a DCG room was employed to avoid the problem of the commutator that had appeared in the former year. A soundness of DCG was maintained by doing the careful daily and annual checks. The results of these checks showed that insulation performance maintained good condition.

III THEORY AND ANALYSIS

The principal objective of theoretical and analytical studies is to understand physics of tokamak plasmas. Much progress was made on analyzing dynamics of the internal transport barrier in JT-60U reverse shear plasmas. Progress was also made on the study of micro and macro instabilities. The NEXT (Numerical EXperiment of Tokamak) project has been progressed in order to investigate complex physical processes in core plasmas, such as transport and MHD, and in divertor plasma by using recently advanced computer resources. Remarkable progress was made on the development of divertor simulation codes.

1. Confinement and Transport

The global confinement and the local transport properties of improved core confinement plasmas with internal transport barrier (ITB) in JT-60U have been studied in connection with E_r shear formation. Both electron and ion thermal diffusivity, χ_e and χ_i decrease as the increase of $|dE_r/dr|$ [1-1]. The estimated ExB shearing rate, $v_{E \times B}$, becomes almost the same as the linear growth rate of the drift microinstability, ω_L , at the ITB layer in the box type ITB [1-2].

The effects of plasma rotation on the characteristics of ITB and core confinement properties are studied in JT-60U reversed shear plasmas. The combination of on-axis and off-axis tangential NBI in the co and counter directions in JT-60U allows various profiles of the momentum input and toroidal rotation. When the toroidal momentum input is almost balanced, the profile of E_r shear does not change and the ITB is retained. On the other hand, when the toroidal momentum input is unbalanced in the co or counter directions, the E_r shear decreases and the pressure gradient of ITB is remarkably relaxed [1-3].

New features of the space-time evolution of the ITB were highlighted during recent JT-60U reverse shear (RS) experiments. An ITB evolution in RS plasmas is often a combination of the fast time-scale processes and the gradual ones. Fast time-scale processes are the common intrinsic features of JT-60U RS plasmas and are seen as the simultaneous (within a few milliseconds) rise and decay of electron temperature (T_e) on two zones separated by a region without variation of T_e ("bipolar" perturbation shown by Fig. III.1-1). The region without variation of T_e is located near the position of the minimum safety factor profile for many fast processes. The present robust result is that the region of fast-time-scale improvements of electron heat diffusivity χ_e is wide in space (around 0.3 of the minor radius) and well extended to the zone of T_e decay. The decrement of χ_e , $\Delta\chi_e$ is 0.2 - 0.4 m²/s for this case (Fig. III.1-2) [1-4].

A new source of Heat Pulse Propagation (HPP) is found in JT-60U RS plasmas. HPP is created by the abrupt variation of heat diffusivity described above. For such an event, a strong T_e rise (~20 keV/s) occurs in a localized region (~4 cm) initially. The HPP is studied

analytically and numerically. Values of the electron heat diffusivity as low as $\sim 0.1 \text{ m}^2/\text{s}$ are found in the ITB region. An important consequence of HPP analysis is an absence of "heat pinch" in this region [1-5].

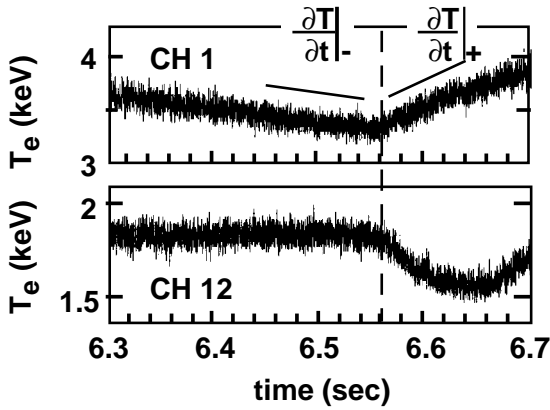


Fig. III.1-1 Evolution of T_e measured on Innermost (CH1) and outermost (CH12) channels of the heterodyne radiometer.

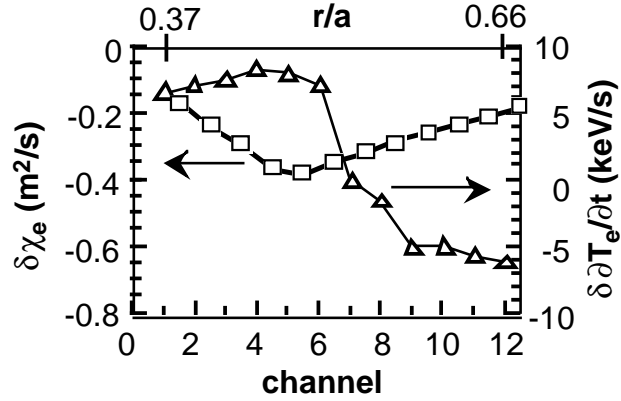


Fig. III.1-2 Profile of $\delta\chi_e$ (squares) calculated from $\delta\partial T_e / \partial t$ (triangles), where $\delta\partial T_e / \partial t = \partial T_e / \partial t \uparrow - \partial T_e / \partial t \downarrow$.

The particle and heat transport in an internal transport barrier (ITB) is investigated with taking account of a finite orbit width and a radial electric field. The Orbit Following Monte Carlo (OFMC) code is used to follow the drift orbit in a radial electric field with the Coulomb collision effect. It is shown that inward particle/heat flows are induced in ITB [1-6].

References

- [1-1] Shirai H., Kikuchi M., Takizuka T., et al., "Reduced Transport and E_r Shearing in Improved Confinement Regimes in JT-60U", Nucl. Fusion, **39** 1713 (1999)
- [1-2] Shirai H., Kikuchi M., Takizuka T., Azumi M., "Improved Confinement and Neoclassical Effect", J. Plasma and Fusion Research, **75** 444 (1999) (in Japanese).
- [1-3] Shirai H., Kikuchi M., Takizuka T., et al., "Role of Radial Electric Field and Plasma Rotation in the Time Evolution of Internal Transport Barrier in JT-60U", Plasma Phys. Control. Fusion, **42** A109 (2000).
- [1-4] Neudatchin S.V., Takizuka T., Shirai H., et al., "Abrupt in Time and Wide in Space Variations of Heat Diffusivity during ITB Formation in JT-60U Reverse Shear Discharges", Plasma Phys. Control. Fusion, **41** L39 (1999).
- [1-5] Neudatchin S.V., Takizuka T., Shirai H., et al., "Analysis of Internal Transport Barrier Heat Diffusivity from Heat Pulse Propagation Created by Abrupt Variation of Diffusivity in JT-60U Reverse Shear Plasmas", JAERI-Research 99-063 (1999).
- [1-6] Hamamatsu K., Takizuka T., Shirai H., et al., "Monte Carlo Simulation of Particle and Heat Transport in Internal Transport Barrier", Proceedings of the 26th European Conference on Controlled Fusion and Plasma Physics (EPS, Maastricht, 1999) Vol. 23J 421-424 (1999).

2. Stability

The effect on vertical stability of a strong β_p -collapse in the highly elongated TCV (Tokamak Configuration Variable) tokamak was investigated computationally and experimentally. The essential mechanism of the β_p -collapse-induced VDE was confirmed to be

an intense enhancement of the vertical instability due to a large and sudden degradation of the n -index produced by eddy currents [2-1].

Numerical analysis of the island width of the neoclassical tearing mode, which is induced by the helical bootstrap current along the island, have been carried out to clarify effects of profiles on stability and to obtain conditions for stabilization by electron cyclotron current drive (ECCD). The saturated island grows up to some 10% of the minor radius at the beta value well below the ideal kink limit. The saturated island width of m/n mode can be small when the magnetic shear is large and the pressure gradient is low at the corresponding rational surface. A localized additional current at the O-point of the island by the ECCD significantly stabilizes the mode [2-2].

The linear stability and nonlinear behaviors of the tearing mode were systematically studied for non-monotonic q -profiles in cylindrical geometry and some new features about the double tearing mode have been revealed [2-3]. The linear growth rate of the tearing mode changes its dependence on the plasma resistivity with different radial separation between the resonant surfaces, r_r . For small r_r , it scales as the resistive internal mode $\sim r_r^{1/3}$ and, as r_r becomes larger, it tends to the standard tearing mode $\sim r_r^{3/5}$. The nonlinear behavior of the tearing mode primarily reflects the features of the linear instability.

Linear and nonlinear stability for double tearing mode with poloidal rotation are examined. Weak differential rotation between each mode rational surfaces can't affect on linear growth rate but it can prevent core crash. Larger differential rotation suppresses the double tearing mode in some case [2-4].

Simulations using a reduced set of resistive MHD equations in cylindrical geometry are carried out and an attempt is made to find the plasma response effects on the externally applied helical field. We show that the deviation from a vacuum model is mainly comes from the perturbed current due to a helical deformation for a low frequency case. For a high frequency case, the shielding current near the resonant surface also affects the penetrating process [2-5].

A new eigenvalue method for two-dimensional Newcomb equation in an axisymmetric toroidal plasma, such as a tokamak, has been formulated and solved numerically by using a finite element method [2-6]. In the formulation, the weight functions (the kinetic energy integral) and the boundary conditions at rational surfaces are chosen such that the spectra of the eigenvalue problem are comprised of only the real denumerable eigenvalues without continuous spectra. This formulation identifies ideal MHD stable states as eigenstates and enables one to compute the outer-region matching data, essential ingredients in the resistive MHD stability theory, even for a mode close to ideal MHD marginal stability.

The initial evolution process of a forced magnetic reconnection due to an externally imposed boundary perturbation has been reworked by using an improved boundary layer theory [2-7]. It is clarified that the reconnected flux increases on the same time scale as the boundary

perturbation, which excludes the Sweet-Parker time scale and also that an induced surface current on a resonant surface is in such a direction as to oppose the progress of the reconnection.

A gyrokinetic integral eigenvalue code for analyzing global linear mode structure of micro-instability with retaining full wave-particle interaction and finite Larmor radius effect has been developed through a collaboration with KYOTO University. Using this code, linear properties of ion temperature gradient (ITG) [2-8] and electron temperature gradient (ETG) [2-9] modes in negative shear tokamaks has been studied. It was found that the mode structure shows different features compared with that in the normal shear case, suggesting that the transport characteristics could be different. Specifically, it is found that the radial scale length of the ETG mode is influenced by the Debye shielding, so that the slab ETG mode gives an order of magnitude larger transport compared with the conventional normal sheared slab ETG mode.

References

- [2-1] Nakamura Y., Lister J.B., Hofmann F., et al., " p-Collapse-Induced VDE and its Underlying Mechanism in the TCV Tokamak", Proc. 26th European Physical Society Conf. on Controlled Fusion and Plasma Physics, Maarstricht, 14-18 July p. 417 (1999).
- [2-2] Ozeki T., Hamamatsu K., Isayama A. et al., "Effects of Profiles on the Neo-classical Tearing Mode", Joint Meeting of IAEA Technical Committee Meeting on ECRH Physics and Technology for Fusion Devices and The 11th Joint Workshop on Electron Emission and Electron Cyclotron Resonance Heating, (1999).
- [2-3] Ishii Y., Azumi M., Kurita G., "Nonlinear destabilization of double tearing mode", in Proceedings of APS Vol.44, N0.7 (1999) and to be published in Physics of Plasmas.
- [2-4] Tuda T., Kurita. G., Ishii Y. et al., "Velocity Shear Stabilization of Double Tearing Mode", in Proceedings of the 26th European Physical Society Conference on Controlled Fusion and Plasma Physics, (14-18 July 1999 Maarstricht) 433 (1999).
- [2-5] Tuda T., Kobayashi M., Kurita G. et al., "Interaction of Externally applied helical field with tokamak plasma", in Proceedings 7th International Workshop on Plasma Edge Theory in Fusion Devices (4-6 October 1999, Tajimi, Japan), Contribution to Plasma Physics, **40** 256 (2000).
- [2-6] Tokuda S., Watanabe T., "A new Eigenvalue Problem associated with the Two-Dimensional Newcomb Equation without Continuous Spectra", Phys. Plasmas, **6** 3012 (1999).
- [2-7] Ishizawa A., Tokuda S., "Improved Boundary layer Analysis of Forced Magnetic Reconnection due to a Boundary Perturbation", Phys. Plasmas, **7** 875 (2000).
- [2-8] Idomura, Y., Tokuda, S., Wakatani, M., "Gyrokinetic theory of slab ion temperature gradient mode in negative shear tokamaks", Phys. Plasmas, **6** 4658 (1999).
- [2-9] Idomura, Y., Tokuda, S., Wakatani, M., "Gyrokinetic theory of slab electron temperature gradient mode in negative shear tokamaks", Phys. Plasmas, **7** 2456 (2000).

3. Divertor

The thermoelectric instability in divertor plasmas has been studied by using the five-point model. The equilibrium and stability of scrape-off layer (SOL) and divertor plasmas are investigated, taking account of the divertor asymmetry induced externally by the biasing and recycling. In the case of low divertor radiation, there exists a stable equilibrium. On the other hand, in the case of high radiation, there are one unstable and two stable equilibria [3-1, 3-2]. The thermoelectric instability arises at the unstable equilibrium where the SOL current is small. When the externally induced asymmetry is large, one of the stable equilibria only remains and the other equilibria disappear. At the remaining equilibrium, the SOL current increases with the

externally induced asymmetry and the thermoelectric instability does not arise [3-3].

High mach flow associated with X-point MARFE and plasma detachment has been investigated by using B2-Eirene code and a simple model. The redistribution from static into dynamic pressure without large momentum loss is a possible cause of high flow velocity near the ionization front [3-4].

References

- [3-1] Hayashi N., Takizuka T., Hatayama A., Ogasawara M., "Numerical Analysis of Thermoelectric Instability in Tokamak Divertor", *J. Nucl. Mater.*, **266-269** 526 (1999).
- [3-2] Shibata Y., Hatayama A., Hayashi N., Ogasawara M., "Numerical Simulation of Divertor Asymmetry Caused by Thermoelectric Instability", 7th Int. Workshop on Plasma Edge Theory in Fusion Devices, 4-6 October, (1999).
- [3-3] Hayashi N., Takizuka T., Shimizu K., "Thermoelectric Instability in Externally Induced Asymmetric Divertor Plasmas", 7th Int. Workshop on Plasma Edge Theory in Fusion Devices, 4-6 October, (1999).
- [3-4] Hatayama A., Segawa H., Schneider R., Coster D., Hayashi N., Sakurai S., and Asakura N., "High Mach Flow Associated with X-point MARFE and Plasma Detachment", JAERI Int. Meeting on Plasma Edge Issues for Existing Tokamaks and Next Step Devices, 15-16 December, (1999).

4. Numerical Experiment of Tokamak (NEXT)

4.1 Development of Computational Algorithm

A fully compressible nonlinear MHD code has been developed in the torus geometry to investigate the dynamics of collapse events in high beta plasmas. The code is based on the cell-centered finite-volume method in the poloidal plane, and on the pseudo-spectral method in the toroidal direction. Thus, the nonlinear dynamics is readily simulated without any singularities at the magnetic axis. However, in general, the numerical MHD code may generate non-zero divergence of the magnetic field. Therefore, in order to maintain the divergence free constraint of the magnetic field numerically, only the poloidal component of the rotation is defined at the edges of the discrete element in our code. As a result, the divergence free condition is naturally satisfied, and the numerical instabilities caused by unphysical magnetic monopole can be removed [4.1-1].

References

- [4.1-1] Miyoshi T. and NEXT group, "A spatial discretization of the MHD equations based on the finite volume - spectral method", JAERI-Research, 2000-023 (2000)

4.2 Transport and MHD Simulation

In order to clarify the kinetic effects on the MHD phenomena in the Reversed Shear Configuration (RSC) due to the particle properties of plasma such as the electron inertia, we have extended the previous gyro-kinetic simulation to the RSC. Using these simulation models, we study the linear and nonlinear dynamics of the kinetic double tearing modes. It is shown that by the coupling of two perturbations originated in each resonant surface, these modes grow up at the Alfvén time scale. It is also found that not only $m=1$ mode but also $m=2$ mode induce the internal collapse. After the internal collapse, the radial electric field grows by the kinetic effect

due to the density gradient [4.2-1, 4.1-2].

The new theoretical model, which determines the penetration depth of a compact toroid (CT) injected into a magnetized target plasma region, is represented from the result of MHD simulations. In the penetration process, the CT is influenced by the plasma compressibility, the magnetic pressure force, the magnetic tension force and magnetic reconnection between the CT magnetic field and the target one and so on. How these physical mechanisms affect the penetration process of the CT is examined. As a result, it is revealed that 1) the magnetic tension force, which is caused by the bent target magnetic field through the CT penetration process, effectively decelerates the CT, 2) magnetic reconnection between the CT magnetic field and the target magnetic field relaxes the CT deceleration [4.1-3].

References

- [4.2-1] Matsumoto T., Tokuda S., Kishimoto Y., et al., "Gyro-Kinetic Particle Simulation of $m=1$ Internal Kink Mode in the Presence of Density Gradient", *J. Plasma and Fusion Res.*, **75** 1188 (1999).
- [4.2-2] Matsumoto T., Tokuda S., Kishimoto, Y., et al., "Complex Behavior of Internal Collapse Due to Self-generated Radial Electric Field", *J. Plasma and Fusion Res. SERIES*, Vol.2, 97 (1999).
- [4.2-3] Suzuki Y., Hayashi T. and NEXT group, "Three-Dimensional Dynamics of a Compact Torus Injected into Magnetized Plasmas II", *J. Plasma and Fusion Res.*, **76** 288 (2000), in Japanese.

4.3 Divertor Simulation

We have developed a two-dimensional divertor simulation code, SOLDOR, with a fluid model by adopting the TVD scheme to accurately solve steep profiles. Non-orthogonal meshes can be treated, which are superior for complex divertor geometries. Transport of neutral particles is calculated by a Monte-Carlo method. We have obtained numerical solutions with high convergence speed and high accuracy. Simulation results showed that a W-shaped divertor configuration in JT-60U enhances the particle recycling efficiently, and the cold and dense plasma is easily formed near the divertor plate. It was also shown the detached divertor plasma is formed when the SOL plasma density becomes much higher [4.3-1].

Effect of radial electric field on SOL plasma and sheath formation is studied by the use of a particle simulation code PARASOL [4.3-2]. The flow pattern and the density profile in the SOL plasma become asymmetric due to the $E_r \times B$ drift. The condition of the sheath formation is clarified; at the sheath entrance, the flow velocity normal to the divertor plate is larger than a specific sound speed projected in the normal direction. The asymmetry of the SOL plasma is principally brought by this boundary condition. The asymmetry becomes large with the increase of $E_r \times B$ drift velocity. When the velocity exceeds a critical value, the detached divertor with very low density is formed in a divertor region where $E_r \times B$ drift flows out from the plate.

References

- [4.3-1] Shimizu K., Takizuka T., Hirayama T., "A Time Dependent 2D Divertor Code with TVD Scheme for Complex Divertor Configurations", 41th Annual Meeting of APS, Seattle, (1999).
- [4.3-2] Takizuka T., Hosokawa M., "Particle Simulation Study of the Effect of Radial Electric Field on Scrape-off Layer Plasma and Sheath Formation", *Contrib. Plasma Phys.*, **40** 471 (2000).

IV. FUSION REACTOR DESIGN AND SAFETY RELATED RESEARCH

1. Fusion Reactor Design

Based on the previous design studies of a Steady-State Tokamak Reactor (SSTR) in 1990, Advanced SSTR (A-SSTR)[1] in 1996 and a concept of DREAM reactor [2], a new tokamak fusion power reactor (A-SSTR2) which meets both economical and environmental requirements was developed in 1999.

Table 1 shows basic parameters of A-SSTR2. In the A-SSTR2, a combination of high toroidal field (11T on plasma axis and peak field of 23T) and moderate beta ($\beta_N=4$) is chosen for achieving the high fusion power (4 GW) and the compact machine size ($R_p=6.2$ m). Eliminating the center solenoid (CS) coil generates the space for the supporting structure required by the enormous electromagnetic force on the TF coils. Numerical simulation revealed the possible plasma equilibrium solution, plasma break down and plasma current ramp with CS-less configuration. It takes about 2000 s for the initial current ramp-up phase up to the plasma current of 2 MA. The ignition approach time from 2 MA to 12 MA is about 22 hours, where the linkage flux of -52.4 Vs is taken into account. For the plasma vertical position control, the passive shell structure is located behind the blanket structures. The shell structure is made of a low activation vanadium alloy with a resistivity of $4.8 \times 10^{-7} \mu$ and the thickness of 5 cm can suppress the vertical instability growth rate to 40 sec^{-1} . The MHD stability against the ballooning mode and the ideal low n kink-modes are confirmed by ERRATO-J code. The n=1 and n=2 kink modes can be avoided by the shell position closer than 1.4 and 1.2 times of the plasma minor radius, respectively. As to the divertor thermal condition, it was found that 2.2 % Ar seeding or 0.5 % Kr seeding into the divertor plasma region could lower the thermal power onto the divertor plate from 460 MW to 100 MW and the plasma temperature from 200 eV to 20~30 eV.

Table 1 A-SSTR2 Parameters

Plasma current	12MA
Major radius	6.2m
Aspect ratio	4
Toroidal field	11T
Max. Toroidal field	23T
Fusion power	4.0GW
Current drive	60MW
Normalized beta	4.0
Electron density	$2.0 \times 10^{20} \text{m}^{-3}$
Max. Neutron load	8MW/m ²
Blanket heat flux	2MW/m ²
Max. coolant temp.	900°C
Coolant	He

References

- [1-1] Kikuchi, M., Fusion Technology 30(3) Part 2B (1996)1631.
- [1-2] Nishio S., et al., 16th IAEA Fusion Energy Conf. Vol 3 (1997) 693.

2. Fusion Safety

2.1 Study of In-vessel Abnormal Events

This study aims to prepare analytical evaluation techniques and codes to guarantee and enhance the safety of the future fusion reactors.

In the verification on the TRAC-BF1 code to analyze the ingress of coolant event (ICE) phenomenon^[2-1], we participated in the benchmark calculation of thermohydraulic analysis code for

fusion reactor carried out under the IEA international cooperation. In the benchmark meeting, the comparative discussion of the calculation results by thermohydraulic analysis codes (CATHARE, PAXITR, MELCOR, INTRA, CONSEN, TRAC-BF1, etc.) was carried out for the several problems distributed in advance. The TRAC-BF1 code showed partly different results in comparison with other codes, probably due to the difference of constitutive equations or steam tables used in each code.

In order to evaluate the structural integrity of the power reactor, the stability analysis of a crack in the breeder blanket first wall was carried out with ADINA code for the DREAM reactor. It was revealed that the area around the crack was in the compression stress state under the condition without thermal bending, creep and fatigue.

The loss of vacuum accident (LOVA) phenomenon of the fusion reactor was analyzed using the STREAM code. It was confirmed that the replacement flow behavior could be simulated by dividing more than 10 elements for a breach of the vacuum vessel using the turbulent flow analysis model in the compressible fluid. The construction of the physical model simulating the LOVA experimental result was almost finished.

In the improvement of the DYNAS code^[2-21], the time response of inventory change in pulse operation was tracked. Multistage evaluation model of the isotope separation system column was made, and simple calculation code development in search of the equilibrium solution was almost finished. The man-machine interface function was improved.

2.2 Comparison of the Biological Hazard Potential in Fusion Reactor, Light-water Reactor and Coal-fired Power Plant

Radiological toxic hazard potential to be taken in the body through the inhalation or the ingestion is compared among all the radioactive materials contained in a fusion reactor, a pressurized light water reactor and a coal-fired power plant.

A fusion prototype reactor SSTR (1.08 million kWe) with the low activation steel (F82H) as a structure material was analyzed with the ANISN code to calculate the radioactive nuclides, assuming the blanket is replaced in every two years, and other structures are run for 30 years at the plant availability factor 100%. Tritium inventory of 4.5kg is taken into consideration in this evaluation.

A pressurized light water reactor power plant generating one million kW electricity is selected as a typical light water reactor. Only nuclear fuel was taken into consideration in this evaluation, and the irradiated structural materials were ignored. The nuclear fuel uses the uranium dioxide (UO₂) of 4.1% enrichment to the burn-up of 33,000 MWd/t, generating spent fuels of 25 tons per year. The radiological toxic hazard potential and the attenuation throughout the long term after the 30 years operation were evaluated by using ORIGEN2 code.

Concerning fire-powered plant, coal ashes, that are the fly ashes mixed with the solid, are

evaluated in a coal-fired power plant with one million kW electricity. According to the literature, the amounts of coal burnt by operating 1 million kW coal-fired power plant for 30 years and its ash are 0.9 and 0.21 hundred million tons, respectively. Time change of the radiological toxic hazard potential of coal ash discharged from the coal-fired power plant was obtained by using the ORIGEN2 code from radionuclides contained in the coal.

Comparison of the radiological toxic hazard potentials concerning with the inhalation and the ingestion intake is shown in Figure IV.2-1. The fusion reactor SSTR has smaller hazard potentials than the light water reactor PWR all the time. The ratio of hazard potentials between the fusion reactor and the light water reactor becomes 100 ~ 1000 times just after the operation and 1000 ~ 10000 times after 1 year. Since then, the difference rapidly increases and becomes about 1000000 ~ 10000000 times after 100 years. In comparison with coal-fired power plant, hazard potential of a fusion reactor is 100 ~ 1000 larger just after the operation. It becomes equivalent to that of the coal-fired power plant in about 20 years, because the coal ash contains long life radio nuclides.

References

- [2-1] Kurihara R., Ajima T., Ueda S., Seki Y., “3-D Analysis on Ingress of Coolant Event in ITER Vacuum Vessel Using Modified TRAC-BF1”, Proceedings of ISFNT-5, Rome (1999).
- [2-2] Aoki I., Seki Y., Sasaki K., et al., “Development of Dynamic Simulation Code for Fuel Cycle of Fusion Reactor”, JAERI-Data/Code 99-004 (1999).

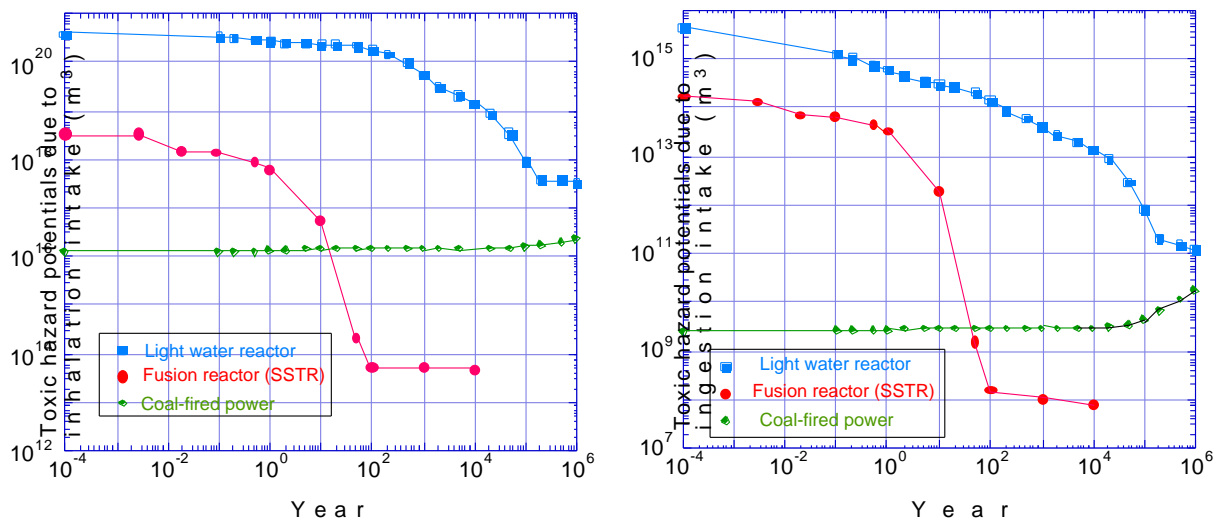


Fig. IV.2-1 Comparison of the radiological toxic hazard potentials due to inhalation intake, in the fusion reactor, the light water reactor and the coal-fired power plant. Standards are U.S.A. 10 CFR Pt.20 App. B Table 2 (Effluent Concentration).

Appendix A.1 Publication List (April 1999 - March 2000)

A.1.1 List of JAERI report

- 1) Fujiwara Y., Hanada M., Miyamoto K., et al., "Thermo-mechanical Analysis of an Acceleration Grid for the ITER-NBI System", JAERI-Tech 99-051 (1999).
- 2) Fujiwara Y., Inoue T., Miyamoto K., et al., "Experimental Study on the Influence of Radiation on High-voltage Insulation Gases", JAERI-Research 99-071 (1999).
- 3) Hashimoto M., Morimoto I., Zheng X., et al., "Evaluation of Ferromagnetic Materials for Induction Linacs", JAERI-Research 2000-18 (2000).
- 4) Hoek M., Nishitani T., Takahashi H., et al., "The JT-60U 2.45 MeV Neutron Time-of-flight Spectrometer", JAERI-Research 99-061 (1999).
- 5) Ida M., Nakamura H., Sugimoto M., et al., "IFMIF International Fusion Materials Irradiation Facility Conceptual Design Activity, Reduced Cost Report; A Supplement to the CDA by the IFMIF Team", JAERI-Tech 2000-014 (2000).
- 6) Department of Fusion Plasma Research, "Proc. of 6th IAEA TCM on Energetic Particles in Magnetic Confinement Systems, Oct. 1999, Naka, Japan", JAERI-Conf 2000-004 (2000).
- 7) Department of Fusion Plasma Research, "Proc. of the 5th Australia-Japan Workshop on Plasma Diagnostics, December 15-17, 1999, Naka, Japan", JAERI Conf 2000-007 (2000).
- 8) Ikeda Y., "Basic Design Study of the Injection System of the 110GHz Local Heating and Current Drive System on JT-60U", JAERI-Research 99-061 (1999).
- 9) Inoue T., Miyamoto K., Nagase A., et al., "Steering of High Energy Negative Ion Beam and Design of Beam Focusing/Deflection Compensation for JT-60U Large Negative Ion Source", JAERI-Tech 2000-23 (2000).
- 10) Itoh T., Yamazaki H., Usui K., et al., "Surface Level Measurement of a Liquid Cesium with Float with Marker Magnet for Cesium Feeding System in the Negative Ion Source", JAERI-Tech 99-066 (1999).
- 11) Iwai Y., Yamanishi T. and Nishi M., "Study on Cascade Configuration and Hydrogen Isotope Inventory of Cryogenic Distillation Columns for Isotope Separation System of the ITER Tritium Plant", JAERI-Tech 2000-002, (2000) (in Japanese).
- 12) JT-60 Team, "Review of JT-60U Experimental Results in 1998", JAERI-Research 99-048 (1999).
- 13) Koizumi N., "Non-uniform Current Distribution in a Force-cooled Superconductor under Changing Magnetic Field", JAERI-Research 99-076 (2000).
- 14) Liqun HU., Akino N. and Ebisawa N., "Power Loading on the Beanline Components and Beam Divergence of the Negative-Ion Based NBI System for JT-60U", JAERI-Tech 99-057 (1999).
- 15) Maekawa F., Wada M. and Ikeda Y., "Decay Heat Experiment and Validation of Calculation Code Systems for Fusion Reactor", JAERI-Research 99-055 (1999).
- 16) Morimoto I., Kishiro J., Takayama K., et al., "Beam Transport Study of kA Class on the Induction Linac", JAERI-Research 2000-8 (2000).

- 17) Neudatchin S.V., Takizuka T., Shirai H., et al., "Analysis of Internal Transport Barrier Heat Diffusivity from Heat Pulse Propagation Created by Abrupt Variation of Diffusivity in JT-60U Reverse Shear Plasmas", JAERI-Research 99-063 (1999).
- 18) Ohmori J. and Araki M., "Assessment of Buckling for Vacuum Vessel and Back Plate of RC-ITER (IAM-V2)", JAERI-Tech 2000-06 (2000).
- 19) Oka K., et al., "Design of Remote Handling Equipment for the ITER NBI", JAERI-Tech 99-055 (1999).
- 20) Oka K., et al., "Development of Pipe Welding Cutting and Inspection Tools for the ITER Blanket", JAERI-Tech 99-048 (1999).
- 21) Oya Y., Shu W., Ohira S., et al., "Results of Preliminary Experiments on Tritium Decontamination by UV Irradiation", JAERI-Tech 2000-010 (2000).
- 22) Sugai H., "Study on Defect State and Tritium Behavior in Neutron-irradiated Li-Al Alloy", JAERI-Research 99-041 (1999).
- 23) Suzuki T., Morimoto I., Zheng X., et al., "Design of Alternately-slanted Focusing Wiggler for mm wave FEL and the Evaluation of FEL Performance", JAERI-Research 99-025 (1999).
- 24) Taguchi K., et al., "Development of Super Elastic Alloy Seal Gasket", JAERI-Tech 99-079 (1999).
- 25) Watanabe K., Higa O., Kawashima S., et al., "Design of Neutral Beam Injection Power Supplies for ITER", JAERI-Tech 2000-033 (2000).
- 26) Yamazaki H., Itoh T., Usui K., et al., "Development of Heat Conduction Type Cesium Injection Device for Negative-Ion Source for JT-60U", JAERI-Tech 99-054 (1999) (in Japanese).

A.1.2 List of papers published in journals

- 1) Ando T., Hiyama T., Takahashi Y., et al., "Completion of the ITER CS Model Coil-Outer Module Fabrication", IEEE Trans. Appl. Supercond., **10** 568 (2000).
- 2) Ando T., Hiyama T., Takahashi Y., et al., "Development of a 13T-640MJ Superconducting Pulsed Coil for Fusion Machines", Trans. IEE Japan, **120-B** 449 (2000) (in Japanese).
- 3) Ando T., Hiyama T., Takahashi Y., et al., "Fabrication of ITER Central Solenoid Model Coil -Outer Module-", IEEE Trans. Appl. Supercond., **9** 6281 (1999).
- 4) Asakura N., Hosogane N., Itami K., et al., "Role of Divertor Geometry on Detachment and Core Plasma Performance in JT-60U", J. Nucl. Mater., **266-269** 182 (1999).
- 5) Asakura N., Sakurai S., Hosogane N., et al., "Heat and Particle Transport of SOL and Divertor Plasma in the W-shaped Divertor on JT-60U", Nucl. Fusion, **39** 1983 (1999).
- 6) Asakura N., Sakurai S., Shimada M., et al., "Measurement of Natural Plasma Flow along the Field Lines in the Scrape-off Layer on the JT-60U Divertor Tokamak", Phys. Rev. Lett., **84** 3093 (2000).
- 7) Bak P. E., Yoshino R., Asakura N., et al., "Identification of Unstable Periodic Orbit in Inter-Edge-Localized-Mode Intervals in JT-60U", Phys. Rev. Lett., **83** 1339 (1999).
- 8) Boscary J., Araki M., Suzuki S., et al., "Critical Heat Flux in Subcooled Water Flow of One-side-heated Screw Tubes", Fusion Technol., **35** 289 (1999).
- 9) Dnestrovskii Yu.N., Takizuka T., Shirai H., et al., "Test of Canonical Profiles and Semi-empirical Transport Models with JT-60U Plasmas", Nucl. Fusion, **39** 2089 (1999).
- 10) Fujita T., Kamada Y., Ishida S., et al., "High Performance Experiments in JT-60U Reversed Shear Discharges", Nucl. Fusion, **39** 1627 (1999).
- 11) Fukuda T., Takizuka T., Tsuchiya K., et al., "Reduction of L-H Transition Threshold Power under W-shaped Pumped Divertor Geometry in JT-60U", Plasma Phys. Control. Fusion, **43** A289 (2000).
- 12) Fukuda T. and the JT-60 Team, "Active Feedback Control of Steady-state Improved Confinement Discharges in JT-60U", Fusion Eng. Des., **46** 337 (1999).
- 13) Fukumoto N., Nagata M., Uyama T., et al., "Specification of Compact Toroid Injector and Initial Injection Experiment into Tokamak Plasma", Trans. IEE Japan, **119-A** 1300 (1999).
- 14) Hamajima K., Hanai T., Wachi Y., et al., "AC Loss Performance of 100kwh SMES Model Coil", IEEE Trans. Appl. Super., **10** 812 (2000).
- 15) Hayashi N., Takizuka T., Hatayama A., et al., "Numerical Analysis of Thermoelectric Instability in Tokamak Divertor", J. Nucl. Mater., **266-269** 526 (1999).
- 16) Hayashi T., Kobayashi K. and Nishi M., "Tritium Confinement and Detritiation Demonstration Program for Fusion Reactor Rooms using Caisson Assembly for Tritium Safety Study (CATS) at TPL/JAERI", J. Health Phys., **31** 112 (2000) (in Japanese).
- 17) Higashijima S. and the JT-60 Team, "Wall Conditioning to Control Impurity and Hydrogen Isotope Recycling in JT-60U", J. Plasma Fusion Res., **75** 1297 (1999) (in Japanese).

- 18) Higashijima S., Kubo H., Sugie T., et al., "Carbon Impurity Behavior in W-shaped Pumped Divertor of JT-60U", *J. Nucl. Mater.*, **266-269** 1078 (1999).
- 19) Hiroki S., Ladd P., Shaubel K., et al., "Leak Detection System in ITER", *Fusion Eng. Des.*, **46** 11 (1999).
- 20) Hoek M., Nishitani T., Takahashi H., et al., "Results from Monte Carlo Simulation of the Neutron Transport of the New 2.45 MeV Neutron Time-of-flight Spectrometer for the JT-60U Tokamak", *Fusion Eng. Des.*, **45** 437 (1999).
- 21) Honda T., Bartels H.-W., Inabe T., et al., "Analysis of Loss of Vacuum Accident (LOVA) in ITER", *Fusion Eng. Des.*, **47** 361 (2000).
- 22) Ide S. and the JT-60 Team, "Latest Progress in Steady State Plasma Research on Japan Atomic Energy Research Institute Tokamak-60 Upgrade", *Phys. Plasmas*, **7** 1927 (2000).
- 23) Ide S., Naito O., Oikawa T., et al., "LHCD Current Profile Control Experiments towards Steady State Improved Confinement on JT-60U", *Nucl. Fusion*, **40** 445 (2000).
- 24) Ido T., Kamiya K., Hamada Y., et al., "Behavior of Sample Volumes of the Heavy Ion Beam Probe on JFT-2M", *Plasma Phys. Control. Fusion*, **41** 1013 (1999).
- 25) Ido T., Kamiya K., Miura Y., et al., "Temporal Behavior of the Potential and Fluctuations at the L/H Transition on JFT-2M", *Plasma Phys. Control. Fusion*, **42** A309 (2000).
- 26) Idomura Y., Tokuda S. and Wakatani M., "Gyrokinetic Theory of Slab Ion Temperature Gradient Mode in Negative Shear Tokamaks", *Phys. Plasmas*, **6** 4658 (1999).
- 27) Iida H., Valenza D., Plenteda R., et al., "Radiation Shielding for ITER to Allow for Hands-on Maintenance inside the Cryostat", *J. Nucl. Sci. Technol.*, **Supplement 1** 235 (2000).
- 28) Inoue T., Pietro E.Di., Mondino P.L., et al., "Neutral Beams for the International Thermonuclear Experimental Reactor", *Rev. Sci. Instrum.*, **71** 744 (2000).
- 29) Ishida S. and the JT-60 Team, "JT-60U High Performance Regimes", *Nucl. Fusion*, **39** 1211 (1999).
- 30) Ishijima T., Kubo H., Shimada M., et al., "Radiation and Spectroscopy Analysis of Divertor Discharges with Neon Gas Puff in JT-60U", *Plasma Phys. Control. Fusion*, **41** 1155 (1999).
- 31) Ishiyama S., Akiba M. and Eto M., "Thermal and Irradiation Induced Stress Analysis on Relevant Target Plate Structure of the Divertor for Fusion Experimental Reactors", *J. Nucl. Sci. Technol.*, **37** 90 (2000).
- 32) Ishizawa A. and Tokuda S., "Improved Boundary Layer Analysis of Forced Magnetic Reconnection due to a Boundary Perturbation", *Phys. Plasmas*, **7** 875 (2000).
- 33) Isobe K., Hatano Y., Sugisaki, et al., "Observation of Spatial Distribution of Tritium in Zirconium Alloy with Microautoradiography", *J. Nucl. Mater.*, **271-272** 326 (1999).
- 34) Itami K., Hosogane N., Konoshima S., et al., "Radiative Plasma by Impurity Seeding in W-shaped Pumped Divertor Experiment of JT-60U", *J. Nucl. Mater.*, **266-269** 1097 (1999).
- 35) ITER Physics Basic Editors*, et al., (* Perkins F.W., Post D.E., Azumi M., et al.) "ITER Physics Basis, Chapter 1: Overview and Summary", *Nucl. Fusion*, **39** 2137 (1999).

- 36) ITER Physics Expert Groups* on Confinement and Transport and Confinement Modelling and Database, et al., (* Wakatani M., Mukhovatov V.S., Mori M., et al.) "ITER Physics Basis, Chapter 2: Plasma Confinement and Transport", Nucl. Fusion, **39** 2175 (1999).
- 37) ITER Physics Expert Group* on Disruptions, Plasma Control, and MHD, et al., (* Mirnov S., Wesley J., Tokuda S., et al.) "ITER Physics Basis, Chapter 3: MHD Stability, Operational Limits and Disruptions", Nucl. Fusion, **39** 2251 (1999).
- 38) ITER Physics Expert Group* on Divertor, et al., (* Stambaugh R., Janeschitz G., Hosogane N., et al.) "ITER Physics Basis, Chapter 4: Power and Particle Control", Nucl. Fusion, **39** 2391 (1999).
- 39) ITER Physics Expert Group* on Energetic Particles, Heating and Current Drive, et al., (* Jacquinot J., Putvinski S., Tobita K., et al.) "ITER Physics Basis, Chapter 5: Physics of Energetic Ions", Nucl. Fusion, **39** 2471 (1999).
- 40) ITER Physics Expert Group* on Energetic Particles, Heating and Current Drive, et al., (* Jacquinot J., Putvinski S., Tobita K., et al.) "ITER Physics Basis, Chapter 6: Plasma Auxiliary Heating and Current Drive ", Nucl. Fusion, **39** 2495 (1999).
- 41) ITER Physics Expert Group* on Diagnostics, et al., (* Young K.M., Costley A.E., Nagashima A., et al.) "ITER Physics Basis, Chapter 7: Measurement of Plasma Parameters", Nucl. Fusion, **39** 2541 (1999).
- 42) ITER Physics Expert Group* on Disruptions, Plasma Control, and MHD, et al., (* Mirnov S., Wesley J., Tokuda S., et al.) "ITER Physics Basis, Chapter 8: Plasma Operation and Control", Nucl. Fusion, **39** 2577 (1999).
- 43) ITER Physics Basic Editors*, et al., (* Perkins F.W., Post D.E., Azumi M., et al.) "ITER Physics Basis, Chapter 9: Opportunities for Reactor Scale Experimental Physics", Nucl. Fusion, **39** 2627 (1999).
- 44) Kamada Y., Hatae T., Fukuda T., et al., "Growth of the Edge Pedestal in JT-60U ELMy H-mode", Plasma Phys. Control. Fusion, **41** 1371 (1999).
- 45) Kamada Y., Isayama A., Oikawa T., et al., "Long Sustainment of JT-60U Plasmas with High Integrated Performance", Nucl. Fusion, **39** 1845 (1999).
- 46) Kamada Y. and the JT-60 Team, "Extension of the JT-60U Plasma Regimes toward the Next-step Experimental Reactor", Plasma Phys. Control. Fusion, **41** B77 (1999).
- 47) Kashiwagi M., Ido S. and Okumura Y., "Computational Studies on Ion Source Plasmas of the Neutral Beam Injection System", Rev. Sci. Instrum., **71** 747 (2000).
- 48) Kawai M., Kazawa M., Mogaki K., et al., "Study of Plasma Uniformity on JT-60 Negative Ion Source," Rev. Sci. Instrum., **71** 755 (2000).
- 49) Kawamura Y., Enoda M., et al., "Adsorption Isotherms of Various Adsorbents at Liquid Nitrogen Temperature", Fusion Technol., **37** 536 (2000).
- 50) Kawano Y., Chiba S., Shirai H., et al., "Dual CO₂ Laser Polarimeter for Faraday Rotation Measurement in Tokamak Plasmas", Rev. Sci. Instrum., **70** 714 (1999).
- 51) Kawano Y., Chiba S., Shirai H., et al., "First Measurement of Tangential Faraday Rotation of CO₂ Laser Wave in a Tokamak Plasma", Rev. Sci. Instrum., **70** 1430 (1999).

- 52) Kawashima H., Sengoku S., Ogawa T., et al., "Study of a Closed Divertor with Strong Gas Puffing on JFT-2M", Nucl. Fusion, **39** 1679 (1999).
- 53) Kinsho M., Sugimoto M., Seki M., et al., "Development of High Intensity Deuteron Ion Source for the Fusion Intense Neutron Source", Rev. Sci. Instrum., **71** 963 (2000).
- 54) Kishimoto Y., Kim J. Y., Horton W., et al., "Discontinuity Model for Internal Transport Barrier Formation in Reversed Shear Plasmas", Nucl. Fusion, **40** 667 (2000).
- 55) Kishimoto Y. and Tajima T., "Strong Coupling between Clusters and Radiation", "High Field Science", Eds. T. Tajima, K. Mima, and H. Baldis (Plenum, NY, 1999) 85.
- 56) Kobayashi M., Tuda T., Tashiro K., et al., "Interaction of Externally Applied Rotating Helical Field with Tokamak Plasma", Nucl. Fusion, **40** 181 (2000).
- 57) Koizumi N., Ando T., Matsui K., et al., "Development of Nb₃Al Superconductors for International Thermometer Experimental Reactor (ITER)", Cryogenics, **39** 155 (1999).
- 58) Koizumi N., Ando T., Matusi K., et al., "Development of Nb₃Al Superconductors for ITER", IEEE Trans. Appl. Supercond., **9** 2688 (1999).
- 59) Koizumi N., Azuma K., Macfall K., et al., "Quasi-two-dimensional Numerical Mode for Stability Simulation of a Cable-in-conduit Conductor", Cryogenic, **39** 495 (1999).
- 60) Koizumi N., Takahashi Y., Kato T., et al., "Induced Circulation Current in a Conductor Consisting of Strands Coated with High Resistive Layer", Cryogenic Eng., **35** 132 (2000) (in Japanese).
- 61) Koizumi N., Takahashi Y., Tsuji H., et al., "Analysis of Current Distribution after Normal Transition in Multi-strand Cable using Distributed Model Circuit", Cryogenic Eng., **34** 395 (1999) (in Japanese).
- 62) Konno C., Maekawa F., Oyama Y., et al., "Experimental Investigation on Streaming due to a Gap between Blanket Modules in ITER", J. Nuc. Sci. Technol., **Supplement 1** 540 (2000).
- 63) Konno C., Maekawa F., Wada M., et al., "Analysis of Iron and Concrete Shielding Experiments for 43 and 68 MeV p-7Li Neutrons with LA150", J. Nucl. Sci. Technol., **Supplement 1** 187 (2000).
- 64) Kubo H., Goto M., Takenaga H., et al., "Study of Intensity Ratios of He I Lines (668 nm, 706 nm and 728 nm) for Measurement of Electron Temperature and Density in the JT-60U Divertor Plasma", J. Plasma Fusion Res. **75** 945 (1999).
- 65) Kubo H., Takenaga H., Kumagai A., et al., "Spectral Profile of the He I Singlet Line (667.82nm) Emitted from the Divertor Region of JT-60U", Plasma Phys. Control. Fusion, **41** 747 (1999).
- 66) Kumagai A., Kubo H., Takenaga H. et al., "Spatial Variation of D_α Line Spectral Profile and Emission Process in the Divertor Region of JT-60U", Plasma Phys. Control. Fusion, **42** 529 (2000).
- 67) Kurihara K., Kawamata Y., Akiba K., et al., "Plasma Real-time Control System for Advanced Tokamak Operation Scenarios in JT-60", Nucl. Sci., **47** 205 (2000).
- 68) Kuriyama M., Akino N., Ebisawa N., et al., "Power Flow in the Negative-ion Based Neutral Beam Injection for JT-60", Rev. Sci. Instrum., **71** 751 (2000).
- 69) Kusama Y. and the JT-60 Team, "Recent Progress in High Performance and Steady-state Experiments on the Japan Atomic Energy Research Institute Tokamak-60 Up-grade with W-shaped Divertor", Phys. Plasmas, **6** 1935 (1999).

- 70) Kusama Y., Kramer G. J., Saigusa M., et al., "Characteristics of Alfvén Eigenmodes, Burst Modes and Chirping Modes in the Alfvén Frequency Range Driven by Negative Ion Based Neutral Beam Injection in JT-60U", Nucl. Fusion, **39** 1837 (1999).
- 71) Kusama Y., Kimura H., Nemoto M., et al., "Production and Confinement Characteristics of ICRF-accelerated Energetic Ions in JT-60U Negative-shear Plasma", Plasma Phys. Control. Fusion, **41** 625 (1999).
- 72) Kusama Y., Fu G.Y., Kramer G.J., et al., "Destabilization of Ellipticity-induced Alfvén Eigenmodes during ICRF Heating and Stabilization by Negative-ion-based Neutral Beam Injection in JT-60U", Plasma Phys. Control. Fusion, **41** 1167 (1999).
- 73) Leonard A.W., Hermann A., Itami K., et al., "The Impact of ELMs on the ITER Divertor", J. Nucl. Mater., **266-269** 109 (1999).
- 74) Loarte A., Bosch S., Shimada M., et al., "Multi-machine Scaling of the Divertor Peak Heat Flux and Width for L-mode and H-mode Discharges", J. Nucl. Mater., **266-269** 587 (1999).
- 75) Loarte A., Kukushkin A.S., Shimada M., et al., "Comparison of B2-EIRENE Calculations with Multi-machine Experimental Measurements", J. Nucl. Mater., **266-269** 1123 (1999).
- 76) Maeda M., Uehara K. and Amemiya H., "Measuring Method for Mach Number in Tokamak Edge Plasma Using Probes", Jpn. J. Appl. Phys., **38** 2971 (1999).
- 77) Maekawa F., et al., "Benchmark Experiment on Vanadium with D-T Neutrons and Validation of Evaluated Nuclear Data Libraries by Analysis of the Experiment", J. Nucl. Sci. Technol., **36** 242 (1999).
- 78) Maekawa F., et al., "Investigation of Prediction Capability of Nuclear Design Parameters for Gap Configuration in ITER through Analysis of the FNS Gap Streaming Experiment", J. Nucl. Sci. Technol., **Supplement 1** 263 (2000).
- 79) Maekawa F. and Ikeda Y., "Decay Heat Experiment on Thirty-Two Fusion Reactor Relevant Materials Irradiated by 14-MeV Neutrons", Fusion Eng. Des., **47** 377 (2000).
- 80) Maekawa F., Moellendorff U., Wilson P., et al., "Determination of Deuterium-Beryllium Neutron Source Spectrum by Multi-Foil Activation Technique" Fusion Technol., **36** 165(1999).
- 81) Maekawa F., Wada M. and Ikeda Y., "Development of Whole Energy Absorption Spectrometer for Decay Heat Measurement" Nucl. Instrum. Meth., **A450** 467 (2000).
- 82) Manickam J., Fujita T., Gorelenkov N., et al., "Localized MHD Activity near Internal Transport Barriers in JT-60U and TFTR", Nucl. Fusion, **39** 1819 (1999).
- 83) Matsukawa M., Miura, Y.M., Terakado, T., et al., "Preparations in the JT-60 Power Supply for Pulse Operation Test of ITER CS Model Coil", IEEE Trans. Appl. Supercond., **10** 1410 (2000).
- 84) Matsumoto T., Tokuda S., Kishimoto Y., et al., "Gyro-Kinetic Particle Simulation of m=1 Internal Kink Mode in the Presence of Density Gradient", J. Plasma Fusion Res., **75** 1188 (1999).
- 85) Matsumoto T., Tokuda S., Kishimoto, Y., et al., "Complex Behavior of Internal Collapse Due to Self-generated Radial Electric Field", J. Plasma Fusion Res., **SERIES 2** 97 (1999).
- 86) Miura, Y.M., Matsukawa M. and Nakano H., "A New Method of Switching Pulses Generation in Three-Phase PWM Current Source Type Converter", Trans. IEE Japan, **119D** 1022 (1999) (in Japanese).

- 87) Miyamoto N., Fujiwara Y., Miyamoto K., et al., "Steady State Operation of an Ampere-class Hydrogen Negative Ion Source", *Rev. Sci. Instrum.*, **71** 738 (2000).
- 88) Mondino P.L., Bayetti P., Okumura Y., et al., "ITER Neutral Beam System", *Nucl. Fusion*, **40** 501 (2000).
- 89) Murayama S., Sekine C., Nakano T., et al., "Spin-density-wave Transition and mSR in the Heavy-fermion Ce(Ru,T)₂Si₂, T=Rh, Pd", *Physics of Strongly Correlated Electron Systems JJAP*, **Series 11** 15 (2000).
- 90) Murayama S., Sekine C., Yotsuya S., et al., "Magnetic Properties of Heavy-fermion Ce(Ru_{1-x}Pdx)₂Si₂", *Physica*, **B281&282** 343 (2000).
- 91) Naito O., Yoshida H., Kitamura S., et al., "How Many Wavelength Channels Do We Need in Thomson Scattering Diagnostics?", *Rev. Sci. Instrum.*, **70** 3780 (1999).
- 92) Naitou H., Kobayashi T. and Tokuda S., "Stabilization of the Kinetic Internal Kink Mode by a Sheared Poloidal Flow", *J. Plasma Phys.*, **61** 543 (1999).
- 93) Neudatchin S.V., Takizuka T., Shirai H., et al., "Abrupt in Time and Wide in Space Variations of Heat Diffusivity during ITB Formation in JT-60U Reverse Shear Discharges", *Plasma Phys. Control. Fusion*, **41** L39-L47 (1999).
- 94) Neyatani Y., Yoshino R., Nakamura Y., et al., "Characteristics of Halo Current in JT- 60U", *Nucl. Fusion*, **39** 559 (1999).
- 95) O'hira S., Hayashi T., Nakamura H., et al., "Improvement of Tritium Accountancy Technology for the ITER Fuel Cycle Safety Enhancement", *Nucl. Fusion*, **40** 519 (2000).
- 96) Oda T., Hirohata Y., Hino T., et al., "Hydrogen Retention of V-alloy under Plasma Irradiation of JFT-2M", *J. Vac. Soc. Jpn.*, **43** 325 (2000).
- 97) Ogawa H., Miura Y., Fukumoto N., et al., "Studies of Boundary Plasmas and Fueling on the JFT-2M", *J. Nucl. Mater.*, **266-269** 623 (1999).
- 98) Ogawa T., Fukumoto N., Nagata M., et al., "Compact Toroid Injection Experiment in JFT-2M", *Nucl. Fusion*, **39** 1911 (1999).
- 99) Oguri H., Tomisawa T., Kinsho M., et al., "Development of a H-ion Source for the High Intensity Proton Linac at Japan Atomic Energy Research Institute", *Rev. Sci. Instrum.*, **71** 975 (2000).
- 100) Oikawa T., Ushigusa K., Forest C. B., et al., "Heating and Non-inductive Current Drive by Negative Ion Based NBI in JT-60U", *Nucl. Fusion*, **40** 435 (2000).
- 101) Okumura Y., Fujiwara Y., Kashiwagi M., et al., "Negative Hydrogen Ion Source for Tokamak Neutral Beam Injector", *Rev. Sci. Instrum.*, **71** 1219 (2000).
- 102) Okumura Y., "Technologies of a Large Ion Source and High Heat Flux Handling for Fusion", *Energy Humanity*, **47** 38 (1999) (in Japanese).
- 103) Porter G.D., Davies S., Shimada M., et al., "Analysis of Separatrix Plasma Parameters Using Local and Multi-machine Databases", *J. Nucl. Mater.*, **266-269** 917 (1999).
- 104) Raffray A., Schlosser J., Akiba M., et al., "Critical Heat Flux Analysis and R&D for the Design of the ITER Divertor", *Fusion Eng. Des.*, **45** 377 (1999).

- 105) Sakasai A., Takenaga H., Hosogane N., et al., "Helium Exhaust in ELMy H-mode Plasmas with W-shaped Pumped Divertor of JT-60U", J. Nucl. Mater., **266-269** 312 (1999).
- 106) Sato M., Miura Y., Kimura H., et al., "Advanced Material Tokamak Experiment (AMTEX) Program with Ferritic Steel on JFT-2M", J. Plasma Fusion Res., **75** 741 (1999).
- 107) Sentoku Y., Ruhl H., Kishimoto Y., et al., "Plasma Jet Formation and Magnetic-field Generation in the Intense Laser Plasma under Oblique Incidence", Phys. Plasmas, **6** 2855 (1999).
- 108) Shimada M. and Ohkawa T., "Effect of Gyro-motion of Incident Ions on Inboard-outboard Asymmetry in Divertor Plasmas", J. Nucl. Mater., **266-269** 906 (1999).
- 109) Shinohara K., Nazikian R., Fujita T., et al., "Core Correlation Reflectometer at the JT-60U Tokamak", Rev. Sci. Instrum., **70** 4246 (1999).
- 110) Shirai H., Kikuchi M., Takizuka T., et al., "Improved Confinement and Neoclassical Effect", J. Plasma Fusion Res., **75** 444 (1999) (in Japanese).
- 111) Shirai H., Kikuchi M., Takizuka T., et al., "Reduced Transport and Er Shearing in Improved Confinement Regimes in JT-60U", Nucl. Fusion, **39** 1713 (1999).
- 112) Shu W., "General Formula of Tritium Permeation through Plasma Facing Materials", J. Plasma Fusion Research, **75** 409 (1999) (in Japanese).
- 113) Smith D.L., Maekawa F. and Ikeda Y., "Observation of Uranium Photo-Fission by 16N Decay Gamma Rays from Water Activated by D-T Fusion Neutrons", Fusion Eng. Des., **47** 403 (2000).
- 114) Sugimoto M., Isono T., Koizumi N., et al., "An Evaluation of the Inlet Flow Reduction for a Cable in Conduit Conductor by Rapid Heating", Cryogenics, **39** 939 (1999).
- 115) Sugimoto M., Isono T., Koizumi N., et al., "R&D Activity of SAGBO Avoidance for the CS Insert Fabrication", IEEE Trans. Appl. Supercond., **9** 636 (1999).
- 116) Sugimoto M., Kato T., Isono T., et al., "Flow Reduction by AC Losses for a Forced Flow Superconducting Coil with a Cable-in-conduit Conductor", Cryogenics, **39** 323 (1999).
- 117) Sugimoto M., "Completion of CS Insert Fabrication", IEEE Trans. Appl. Supercond., **10** 564 (1999).
- 118) Suzuki S., Sato K., Ezato K., et al., "Development of Divertor High Heat Flux Component for ITER in JAERI", Physica Scripta, **T81** 89 (1999).
- 119) Suzuki Y., Watanabe T., Sato T., et al., "Three-Dimensional Dynamics of a Compact Torus Injected into Magnetized Plasmas", J. Plasma Fusion Res., **75** (CD-ROM) (1999).
- 120) Suzuki Y., Watanabe T., Sato T., et al., "Three-Dimensional Dynamics of an Accelerated Compact Toroid in a Cylindrical Conductor", J. Plasma Fusion Res., **SERIES 2** 271 (1999).
- 121) Suzuki Y., Watanabe T., Sato T., et al., "Three-Dimensional Simulation Study of Compact Toroid Injection into Magnetized Plasmas", Chinese Physics Letters, **95** (2000).
- 122) Suzuki Y., Hayashi T. and NEXT group, "Three-Dimensional Dynamics of a Compact Torus Injected into Magnetized Plasmas II", J. Plasma Fusion Res., **76** 288 (2000) (in Japanese).
- 123) Suzuki Y., Watanabe T., Sato T., et al., "Three Dimensional Simulation Study of Spheromak Injection into Magnetized Plasma", Nucl. Fusion, **40** 277 (2000).

- 124) Takahashi Y., Nunoya Y., Nishijima G., et al., "Development of 46 kA Nb₃Sn Conductor Joint for ITER Model Coils", IEEE Trans. Appl. Supercond., **10** 580 (2000).
- 125) Takenaga H., Nagashima K., Sakasai A., et al., "Particle Confinement and Transport in JT-60U", Nucl. Fusion, **39** 1917 (1999).
- 126) Takenaga H., Sakasai A., Koide Y., et al., "Impurity Transport in Reversed Shear and ELMy H-mode Plasmas of JT-60U", J. Plasma Fusion Res., **75** 952 (1999).
- 127) Takigami H., Mitchell N., Okuno K., et al., "Predicted Thermohydraulic Performance of the ITER Central Solenoid Model Coil Conductors", IEEE Trans. Supercond., **10** 1070 (2000).
- 128) Tamai H., Asakura N., Hosogane N., et al., "Behaviour of Divertor Neutral Pressure at the Onset of an X-point MARFE in JT-60U", J. Plasma Fusion Res., **74** 1336 (1998).
- 129) Tamai H., Takenaga H., Asakura N., et al., "Particle Control and Behaviour of Neutrals in the Pumped W-shaped Divertor of JT-60U", J. Nucl. Mater., **266-269** 1219 (1999).
- 130) Tanimura Y., Kaneko J., Katagiri M., et al., "High-temperature Operation of a Radiation Detector Made of a Type Iia Diamond Single Crystal Synthesized by a HP/HT Method", Nucl. Instrum. Meth., **A443** 325 (2000).
- 131) Taylor N.P., Ikeda Y., Maekawa F., et al., "Experimental Validation of Calculations of Decay Heat Induced by 14 MeV Neutrons Activation of ITER Materials", Fusion Eng. Des., **45** 75 (1999).
- 132) Tchernychov F.V., Kusama Y., Nemoto M., et al., "Charge-exchange Measurements of D-D Triton Distribution Functions in High Power Neutral Beam Heating on JT-60U", Plasma Phys. Control. Fusion, **41** 1291(1999).
- 133) Tivey R., Ando T., Antipenkov A., et al., "ITER Divertor Design Issues and Research and Development", Fusion Eng. Des., **46** 207 (1999).
- 134) Tobita K., Hamamatsu K., Takizuka T., et al., "Numerical Analysis of Ripple Loss in Reversed Shear Tokamak Operation", J. Plasma Fusion Res., **75** 582 (1999) (in Japanese).
- 135) Tokuda S. and Watanabe T., "A New Eigenvalue Problem Associated with the Two-Dimensional Newcomb Equation without Continuous Spectra", Phys. Plasmas, **6** 3012 (1999).
- 136) Tokuda S. and Yoshino R., "Simulation Study on Collisionless Loss of Runaway Electrons by Magnetic Perturbations in a Tokamak", Nucl. Fusion, **39** 1123 (1999).
- 137) Tsintsadze L. N., Tajima T., Kishimoto Y., et al., "Generation of Low-Frequency Electromagnetic Waves by Spectrally Broad Intense Laser Pulses in a Plasma", Physica Scripta, **T84** 94 (2000).
- 138) Tsuneoka M., Asaka T., Nakayama N., et al., "Development of High Frequency Step-up Transformer for DC-DC Converter", Trans. IEEE Japan, **119-D** 1424 (1999).
- 139) Tsuneoka M., Imai T., Bowles E., et al., "The JA Home Team Design of the ITER ECRF Power Supply System", Fusion Eng. Des., **45** 197 (1999).
- 140) Tuda T., Ishii Y. and Kurita G., "Ideal/Resistive Mode Analysis in Reversed Shear Configuration Plasmas", Chinese Physics Letters, **83** (2000).
- 141) Tuda T., Kobayashi M., Kurita G., et al., "Interaction of Externally Applied Helical Field with Tokamak Plasma", Contribution to Plasma Phys., **40** 256 (2000).

- 142) Uda M., Ishitsuka E., Sato K., et al., "Thermal Shock Test of Neutron Irradiated Carbon Fiber Reinforced Carbon Composites with OHBIS", *Physica Scripta*, **T81** 98 (1999).
- 143) Watanabe K., Fujiwara Y., Hanada M., et al., "Hydrogen Negative Ion Beam Acceleration in a Multiaperture Five-stage Electrostatic Accelerator", *Rev. Sci. Instrum.*, **71** 1231 (2000).
- 144) Yamagiwa M., Koga J.K., Kishimoto Y., et al., "Ion Explosion and Multi-mega-electron-volt Ion Generation from an Underdense Plasma Layer Irradiated by a Relativistically Intense Short-pulse Laser", *Phys. Rev.*, **E 60** 5987 (1999).
- 145) Yamanishi T., Kawamura Y., Iwai Y., et al., "Development of a Tritium Fuel Processing System using an Electrolytic Reactor for ITER", *Nucl. Fusion*, **40** 515 (2000).
- 146) Yonekawa, I., Totsuka, T., Akasaka., et al., "Remodeling of JT-60 Discharge Control System," *Fusion Eng. Des.*, **48** 17 (2000).
- 147) Yoshida K., Krivchenkov K, Sborchia C., et al., "Pancake-wound Central Solenoid Coil for RC-ITER", *IEEE Trans. Supercond.*, **10** 576 (2000).

A.1.3 List of papers published in conference proceedings

- 1) Asakura N., Sakurai S., Hosogane N., et al., "Heat and Particle Transport of Sol/Divertor Plasma in the W-Shaped Divertor on JT-60U", Fusion Energy 1998 (CD-ROM, IAEA, Vienna), EXP4/06 (1999).
- 2) Cardella A., Barabash V., Ioki K., et al., "Application of Beryllium as First Wall Armour for ITER Primary Baffle and Limiter Modules", Proc. of 4th IEA Inter. Workshop on Beryllium Technology for Fusion (Karlsruhe), 192 (1999).
- 3) Costley A.E., Ebisawa K., Edmonds P., et al., "Plasma Diagnostics for RTO/RC-ITER", Proc. of 26th EPS Conf. on Cont. Fusion and Plasma Physics (Maastricht), **23J** 1098 (1999).
- 4) Costley A.E., ITER JCT and Home Teams et al., "ITER Diagnostics: A Successful Experience in International Collaboration", Proc. of 9th Int. Symp. Laser Aided Plasma Diagnostics (Lake Tahoe), 62 (1999).
- 5) Dnestrovski Yu.N., Lysenko S.E., Takizuka T., et al., "Verification of Canonical Profiles and Semi Empirical Transport Models against JT-60U Plasmas", Fusion Energy 1998 (CD-ROM, IAEA, Vienna), THP2/17 (1999).
- 6) Fujita T., Kamada Y., Ishida S., et al., "High Performance Experiments in JT-60U Reversed Shear Discharges", Fusion Energy 1998 (CD-ROM, IAEA, Vienna), EX1/2 (1999).
- 7) Fujii T. and Imai T., "Development of ECRF Components and System for ITER and JT-60U Tokamak", Proc. 4th Int. Workshop on Strong Microwaves in Plasmas, **2** 615 (2000).
- 8) Manickam J., Gorelenkov N., Fujita T., et al., "Localized MHD Activity Near Transport Barriers in JT-60U and TFTR", Fusion Energy 1998 (CD-ROM, IAEA, Vienna), EX8/4 (1999).
- 9) Fujiwara Y., Hanada M., Kashiwagi M., et al., "Acceleration Experiment of Hydrogen Negative Ion Beams up to 1MeV Using Multi-aperture Multi-stage Electrostatic Accelerator", Proc. BEAMS 1999 (Kyoto), 87 (1999).
- 10) Fujiwara Y., Kitagawa T., Takayanagi T. et al., "Improvement of Voltage-holding Characteristics of a FRP Insulator by Stress Shield Rings", Proc. of Japanese Electro-Technical Committee Meeting ED-99-176 (1999) (in Japanese).
- 11) Hamada Y., Ido T., Kamiya K., et al., "Fast Potential Changes at H-Mode Transition in the JFT-2M Tokamak", Fusion Energy 1998 (CD-ROM, IAEA, Vienna), PDP/01 (1999).
- 12) Hanada M., Akino N., Ebisawa N., et al., "Development of Multi-Mega Watt Negative Ion Sources and Accelerators for Neutral Beam Injectors", Fusion Energy 1998 (CD-ROM, IAEA, Vienna), FTP/20 (1999).
- 13) Hosogane N., Kubo H., Higashijima S., et al., "Divertor Characteristics and Control on the W-shaped Divertor with Pump of JT-60U", Fusion Energy 1998 (CD-ROM, IAEA, Vienna), EXP4/05 (1999).
- 14) Ide S., Naito O., Oikawa T., et al., "LHCD Current Profile Control Experiments towards Steady State Improved Confinement on JT-60U", Fusion Energy 1998 (CD-ROM, IAEA, Vienna), CD1/4 (1999).
- 15) Ikeda Y., Fujita T., Hamamatsu K., et al., "Resonant RF Activities on JT-60U", Proc. 13th Topical Conf. Appl. of Radio Frequency Power to Plasmas, 279 (1999).
- 16) Ikeda Y., Konno C., Maekawa F., et al., "ITER Relevant Neutronics Experiments at FNS", Fusion Energy 1998 (CD-ROM, IAEA, Vienna), ITERP2/03 (1999).

- 17) Ishida S. and the JT-60 Team "JT-60U High Performance Regimes", Fusion Energy 1998 (CD-ROM, IAEA, Vienna), OV1/1 (1999).
- 18) Ishitsuka E., Sagawa H., Nagashima A., et al., "Neutron Irradiation Test of Optical Components for Fusion Reactor", Effects of Radiation on Materials: 19th Int. Symp, ASTM STP 1366, (West Conshohocken), 1176 (2000).
- 19) Kamada Y., Isayama A., Oikawa T., et al., "Long Sustainment of JT-60U Plasmas with High Integrated Performance", Fusion Energy 1998 (CD-ROM, IAEA, Vienna), EX9/2 (1999).
- 20) Kasugai A., Takahashi K., Sakamoto K., et al., "High Power Operation of Gaussian Beam Gyrotron with CVD Diamond Window for JT-60U", Proc. of Radio Frequency Power in Plasmas, 449 (1999).
- 21) Kawano Y., "Infrared Interferometry / Polarimetry for Fusion Plasma Diagnostics", Proc. of 9th Int. Symp. on Laser-Aided Plasma Diagnostics (Lake Tahoe), 49 (1999).
- 22) Kawashima H., Sengoku S., Ogawa T., et al., "Study of Closed Divertor with Strong Gas-Puff on the JFT-2M", Fusion Energy 1998 (CD-ROM, IAEA, Vienna), EX3/4 (1999).
- 23) Kishimoto Y., Li J.Q., Koide Y., et al., "Discontinuity Model for Internal transport Barrier Formation in Reversed Magnetic Shear Plasmas", Fusion Energy 1998 (CD-ROM, IAEA, Vienna), TH1/2 (1999).
- 24) Kobayashi M., Tuda T., Takamura M., et al., "Experimental Investigation on Penetration of Rotating Magnetic Perturbations into the Tokamak Plasma", Proc. of 26th EPS Conf. on Cont. Fusion and Plasma Physics (Maastricht), 437 (1999).
- 25) Koide Y., Fujita T., Takizuka T., et al., "Formation Condition of Internal Transport Barrier in JT-60U Plasmas", Fusion Energy 1998 (CD-ROM, IAEA, Vienna), EX5/2 (1999).
- 26) Konno C., "TORT Solutions with FNSUNCL3 on 3D Radiation Transport Benchmarks for Simple Geometries with Void Region", Proc. of Mathematics and Computation, Reactor Physics and Environmental Analysis in Nuclear Applications (Madrid), 1755 (1999).
- 27) Kuriyama M., Akino N., Ebisawa N., et al., "Increasing the Beam Power of the JT-60 Negative Ion Based Neutral Beam System," Proc. of 18th Symp. on Fusion Eng (Albuquerque), 133 (1999).
- 28) Kusama Y., Kimura H., Ozeki T., et al., "Alfven Eigenmodes and their Impact on Plasma Characteristics in JT-60U", Fusion Energy 1998 (CD-ROM, IAEA, Vienna), EX8/6 (1999).
- 29) Masaki K., Morimoto M., Sakasai A., et al., "JT-60U W-shaped Divertor with In-out Divertor Pumping Slots," Proc. of 18th Symp. on Fusion Eng. (Albuquerque), 123 (1999).
- 30) Matsukawa M., "A Coil Current Control Method for Power Supply of Nuclear Fusion Devices (in Japanese)", Proc. of the 1999 Japan Ind. Appl. Soc. Conf. (Nagasaki), 3 117 (1999).
- 31) Miura Y.M., Matsukawa M. and Nakano H., "A New PWM Pattern Generation Method for a PWM Converter Applied to a Superconducting Magnet", Proc. of 18th Symp. on Fusion Eng. (Albuquerque), 417 (1999).
- 32) Moriyama S., Fujii T., Kimura H., et al., "Development of All-metal Antenna for ICRF System in Next Generation Tokamaks," Proc. of 18th Symp. on Fusion Eng. (Albuquerque) 399 (1999).
- 33) Nakahira M., Koizumi K., Oka K., et al., "Integration Test of ITER Full-Scale Vacuum Vessel Sector", Fusion Energy 1998 (CD-ROM, IAEA, Vienna), ITERP1/24 (1999).

- 34) Nakamura Y., Lister J.B., Hofmann F., et al., " β_p -Collapse-Induced VDE and its Underlying Mechanism in the TCV Tokamak," Proc. of 26th EPS Conf. on Cont. Fusion and Plasma Physics (Maastricht), 417 (1999).
- 35) Nazikian R., Shinohara K., Yoshino R., et al., "Core Density Fluctuations in Reversed Magnetic Shear Plasmas with Internal Transport Barrier on JT-60U", Fusion Energy 1998 (CD-ROM, IAEA, Vienna), PDP/03 (1999).
- 36) Neyatani Y., Nakamura Y., Yoshino R., et al., "Characteristics of Halo Current in JT-60U", Fusion Energy 1998 (CD-ROM, IAEA, Vienna), EXP3/11 (1999).
- 37) Ogawa T., Ogawa H., Maeno M., et al., "Compact Toroid Injection Experiment in JFT-2M", Fusion Energy 1998 (CD-ROM, IAEA, Vienna), EXP1/16 (1999).
- 38) O'hira S., Hayashi T., Nakamura H., et al., "Improvement of Tritium Accountancy Technology for The ITER Fuel Cycle Safety Enhancement", Fusion Energy 1998 (CD-ROM, IAEA, Vienna), ITERP2/06 (1999).
- 39) Oikawa T., Ushigusa K., Nemoto M., et al., "Heating and Non-Inductive Current Drive by Negative-Ion Based NBI in JT-60U", Fusion Energy 1998 (CD-ROM, IAEA, Vienna), CD1/1 (1999).
- 40) Okumura Y., Fujiwara Y., Hanada M., et al., "Technologies Producing High Current Negative Ion Beams", Proc. of Japanese Electro-technical Committee Meeting, ED-99-175 (1999) (in Japanese).
- 41) Ozeki T., Ishii Y., Tokuda S., et al., "Improvement of MHD Stability in Negative/Weak Shear Configurations for A Stability State Tokamak", Fusion Energy 1998 (CD-ROM, IAEA, Vienna), THP2/31 (1999).
- 42) Sakamoto K., Kasugai A., Tsuneoka M., et al., "Development of High Power Long Pulse Gyrotron for ITER", Fusion Energy 1998 (CD-ROM, IAEA, Vienna), FTP/23 (1999).
- 43) Sakasai A., Takenaga H., Hosogane N., et al., "Steady-State Exhaust of Helium Ash in the W-Shaped Divertor of JT-60U", Fusion Energy 1998 (CD-ROM, IAEA, Vienna), EX6/5 (1999).
- 44) Shirai H., Kikuchi M., Takizuka T., et al., "Reduced Transport and Er Shearing in Improved Confinement Regimes in JT-60U", Fusion Energy 1998 (CD-ROM, IAEA, Vienna), EX5/4 (1999).
- 45) Sinozaki S., Shimono M., Terakado M., et al., "Operation and Control of JT-60U ECRF System," Proc. of 18th Symp. on Fusion Eng. (Albuquerque), 403 (1999).
- 46) Sugihara M., Igitkhanov Yu., Janeschitz G., et al., "Studies on the Scaling of H-mode Pedestal Width in the ITER Multi-machine Pedestal Database", Proc. of 26th EPS Conf. on Cont. Fusion and Plasma Physics (Maastricht), **23J** 1449 (1999).
- 47) Takase K., Seki Y., Akimoto H., et al., "Thermal-Hydraulic Characteristics During Ingress-of-Coolant and Loss-of-Vacuum Events", Fusion Energy 1998 (CD-ROM, IAEA, Vienna), ITERP2/09 (1999).
- 48) Takase H., Senda I., Araki M., et al., "3-D Electromagnetic Transient Characteristics of In-Vessel Components in Tokamak Reactor", Fusion Energy 1998 (CD-ROM, IAEA, Vienna), FTP/28 (1999).
- 49) Takenaga H., Nagashima K., Sakasai A., et al., "Particle Confinement and Transport in JT-60U", Fusion Energy 1998 (CD-ROM, IAEA, Vienna), EXP1/17 (1999).
- 50) Tokuda S., Yoshino R., Matsumoto T., et al., "Simulation Study on Avoiding Runaway Electron Generation by Magnetic Perturbations", Fusion Energy 1998 (CD-ROM, IAEA, Vienna), THP2/26

(1999).

- 51) Tsuchiya Y., Kikuchi K., Minakawa N., et al., "Neutron Diffraction Measurement of Internal Residual Stress of Superconducting Coil Jacket", 6th Int. Conf. on Residual Stress (ICRS-6), 337 (2000).
- 52) Tuda T., Kurita G., Ishii Y. et al., "Velocity Shear Stabilization of Double Tearing Mode", Proc. of 26th EPS Conf. on Cont. Fusion and Plasma Physics (Maastricht), 433 (1999).
- 53) Ushigusa K., Kurita G., Toyoshima N., et al., "Design Optimization of JT-60SU for Steady-State Advanced Operation", Fusion Energy 1998 (CD-ROM, IAEA, Vienna), FTP/12 (1999).
- 54) Watanabe K., Fujiwara Y., Hanada M., et al., "Voltage Holding and Beam Acceleration Characteristics of 1MeV Negative Ion Accelerator", Proc. of Japanese Electro-technical Committee Meeting, ED-99-177 (1999) (in Japanese).
- 55) Yamada M., Ioki K., Cardella A., et al., "Status of Blanket Design for RTO/RC ITER", Proc. of 4th IEA International Workshop on Beryllium Technology for Fusion (Karlsruhe), 186 (1999).
- 56) Yamanishi T., Kawamura Y., Iwai Y., et al., "Development of Tritium Fuel Processing Systems Using Electrolytic Reactor for ITER", Fusion Energy 1998 (CD-ROM, IAEA, Vienna), ITERP2/05 (1999).
- 57) Yoshino R., Neyatani Y., Tokuda S., et al., "Characterization of Disruption Phenomenology in ITER", Fusion Energy 1998 (CD-ROM, IAEA, Vienna), ITERP1/14 (1999).

A.1.4 List of other papers

- 1) Abe T., Kasai S., Hiroki S., et al., "Development of Fuel Injection Technology and Vacuum Pumps" J. Plasma Fusion Res., **75 Supplement** 62 (1999) (in Japanese).
- 2) Akiba M. and Suzuki S., "Development of Divertor Technology" J. Plasma Fusion Res., **75 Supplement** 26 (1999) (in Japanese).
- 3) Ando T., Takahashi Y., Nakajima H., et al., "Superconducting Magnet System Technology" J. Plasma Fusion Res., **75 Supplement** 7 (1999) (in Japanese).
- 4) Fujisawa N., "Burn Control in Tokamak Fusion Reactors Burn Control in ITER" J. Plasma Fusion Res., **75** 1366 (1999) (in Japanese).
- 5) Fukuyama A. and Ozeki T., "Linear Theory of Alfvén Eigenmodes in Tokamak Plasmas" J. Plasma Fusion Res., **75** 537 (1999) (in Japanese).
- 6) Fukuyama A., Takase Y., Ide S., et al., "Physics of Heating and Current Drive" J. Plasma Fusion Res., **76** 127 (1999) (in Japanese).
- 7) Imai T., Sakamoto K. and Moriyama S., "RF Heating and Current Drive Technology" J. Plasma Fusion Res., **75 Supplement** 72 (1999) (in Japanese).
- 8) Kimura H., "Report on JFT-2M Research Collaborating Meeting" J. Plasma Fusion Res., **75** 758 (1999) (in Japanese).
- 9) Kishimoto H., Fujiwara M., Tamano T., et al., "Introduction of ITER Physics R&D", J. Plasma Fusion Res., **76** 19 (2000) (in Japanese).
- 10) Koizumi K., "Vacuum Vessel and Related Technologies" J. Plasma Fusion Res., **75 Supplement** 20 (1999) (in Japanese).
- 11) Kurihara K., "Plasma Equilibrium Analysis for Tokamak Experiments" J. Plasma Fusion Res., **76** 65 (1999) (in Japanese).
- 12) Kusama Y. and Kimura H., "Experimental Studies of Alfvén Eigenmodes in Tokamaks and Critical Issues" J. Plasma Fusion Res., **75**, 525 (1999) (in Japanese).
- 13) Loarer T., Horton L. D., Kubo H., et al., "D_α Measurements in the JET Divertor with the Divertor Periscope Diagnostic", JET-R (99) 05 (1999).
- 14) Matsuda S., "Prospectives of Fusion Technology Development, New Technology of Fusion Engineering", J. Atomic Energy Soc. Japan, **41** 735 (1999) (in Japanese).
- 15) Ninomiya H., Wakatani M., Tamano T., et al., "Prospect of ITER Physics R&D" J. Plasma Fusion Res., **76** 163 (2000) (in Japanese).
- 16) Nishitani T., Sugie T. and Kasai S., "Development of Diagnostic Components" J. Plasma Fusion Res., **75 Supplement** 79 (1999) (in Japanese).
- 17) Ohara Y., Takeuchi H. and Kawamura H., "Development of Blanket" J. Plasma Fusion Res., **75 Supplement** 35 (1999) (in Japanese).
- 18) Ohmori J., Nakahira M., Tada E., et al., "V.2.1; Clearance TS-VV", ITER/EDA Task Report- INT9025 (June 14, 1999).

- 19) Ohmori J., Nakahira M., Tada E., et al., "V.2.2; Clearance VV-SB", ITER/EDA Task Report- INT9026 (June 15, 1999).
- 20) Ohmori J., Satoh Sa., Sato Sh., et al., "V.1.2; Nuclear Response Analysis in TFC and VV", ITER/EDA Task Report- INT9009 rev.1 (June 9, 1999).
- 21) Okumura Y. and Watanabe K., "NBI Heating and Current Drive System" J. Plasma Fusion Res., **76** 65 (1999) (in Japanese).
- 22) Shibanuma K. and Obara K., "Development of Remote Maintenance Technology" J. Plasma Fusion Res., **75 Supplement** 45 (1999) (in Japanese).
- 23) Shiho M., "Application of Intense Charged Particle Beams" J. Plasma Fusion Res., **75** 1280 (1999) (in Japanese).
- 24) Shimada M., Hosogane N. and Itami K., "Divertor Physics" J. Plasma Fusion Res., **76** 41 (1999) (in Japanese).
- 25) Takase H., Nishino T., Shoji T., et al., "III.4.2; Further Studies on Steady State Operation Capability: Higher Triangularity, Higher Elongation, Changing Aspect Ratio", ITER/EDA Task Report- INT9002 (May 7, 1999), INT9015 (June 8, 1999).
- 26) Takase H., Shoji T., Fujieda H., et al., "III.4.3; Optimisation of Plasma Profile: Heating and Current Drive Efficiency, Dilution of Fuel with Hydrogen, Heating Capability of Hydrogen Beam", ITER/EDA Task Report- INT9001 (May 7, 1999), INT9016 (June 8, 1999).
- 27) Takase H., Shoji T., Fujieda H., et al., "IV.4.2; Calculation of Stopping Voltages at Minor VDE - Static and Dynamic Analyses of Plasma Vertical Stability", ITER/EDA Task Report- INT9003 (May 7, 1999), INT9014 (June 8, 1999).
- 28) Tobita K. and Fukuyama A., "Physics of Energetic Particles" J. Plasma Fusion Res., **76** 138 (1999) (in Japanese).
- 29) Ueda S., Kurihara R., Seki Y., et al., "Safety R&D" J. Plasma Fusion Res., **76** 88 (1999) (in Japanese).
- 30) Wakatani M., Ohyabu N., Kamada Y., et al., "Confinement and Transport in High Performance Plasmas" J. Plasma Fusion Res., **76** 21 (1999) (in Japanese).
- 31) Wakatani M., Shimada M., Tamano T., et al., "ITER-Project (International Thermonuclear Experimental Reactor)", BUTSURI, **54** 417 (1999) (in Japanese).
- 32) Yamanishi T., O'hira S., Hayashi T., et al., "Development of Tritium Technology" J. Plasma Fusion Res., **75 Supplement** 55 (1999) (in Japanese).
- 33) Yoshino R., "Burn Control in Tokamak Fusion Reactors Disruption and Fast Plasma Shutdown" J. Plasma Fusion Res., **75** 1360 (1999) (in Japanese).
- 34) Yoshino R., Ozeki T., Tokuda S., et al., "Disruption, MHD and Plasma Control" J. Plasma Fusion Res., **76** 116 (1999) (in Japanese).
- 35) Zushi H., Sugie T., Kusama Y., et al., "Plasma Diagnostics" J. Plasma Fusion Res., **76** 145 (1999) (in Japanese).

Appendix A.2 Personnel

Scientific Staff in the Naka Fusion Research Establishment (April 1999 - March 2000)

Naka Fusion Research Establishment

OHTA Mitsuru	(Director General)
MIYAMOTO Kenro	(Invited Researcher)
NISHIKAWA Kyoji	(Invited Researcher)
KAWASAKI Sunao	(Invited Researcher)
SHIMAMOTO Susumu	(Invited Researcher)
KOYAMA Akira	(Invited Researcher)
KONDO Tatsuo	(Invited Researcher)
SEKIMURA Naoto	(Invited Researcher)
AZUMI Masafumi	
YAMAMOTO Takumi	(Staff for Director General)
YOSHIDA Hidetoshi	(Staff for Director General)
IIZUKA Takayuki	(Staff for Director General)

Department of Administrative Services

HINO Syuji	(Director)
KAMBARA Yoyu	(Deputy Director)

Department of Fusion Plasma Research

FUNAHASHI Akimasa	(Director)
NINOMIYA Hiromasa	(Deputy Director)
MAENO Masaki	
KAWANO Yoshikatsu	(Administrative Manager)

Tokamak Program Division

KIKUCHI Mitsuru	(General Manager)	
ARAI Masaru (*13)	ISHIDA Shinichi	KAWANO Yasunori
KURITA Gen-ichi	MORI Katsuharu (*13)	OGURI Shigeru (*13)
OIKAWA Akira	SAKASAI Akira	TAKENAGA Hidenobu
TOBITA Kenji	YAMAZAKI Takeshi (*13)	

Plasma Analysis Division

OZEKI Takahisa	(General Manager)	
HAMAMATSU Kiyotaka	HAYASHI Nobuhiko	KOIWA Motonao (*29)
MATSUDA Toshiaki	NAITO Osamu	NAKAMURA Yukiharu
NEUDATCHIN Sergei V. (*9)	OHSHIMA Takayuki	SAKATA Shinya
SATO Minoru	SHIMIZU Katsuhiro	SHIRAI Hiroshi
SUZUKI Masahei (*29)	SUZUKI Mitsuhiro (*25)	TAKIZUKA Tomonori
TSUGITA Tomonori		

Large Tokamak Experiment Division I

NINOMIYA Hiromasa	(General Manager)	
CHIBA Shinichi	FUJITA Takaaki	FUKUDA Takeshi

HAMANO Takashi (*24)	HOEK Magnus (*30)	INOUE Akira (*24)
ISAYAMA Akihiko	IWASE Makoto (*27)	KAMADA Yutaka
KASHIWABARA Tsuneo (*21)	KITAMURA Shigeru	KOIDE Yoshihiko
KOKUSEN Shigeharu (*21)	KRAMER Gerrit Jakob (*9)	KUSAMA Yoshinori
MIRNOV Maxim (*30)	MORIOKA Atsuhiko	NAGAYA Susumu
NEMOTO Masahiro	NISHITANI Takeo	OIKAWA Toshihiro
SAKAMOTO Yoshiteru	SAKUMA Takeshi (*24)	SHIBATA Yasunari (*20)
SHITOMI Morimasa	SUNAOshi Hidenori	SUZUKI Takahiro
TAKEJI Satoru	TAKI Yoshiaki (*21)	TSUCHIYA Katsuhiko
TSUKAHARA Yoshimitu	UEHARA Kazuya	URAMOTO Yasuyuki
URANO Hajime (*6)		

Large Tokamak Experiment Division II

YOSHINO Ryuji	(General Manager)	
ASAKURA Nobuyuki	BAK Paul Eric (*30)	BAKHTIARI Mohammad (*34)
HATAE Takaki	HIGASHIJIMA Satoru	IDE Shunsuke
ISHIJIMA Tatsuo (*2)	ITAMI Kiyoshi	KONDOH Takashi
KONOSHIMA Shigeru	KUBO Hirotaka	LEE Seishu (*27)
NAKANO Tomohide	OYAMA Naoyuki (*27)	SAKURAI Shinji
SHINOHARA Kouji	SUGIE Tatsuo	TAMAI Hiroshi

Plasma Theory Laboratory

KISHIMOTO Yasuaki	(Head)	
DETTRICK Sean (*30)	ISHII Yasutomo	ISHIZAWA Akihiro (*27)
LI Jiquan (*30)	MATSUMOTO Taro	MIYOSHI Takahiro (*27)
SUGAHARA Akihiro (*29)	SUZUKI Yoshio (*27)	TOKUDA Shinji
TUDA Takashi		

Experimental Plasma Physics Laboratory

KIMURA Haruyuki	(Head)	
HOSHINO Katsumichi	ISEI Nobuaki	KAWAKAMI Tomohide
KAWASHIMA Hisato	MAEDA Mitsuru (*12)	MIURA Yukitoshi
OGAWA Hiroaki	OGAWA Toshihide	OASA Kazumi
SATO Masayasu	SENGOKU Seio	SHIINA Tomio
TSUZUKI Kazuhiro		

Reactor System Laboratory

USHIGUSA Kenkichi	(Head)	
AOKI Isao	AJIMA Toshio(*5)	KURIHARA Ryoichi
NISHIO Satoshi	OKADA Hidetoshi (*5)	UEDA Shuzo

Department of Fusion Facilities

SHIMIZU Masatsugu	(Director)
KIMURA Toyoaki	(Deputy Director)

JT-60 Administration Division

OOTAKE Masaki	(General Manager)
---------------	-------------------

JT-60 Facilities Division I

KIMURA Toyoaki	(General Manager)	
ADACHI Hironori (*7)	AKASAKA Hiromi	FURUKAWA Hiroshi (*24)
HATTORI Akio (*13)	KAWAMATA Youichi	KURIHARA Ken-ichi
MATSUKAWA Makoto	MIURA M. Yushi	NODA Masaaki (*13)
OKANO Jun	OHMORI Shunzo	OHMORI Yoshikazu
SEIMIYA Munetaka	TAKANO Shoji	TERAKADO Tsunehisa
TOTSUKA Toshiyuki	UEHARA Toshiaki(*24)	YONEKAWA Izuru

JT-60 Facilities Division II

HOSOGANE Nobuyuki	(General Manager)	
MIYACHI Kengo	(Deputy General Manager)	
ARAI Masaru (*13)	ARAI Takashi	HIRATSUKA Hajime
HONDA Masao	ICHIGE Hisashi	IWAHASHI Takaaki (*21)
KAMINAGA Atsushi	KIKUCHI Hiroshi (*5)	KIZU Kaname
KODAMA Kozo	MASAKI Kei	MASUI Hiroshi (*10)
MIYA Naoyuki	MIYATA Katsuyuki (*5)	MIYO Yasuhiko
MORIMOTO Masaaki (*19)	NAGASHIMA Akira (*13)	OKABE Tomokazu
SASAJIMA Tadayuki	SASAKI Noboru (*5)	YAGYU Jun-ichi

RF Facilities Division

FUJII Tsuneyuki	(General Manager)	
ANNOU Katsuto	IKEDA Yoshitaka	ISAKA Masayoshi
ISHII Kazuhiro (*24)	HAGA Koichi (*21)	HIRANAI Shinichi
HIROI Toshikazu (*31)	KAJIYAMA Eiichi (*21)	MORIYAMA Shinichi
SEKI Masami	SHIMONO Mitsugu	SHINOZAKI Shin-ichi
TERAKADO Masayuki	YOKOKURA Kenji	

NBI Facilities Division

KURIYAMA Masaaki	(General Manager)	
ITOH Takao	(Deputy General Manager)	
AKINO Noboru	EBISAWA Noboru	HONDA Atsushi
GRISHAM Larry (*28)	KAWAI Mikito	KAZAWA Minoru
HU Liquen (*7)	MOGAKI Kazuhiko	OHGA Tokumichi
OHSHIMA Katsumi (*21)	OOHARA Hiroshi	SEKI Hiroshi (*24)
TANAI Yutaka (*24)	TOYOKAWA Yoshiharu (*21)	UMEDA Naotaka
USUI Katsutomi	YAMAGUCHI Masao (*24)	YAMAZAKI Haruhiko (*5)

JFT-2M Facilities Division

KOIKE Tsuneyuki	(General Manager)	
YAMAMOTO Masahiro	(Deputy General Manager)	
AKIYAMA Takashi (*13)	HASEGAWA Koichi	KASHIWA Yoshitoshi
KIKUCHI Kazuo	KIYONO Kimihiro	KOMATA Masao
OKANO Fuminori	SAWAHATA Masayuki	SHIBATA Takatoshi
SUZUKI Sadaaki	TANI Takashi	UMINO Kazumi (*24)

Department of Fusion Engineering Research

MATSUDA Shinzaburo (Director)
SEKI Yasushi (Deputy Director)
NEMOTO Shinichiro (Administrative Manager)

Blanket Engineering Laboratory

OHARA Yoshihiro (Head)
ABE Tetsuya ENOEDA Mikio HATANO Toshihisa
KASAI Satoshi KIKUCHI Shigeto (*33) KOSAKU Yasuo
KURODA Toshimasa (*16) NAKAMURA Jyun-ichi (*26) SATO Satoshi
HIROKI Seiji TANZAWA Sadamitsu

Superconducting Magnet Laboratory

TSUJI Hiroshi (Head)
ANDO Toshinari FU Youkin (*24) HIYAMA Tadao
ISONO Takaaki ISHIO Koutarou (*11) KATO Takashi
KAWANO Katsumi KOIZUMI Norikiyo KUBO Hiroatsu (*3)
MATSUI Kunihiko NAKAJIMA Hideo NISHIJIMA Gen (*27)
NUNOYA Yoshihiko OSHIKIRI Masayuki (*24) SAWADA Kenji (*18)
SHIMBA Toru (*8) SUGIMOTO Makoto TAKAHASHI Yoshikazu
TSUCHIYA Yoshinori (*27) WAKABAYASHI Hiroshi (*24)

NBI Heating Laboratory

OKUMURA Yoshikazu (Head)
AKIBA Masato BANDOURLKO Vassi (*9) DAIRAKU Masayuki
EZATO Koichiro FUJIWARA Yukio KASHIWAGI Yukiko (*27)
HANADA Masaya KITAGAWA Tadashi (*23) MIYAMOTO Kenji
TANIGUCHIA Masaki SATO Kazuyoshi SAWAHATA Osamu (*24)
SUZUKI Satoshi WATANABE Kazuhiro YOKOYAMA Kenji

RF Heating Laboratory

IMAI Tsuyoshi (Head)
IKEDA Yukiharu INOUE Yoji (*22) KASUGAI Atsushi
MAEBARA Sunao OHUCHI Hitoshi (*22) SAKAMOTO Keishi
SHIHO Makoto TAKAHASHI Koji TSUNEOKA Masaki
WATANABE Akihiko (*22) YAMAMOTO Masanori (*5) ZHENG Xiaodong (*27)
SHOYAMA Hiroaki (*27)

Tritium Engineering Laboratory

NISHI Masataka (Head)
MISAKI Yohnosuke (*31) HAYASHI Takumi ISOBE Kanetsugu
IWAI Yasunori KAKUTA Toshiya (*16) KAWAMURA Yoshinori
KOBAYASHI Kazuhiro IAMIZUMI Hideki (*19) NAKAMURA Hirofumi
O'HIRA Shigeru SAKAI Takuhiro (*34) SHU Wataru
SUZUKI Takumi TADOKORO Takahiro (*5) YAMADA Masayuki
YAMANISHI Toshihiko SUZUKI Takumi TADOKORO Takahiro (*5)

YAMADA Masayuki

KONISHI Satoshi

OYA Yasuhisa (*27)

Reactor Structure Laboratory

KOIZUMI Koichi

(Head)

AKOU Kentaro (*16)

ITOU Akira (*8)

KAKUDATE Satoshi

SHIBANUMA Kiyoshi

NAKAHIRA Masataka

OBARA Kenjiro

OKA Kiyoshi

TAGUCHI Kou (*24)

TAKAHASHI Hiroyuki (*5)

TAKIGUCHI Yuji (*33)

TAKEDA Nobukazu

Fusion Neutronics Laborator

TAKEUCHI Hiroshi

(Head)

ABE Yuichi

IDA Mizuho(*8)

KUTSUKAKE Chu

NAKAMURA Hiroo

OGINUMA Yoshikazu (*24)

SEKI Masakazu

SHIBATA Keiichiro(*5)

SUGIMOTO Masayoshi

TANAKA Shigeru

YUTANI Teruaki (*33)

Office of Fusion Material Research Promotion

HISHINUMA Akimichi

(Head)

NAKAMURA Kazuyuki

FURUYA Kazuyuki

Department of ITER Project

KITSUNEZAKI Akio

(Director)

TSUNEMATSU Toshihide

(Deputy Director)

SEKI Masahiro

(Prime Scientist)

SHIMOMURA Yasuo

(Prime Scientist)

FUJISAWA Noboru

INABE Teruo

ODAJIMA Kazuo

Administration Group

OKABE Takashi

(Leader)

Project Management Group

ANDO Toshiro

(Leader)

TSURU Daigo

Joint Central Team Group

SHOJI Teruaki

(Leader)

EBISAWA Katsuyuki (*33)

HONDA Takuro (*5)

HONDA Tsutomu (*33)

HOSHI Yuuichi (*8)

IIDA Hiromasa

IOKI Kimihiro (*19)

INOUE Takashi

KATAOKA Yoshiyuki (*5)

KITAMURA Kazunori (*33)

KOBAYASHI Noriyuki (*33)

KURIBAYASHI Takashi (*8)

MARUYAMA So

MATSUMOTO Hiroshi

MATSUMOTO Yasuhiro (*33)

MATSUNOBU Takashi (*5)

MIKI Nobuharu (*33)

MIZOGUCHI Tadanori (*5)

MOCHIZUKI Eiji (*32)

NISHIKAWA Akira(*8)

OHSAKI Toshio (*16)

OKUNO Kiyoshi

ONOZUKA Masanori (*19)

SATO Kouichi (*1)

SHIMADA Michiya

SUGIHARA Masayoshi	TAKIGAMI Hiroyuki (*33)	YAMADA Masao (*19)
YAMAMOTO Shin	YOSHIDA Hiroshi	YOSHIDA Kiyoshi
YOSHIMURA Hideto (*18)		

Home Team Design Group

SHOJI Teruaki	(Leader)	
ARAKI Masanori	GOTO Yoshinori (*18)	KASHIMURA Shinji (*15)
KATAOKA Takahiro (*18)	KUCHIISHI Keiichi (*5)	MURAKAMI Yoshiki (*33)
OHKAWA Yoshinao	OHMORI Jyunji (*33)	OHNO Isamu (*8)
SAITO Keiji (*5)	SATO Shinichi (*16)	SENDA Ikuoo (*33)
SHIMA Hiroaki (*14)	YAGENJI Akira (*4)	

Safety Evaluation Group

TADA Eisuke	(Leader)	
ARAKI Takao (*33)	HADA Kazuhiko	HASHIMOTO Masayoshi (*8)
ISHIDA Toshikatsu (*16)	MARUO Takeshi	NEYATANI Yuzuru
NOMOTO Kazuhiro (*18)	OHIRA Shigeru	

- *1 Atomic Data Service Corp.
- *2 Cooperative Graduate School System
- *3 Fuji Electric Co., Ltd.
- *4 Hazama-gumi Ltd.
- *5 Hitachi Ltd.
- *6 Hokkaido University
- *7 Institute of Plasma Physics Academia Sinica (China)
- *8 Ishikawajima-Harima Heavy Industries, Ltd.
- *9 JAERI Fellowship
- *10 Japan Expert Clone Corp.
- *11 Japan Steel Works Ltd.
- *12 JST Fellowship
- *13 Kaihatsu Denki Co.
- *14 Kajima Corporation
- *15 Kandenko Corp.
- *16 Kawasaki Heavy Industries, Ltd.
- *17 Mito Software Engineering Co.
- *18 Mitsubishi Electric Co., Ltd.
- *19 Mitsubishi Heavy Industries, Ltd.
- *20 Nagoya University
- *21 Nippon Advanced Technology Co., Ltd.
- *22 Nissei Sangyo Co., Ltd.
- *23 Nissin Electric Co., Ltd.
- *24 Nuclear Engineering Co., Ltd.
- *25 Nuclear Information Service Co.
- *26 Osaka Vacuum Ltd.
- *27 Post-Doctoral Fellow

- *28 Princeton Plasma Physics Laboratory (USA)
- *29 Research Organization for Information Science Technology
- *30 STA Fellowship
- *31 Sumitomo Heavy Industries, Ltd.
- *32 Takenaka Corp.
- *33 Toshiba Corp.
- *34 Utsunomiya University